CHARLES UNIVERSITY IN PRAGUE

FACULTY OF PHARMACY IN HRADEC KRÁLOVÉ

CERAMIDES AND DIMETHYLAMINO ACID DERIVATIVES AS SKIN BARRIER MODULATORS

PhD THESIS

2009

Mgr. Jakub Novotný

I would like to thank my supervisor PharmDr. Kateřina Vávrová, PhD for constant support, patience and valuable advices. I very appreciated help and support of Prof. PharmDr. Alexandr Hrabálek, CSc., my collegues and friends Barbora Janůšová, Michal Novotný, Jaroslav Roh, my family and my girlfriend, Juana Monreal Ferriz. My thanks are also given to Mrs. Iva Vencovská for measuring of IR spectra and Doc. PharmDr. Jiří Kuneš, CSc. for NMR spectra measurement.

Jakub Novotný

April 2009

Prohlašuji, že tato práce je mým původním autorským dílem, které jsem vypracoval samostatně. Veškerá literatura a další zdroje, z nichž jsem při zpracování čerpal, jsou uvedeny v seznamu použité literatury a v práci řádně citovány.

Jakub Novotný

April 2009

TABLE OF CONTENTS

SUMMARY **4**

SOUHRN **6**

1. Transdermal drug delivery **10**

DRUG TRANSPORT ROUTES THROUGH THE HUMAN SKIN 10

TRANSDERMAL PENETRATION ENHANCERS 11

2. Synthesis and Structure-Activity Relationships of Skin Ceramides **18**

SKIN CERAMIDE STRUCTURES 18

STRUCTURE-ACTIVITY RELATIONSHIPS IN SKIN CERAMIDES 19

SYNTHESIS OF SKIN CERAMIDES 22

3. Dimethylamino acid esters as biodegradable and reversible transdermal permeation enhancers: effects of linking chain length, chirality and polyfluorination **59**

4. Short-Chain Ceramides Decrease Skin Barrier Properties **77**

5. Skin Penetration of NBD-Ceramides is Chain Length-Dependent; Long-Chain Lipids Do Not Enter Nucleated Human Epidermis **92**

Curriculum Vitae **107**

Summary

The purpose of this work is to contribute to the understanding of the structure-activity relationships and behavior of the skin ceramides and transdermal penetration enhancers based on dimethylamino acid esters.

First two chapters provide a theoretical background for understanding the main principles of transdermal drug delivery as well as composition and function of stratum corneum barrier. The experimental work is presented in the form of individual publications in chapters three to five.

The first chapter describes transport routes through the human skin and gives an overview of enhancers of transdermal permeation with main accent on their chemical structure, mechanism of action, interaction with stratum corneum components and advantages and drawbacks of their use.

The second chapter brings more detailed information on the specific content and composition of stratum corneum. The main attention is paid to the ceramides - a complex group of lipids that play a crucial role as cell signaling molecules and skin barrier constituents. In the skin, these sphingolipids form a major part of the stratum corneum intercellular lipid matrix, which is the barrier for penetration of most compounds. The development of such a protective layer was a critical step in the evolution of life on a dry land. Moreover, prominent skin diseases such as psoriasis and atopic dermatitis are associated with diminished ceramide levels and may be effectively improved by exogenous ceramides or their analogues. Since ceramides are not obtained from natural sources in pure form, they are of synthetic interest since 1950's. In this chapter, we describe sphingosine syntheses from 1998 until 2008, and the synthetic approaches to the unique epidermal ceramides, including the 6-hydroxysphingosine-based ones, the alpha- and omega-hydroxy forms and the omega-acyloxy species. Moreover, the structural requirements of ceramides for a competent skin barrier are discussed, including acyl chain length, *trans* double bond, acyl alpha-hydroxyl, stereochemistry, omega-linoleyloxy species and ceramide conformation.

Chapter 3 focuses on the synthesis, evaluation of transdermal permeation-enhancing potency, biodegradability and reversibility of action of series of *N*,*N*-dimethylamino acid esters. Effects of chirality, linking chain length and polyfluorination together with the enhancer-drug interaction are discussed. No differences in activity were found between (*R*), (*S*) and racemic dodecyl 2-(dimethylamino)propanoate (DDAIP). Substitution of hydrocarbon tail by fluorocarbon one resulted in loss of activity. Replacement of branched linking chain between nitrogen and ester of DDAIP by linear one markedly improved penetration-enhancing activity with optimum in 4-6C acid derivatives. Dodecyl 6-(dimethylamino)hexanoate (DDAK) was more potent than clinically used skin absorption enhancer DDAIP for theophylline (enhancement ratio of DDAK and DDAIP was 17.3 and 5.9, respectively), hydrocortisone (43.2 and 11.5) and adefovir (13.6 and 2.8), while DDAIP was better enhancer for indomethacin (8.7 and 22.8). DDAK was rapidly metabolized by porcine esterase, and displayed low acute toxicity. Electrical resistance of DDAK-treated skin barrier promptly recovered to control values, showing the reversibility of action of the enhancer. These results suggest that DDAK, a highly effective biodegradable transdermal permeation enhancer for a broad spectrum of drugs, is a promising candidate for future research.

As mentioned above, stratum corneum ceramides are major determinants of skin barrier function. Although their physiological and pathological role has been widely investigated, to date no structure-activity relationships have been established. Study described in chapter 4 concentrates on the synthesis of a series of short-chain ceramide analogues with polar head structure identical to ceramide NS, sphingosine length of 12 carbons and acyl chain length from 2 to 12 carbons. Their effect on skin permeability is evaluated using porcine skin and two model drugs, theophylline and indomethacin, and compared to that of a physiological ceramide NS. The results showed that ceramide chain length was crucial for their barrier properties. Ceramides with 4-8C acyl chain were able to increase skin permeability for both drugs up to 10.8 times with maximum effect at 6C acyl. No increase in permeability was found for ceramide analogues with 2C and 12C acyl and ceramide NS. The same relationships were obtained for skin concentrations of the model drugs. The relationship between ceramide acyl chain length and its ability to perturb skin barrier showed striking similarity to the behavior of short-chain ceramides in sphingomyelin/phospholipid membranes and confirmed that short-chain ceramides do not act as natural ceramides and their use as experimental tools should be cautious.

Topical skin lipid supplementation may provide opportunities for controlling ceramide deficiency in diseases such as atopic dermatitis or psoriasis. However, the exact mechanisms by which exogenous ceramides correct the barrier abnormalities are not known. Although exogenous short-chain NBD-labeled C6-ceramide was shown to rapidly traverse stratum corneum (SC) and to be uptaken and metabolized by viable epidermal layers, no such evidence is available for long-chain ceramides. Thus, the study described in chapter 5 aims at comparing skin penetration of fluorescent NBD-labeled C6, C12, and C24- ceramide and pseudo ceramide 14S24. Fluorescent lipids were synthesized from sphingosine or L-serine ester and omega-NBD-labeled hydroxysuccinimide-activated acids. 24-NBD-lignoceric acid was prepared from dodecan-1,12-diol using lithium tetrachlorocuprate coupling. NBD-ceramide at two concentrations, either alone or in equimolar mixture with cholesterol and lignoceric acid, were applied on viable human skin for 2 and 12 h, respectively. Only short-chain NBD-C6- ceramide reached viable epidermis; NBD-C12- ceramide and both NBD-C24 lipids penetrated solely into several upper SC layers of both intact and acetone-treated skin. These results show that the skin penetration of exogenous ceramide is chain length-dependent and that exogenous long-chain NBD-labeled ceramide and their analogues do not enter viable epidermis. This supports our hypothesis that short-chain ceramide cannot be used as general long-chain ceramide mimics.

Souhrn

Tato práce si klade za cíl přispět k porozumění chování kožních ceramidů a akcelerantů transdermální penetrace založených na esterech dimethylaminokyselin. Zabývá se také vztahem mezi strukturou a účinkem těchto látek.

První dvě kapitoly poskytují teoretický základ pro pochopení složení a funkce *stratum corneum*, která představuje hlavní bariéru pro průnik léčiv a dalších exogenních látek do organismu, a principů transdermálního podání léčiv. Experimentální práce je prezentována ve formě samostatných publikací v kapitolách tři až pět.

Kapitola 1 se zabývá transdermálním podáním léčiv, poukazuje na jeho výhody a limitace. Hlavní pozornost je věnována akcelerantům transdermální penetrace – látkám, které umožňují dočasně snížit bariérové vlastnosti kůže a zajistit dostatečné koncentrace léčivé látky nutné pro lokální či systémový účinek. Akceleranty jsou zde popsány s hlavním důrazem na vlastnosti, chemickou strukturu a mechanismus účinku.

Druhá kapitola přináší informace o specifickém složení lipidické matrix *stratum corneum*. Ceramidy, komplexní skupina lipidů, tvoří hlavní část této intercelulární bariéry pro průnik látek do organismu. Se sníženými hladinami ceramidů jsou spjata závažná kožní onemocnění jako psoriáza či atopická dermatitida. Aplikací ceramidů či jejich analogů může být výrazně zlepšen pacientův stav. Vzhledem k tomu, že nemohou být získány v čisté formě z přírodních zdrojů, jsou zdrojem zájmu syntetických chemiků již od roku 1950. Kapitola 2 popisuje syntézy sfingosinu, publikované od roku 1998 do roku 2008, a syntetické přístupy pro přípravu unikátních kožních ceramidů. Jsou zde diskutovány strukturální požadavky, nutné pro tvorbu kompetentní kožní bariéry, včetně délky acylového řetězce ceramidu, *trans* dvojné vazby, acyl α-hydroxylu, stereochemie a konformace.

Kapitola 3 se zaměřuje na syntézu, hodnocení akcelerační aktivity, biodegradability a reversibility účinku série esterů *N*,*N*-dimethylaminokyselin. Diskutovány jsou vlivy chirality, délky řetězce aminokyselinové části a polyfluorinace alkoholové části společně s interakcí akcelerant – léčivo na účinek akcelerantu. Nebyly zjištěny žádné rozdíly v účinnosti mezi (*R*), (*S*) a racemickým dodecyl 2-(dimethylamino)propanoátem (DDAIP). Substituce uhlovodíkového řetězce za polyfluorovaný měla za následek úplnou ztrátu aktivity. Náhrada rozvětveného spojovacího řetězce mezi aminoskupinou a esterovou funkcí lineárním způsobila výrazné zlepšení penetrační aktivity s optimem u 4-6C derivátů. Dodecyl 6-(dimethylamino)hexanoát (DDAK) byl účinnější než klinicky používaný akcelerant DDAIP pro theofylin (urychlovací poměr DDAK a DDAIP byl 17,3, respektive 5,9), hydrokortizon (43,2 a 11,5) a adefovir (13,6 a 2,8), zatímco DDAIP byl lepší akcelerant pro indomethacin (8,7 a 22,8). DDAK byl relativně rychle metabolizován prasečí esterázou a vykazoval nízkou akutní toxicitu. Elektrický odpor kůže se po časově omezené aplikaci DDAK vrátil na hodnoty shodné s kontrolním vzorkem. Tyto výsledky naznačují, že akcelerant DDAK je, vzhledem k jeho spektru a intenzitě účinku, slibný kandidát pro další výzkum.

Jak již bylo zmíněno, ceramidy *stratum corneum* jsou hlavní determinanty bariérové funkce kůže. Přestože je značná pozornost věnována výzkumu jejich fyziologické a patologické role, nejsou dnes dostupné žádné informace o vztazích mezi strukturou a účinkem na funkci kožní bariéry. Studie popsaná v kapitole 4 se zaměřuje na syntézu krátkých ceramidových analogů s polární hlavou identickou s kožním ceramidem NS, délkou sfingosinové části 12C a délkou acylu od 2C do 12C. Jejich efekt na kožní permeabilitu byl

hodnocen s využitím prasečí kůže a dvou modelových léčiv, theofylinu a indometacinu, a srovnán s přirozeným ceramidem NS. Délka acylového řetězce zásadně změnila vliv ceramidového analogu na funkci kožní bariéry. Ceramidy s krátkým acylovým řetězcem o délce mezi 4-8C zvýšily permeabilitu kůže pro obě léčiva až 10,8x s maximálním účinkem pro 6C acyl. Žádný vzrůst v permeabilitě nebyl zaznamenán při použití analogů s 2C a 12C acylem a u ceramidu NS. Vztahy mezi délkou acylového řetězce ceramidu a jeho schopností rozrušit kožní bariéru vykazují značnou podobnost s chováním krátkých ceramidů ve sfingomyelin-fosfolipidových membránách. Krátké analogy se tedy vždy nechovají jako přirozené ceramidy a jejich experimentální využití musí být opodstatněné.

Předpokládá se, že exogenně podané ceramidy mohou procházet přes *stratum corneum* a vstupovat do živých epidermálních vrstev, ve kterých dochází k jejich vychytávání a metabolizaci v keratinocytech. Tato hypotéza je založena na studii, ve které autoři použili fluorescenčně značený krátký ceramid NBD-C6-Cer. Jak je popsáno v kapitole 4, krátké ceramidy a zvláště C6 derivát se nechovají jako identické kožní sfingolipidy s dlouhým řetězcem a spíše snižují bariérové vlastnosti kůže. Kapitola 5 je zaměřená na srovnání penetrace C6, C12 a C24 fluorescenčně značených ceramidů a pseudoceramidu 14S24 do živé lidské epidermis. Fluorescenční lipidy byly syntetizovány ze sfingosinu či esteru L-serinu a omega-NBD-značených kyselin. Kyselina 24-NBD-lignocerová byla syntetizována z dodekan-1,12-diolu. Značený ceramid byl aplikován ve dvou koncentracích na živou lidskou kůži po dvě, respektive po dvanáct hodin. Pouze krátký NBD-C6-ceramid pronikl do živé epidermis. Penetrace NBD-C12-ceramidu a obou NBD-C24-lipidů byla omezena na svrchní vrstvy *stratum corneum* jak u nepoškozené kůže, tak i u kůže podrobené částečné extrakci lipidů acetonem. Tyto výsledky potvrzují, že chování exogenních ceramidů závisí na délce acylového řetězce; přirozený fluorescenčně značený ceramid s dlouhým řetězcem a jeho analoga zůstávají lokalizována ve *stratum corneum* a nepronikají do živé epidermis.

1. Transdermal drug delivery

On initial inspection, the skin is an unlikely route for systemic drug administration. Indeed, large number of potentially valuable drugs can not alone be used for topical administration because they can not cross the skin barrier and reach the site of action in sufficient quantity. Since transdermal drug delivery offers many advantages over conventional routes of application including avoidance of first pass effect, stable blood levels, easy application and higher compliance of the patient, there is a continuing interest in attempting to circumvent this barrier and unfavorable physico-chemical properties of applied drugs. The drugs administered across the skin presently include clonidine, fentanyl, lidocaine, nicotine, nitroglycerin, estradiol, ethinyl estradiol, norelgestromin, norethindrone, oxybutinin, scopolamine, and testosterone. Among the requirements for these easy-to-deliver drugs belong a small daily dose, molecular weight lower than 500 $g.mol^{-1}$, low melting point and balanced lipophilicity. If the daily dose exceeds 10 mg, then the transdermal delivery might be complicated, more convenient are doses lower than 5mg [1]. A number of various methods have been developed to open the transdermal route to the therapeutics which do not fulfill above mentioned demands, including permeation enhancers, ultrasound, iontophoresis, electroporation, magnetophoresis, photoacustic waves, microneedles, targeted follicular absorption, liposomes and other vesicles, eutectic systems, supersaturated systems, ion pairs etc. [1, 2].

DRUG TRANSPORT ROUTES THROUGH THE HUMAN SKIN

Human skin selectively and effectively inhibits penetration of xenobiotics to the body. Transdermal absorption into the systemic circulation includes the permeation across the horny layer, viable epidermis and the upper dermal layers. The rate-limiting step in absorption of the compound into systemic circulation is the permeation through the *stratum corneum* (SC). The viable epidermis functions as a major barrier only for permeation of extremely lipophilic compounds.

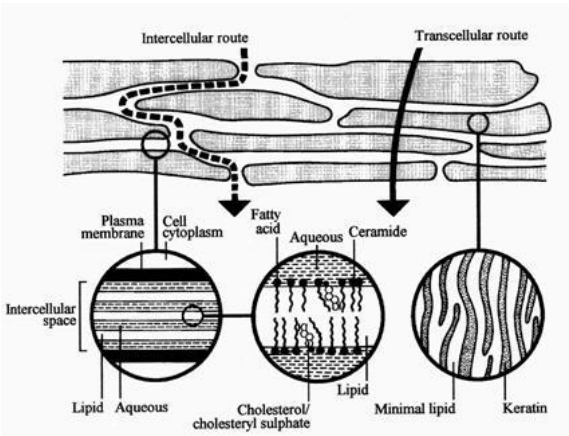

There are three possible routes to reach the viable tissue: via sebaceous glands in hair follicles, through eccrine sweat ducts or across continuous SC. Since the skin appendages occupy only 0.1% of the total human skin surface, the contribution of this route was primarily considered to be small and important only for limited number of charged substances or substances with high molecular weight. Recently it was shown, that follicular penetration may be an important pathway for the penetration of topically administered compounds [3, 4]. The transepidermal route can be divided into transcellular route through the corneocytes and intercellular pathway (Fig 1 - [5]). The more direct route is transcellular. Since the lipid phase is continuous throughout

the SC, the drug has to overcome both the lipophilic structures of SC and hydrophilic environment of the cytoplasm of dead keratinocytes. It has been shown, that intercellular pathway is common for substances with a great polarity spectrum [6, 7]. Relationships between the rate of the skin permeation of various compounds and their physicochemical properties have been also described [8-10].

TRANSDERMAL PENETRATION ENHANCERS

These chemical compounds are designed to reversibly increase the delivery of drugs in therapeutic concentrations into the skin or through the skin into deeper tissues and systemic circulation. Ideally, these compounds should be pharmacologically inert, non-toxic, non-irritating, non-allergic, compatible with the drug and excipients, odorless, tasteless, inexpensive, have good solvent properties, their effect should be immediate, predictable and reversible and they should be chemically and physically stable [11]. Although, there is no single compound possessing all the required properties, many enhancers exhibit most of these attributes and they have been clinically tested or are already commercially available.

Mechanism of the action of penetration enhancers

The mechanisms of action of enhancers are varied and can range from direct influence on the skin barrier to the modification of the formulation. According to Barry's lipid-protein partitioning concept, the direct mode of action of transdermal enhancers is based on lipid interaction, protein modification, and partition changes within the SC [12]. Thus the enhancer can:

a) Act on the SC intracellular keratin, denature it or modify its conformation causing swelling and increased hydration.
b) Affect the desmosomes that maintain the cohesion between corneocytes.
c) Modify the intercellular lipid domains. The interaction with the polar region of the lipidic lamellae is characteristic for small molecules, e.g. water or ethanol. These substances are expected to interfere with hydrogen bonding that provides tight packing of lipid bilayers. The hydrophobic region is the site of action of amphiphilic enhancers possessing similar structural features like natural ceramides. These compounds are likely to be inserted into the lamellae, with their polar head in the polar region and the hydrophobic part between the hydrophobic chains of SC lipids. This may induce disturbance of the lipid packing, lateral fluidization of the lamellae and decrease of the skin barrier resistance [13]. Some enhancers, e.g. oleic acid are likely to be heterogeneously concentrated within domains and act as more permeable pores for polar substances [14]. Some solvents may act via lipid extraction [15, 16].
d) Alter the solvent nature of the SC and thus modify partitioning of the drug or the cosolvent into the tissue.

In addition, penetration enhancer can act indirectly by:

a) Modification of thermodynamic activity of the vehicle.
b) Solubilisation of the permeant in the donor, especially if the solubility of the drug is low.

Overview of the enhancers regarding their chemical structure

Penetration enhancers represent a heterogeneous group of chemical compounds. Regarding the basic structural features they may be divided into several classes.

Water is the most natural enhancer. The hydration of the SC is associated with swelling of the corneocytes and an increase in the water content of the inter-corneocyte lipid bilayers. These phenomena appear to facilitate xenobiotic delivery across the tissue.

Alcohols may influence the transdermal penetration by several mechanisms depending on alkyl chain length. The lower molecular weight alkanols appear to enhance the solubility of drugs in the matrix of SC [17]. The more hydrophobic alcohols may contribute by disruption of SC through the extraction of biochemicals [18].

Activity of polyols, and propylene glycol in particular, are thought to result from solvatation of α-keratin within the SC [2]. Propylene glycol can also modify the solubility in of the drug in the delivery vehicle and work as a cosolvent [19]. The penetration is probably enhanced by a solvent drag effect. Propylene glycol also displays a synergic effect when combined with other permeation enhancers that act on the lipid barrier.

Fatty acids have been used to improve transdermal delivery of wide variety of drugs, e.g. estradiol, progesterone, acyclovir, 5-fluorouracil etc. [11], indicating that these enhancers may be used for wide variety of both hydrophilic and lipophilic permeants. Based on experiments of Aungst the most potent are saturated fatty acids with carbon chain length of C10 – C12 [20, 21]. In contrast, unsaturated fatty acids have the optimum activity at C18. Oleic acid, in relatively low concentration, has been shown to be effective for many drugs, and can work synergistically when delivered from vehicles such as PG.

Esters such as ethyl acetate are relatively small hydrogen bonding species that may enhance permeation by penetrating into the SC and increasing the lipid fluidity by disruption of lipid packing [22]. Moreover, the aliphatic esters may influence partitioning between vehicle and skin by solubilization effects [23].

DMSO is dipolar, aprotic solvent with excellent dissolving power. The mechanism of action is combination of denaturation of intercellular structural proteins of SC, disturbing of SC barrier lipids and their extraction [24]. Unfortunately, DMSO is skin irritating in concentrations over 60% required for penetration enhancement. A group of iminosulfurans, based on DMSO structure was designed to be more lipophilic and effective at lower concentrations (Fig. 2) [25]. This should result in lower skin irritation.

Urea promotes transdermal permeation by facilitating hydration of the SC and formation of hydrophilic diffusion channels within the barrier [26]. The keratolytic properties of urea and its derivatives is other reason for the modest permeation enhancement achieved by use of these compounds. However, application of these substances (Fig. 3) [27] as permeation

enhancers is limited by their inadequate chemical stability, the proteolytic properties and the skin irritating effects [28].

Fig. 2. *S*,*S*-Dimethyl-*N*-(4-bromobenzoyl) iminosulfurane.

Fig. 3. 1-Dodecyl-3-methythiourea.

Derivatives of ω-amino acids include a number of potent enhancers of transdermal penetration. Pyrrolidones are able to promote the penetration of both hydrophilic drugs as well as of lipophilic substances. *N*-methyl-2-pyrrolidone and 5-oxo-pyrrolidin-2-carboxylic acid are the most widely used enhancers of this group. Derivatives of 1-alkyl-2-piperidone promoted the flux of 5-fluorouracil, caffeine, indomethacin, triamcinolon, acetonide and ibuprofen. Michniak prepared a series of alkyl 2-(oxopiperidyl)acetates (Fig. 4) with higher activity for enhancement of hydrocortisone than Azone (Fig. 5), which is the most important derivative of 2-azepanons [29]. Azone is a first compound specifically designed as a transdermal permeation enhancer. It is a very good solvent and possesses overall enhancing activities for a quantity of lipophilic therapeutics, thus being often used as a standard for other sorption accelerants. Nevertheless, it is inconvenient for clinical use due to its irritation potential [30]. Derivatives of alkyl-*N*,*N*-disubstituted amino alkanoates are other effective representatives of this group [31].

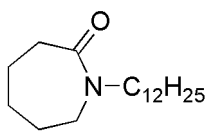

Fig. 4. Dodecyl 2-(2-oxopiperidin-1-yl)acetate.

Fig. 5. 1-Dodecylazepan-2-one.

An α-amino acid derivative, DDAIP (dodecyl 2-(dimethylamino)propanoate), is a therapeutically used permeation enhancer which interacts both with lipid-rich bilayers and keratine-rich layers. The enhancer appears to open new penetration routes and increase the ohmic resistence, capacity properties and fractal dimension of the skin [32]. A series of α-amino acid based enhancers was synthesized by Fisher and Vavrova (Fig. 6) [33, 34].

Carbamates, in particular tramskarbam 12 (Fig. 7), have been reported as excellent penetration enhancers for numerous drugs with wide range of physico-chemical properties with low toxicity and no dermal irritability [35, 36]. The activity is most likely attributed to the structure of the polar head of these compounds, which can be decomposed easily in the mildly acidic environment of the skin. The released carbon dioxide probably interferes with SC lipid packing thus opening the penetration route for the permeant.

Fig. 6. Dodecyl 2-dodecanamidoacetate.

Fig. 7. Transkarbam 12.

Surfactants are frequently used as emulsifiers in formulations for dermal application. They have the potential to cause protein denaturation or extraction, enzyme inactivation, swelling of tissue and extraction of lipid components. Normally, cationic surfactants are more effective than anionic and nonionic compounds. However, nonionic compounds are used because of low skin irritation potential.

Terpenes and terpenoids, as highly lipophilic compounds, influence the non-polar penetration route. Their effect is linked to a disruption of the lipid packing and to a disturbance in the stacking of the bilayers. Terpenes are promising candidates for transdermal enhancers due to their low cutaneous irritation in low concentrations (1-5%), low systemic toxicity and high activity for both lipophilic and hydrophilic compounds [28].

Oxazolidinones benefit from their ability to localize increased concentration of the permeant into SC or into dermis, which results in low systemic permeation [37]. The structural similarity to sphingosine and ceramide like lipids probably causes the lack of effective absorption of the enhancer into lower skin layer where irritation is likely to occur.

Few studies also used phospholipids in non-vesicular form as penetration enhancers. There is evidence that phospholipids interact directly with lipid packing of SC. Nevertheless, phospholipids can occlude the skin surface, which leads to skin hydration and subsequent increase in drug penetration.

Further and more detailed information on transdermal delivery and penetration enhancers can be found in several reviews [24, 28, 38-40].

References

[1] Kanikkannan, N.; Kandimalla, K.; Lamba, S. S.; Singh, M. Structure-activity relationship of chemical penetration enhancers in transdermal drug delivery. *Curr Med Chem*, **2000**, *7*, 593-608.

[2] Barry, B. W. Mode of action of penetration enhancers in human skin. *J Controlled Release*, **1987**, *6*, 85-97.

[3] Lademann, J.; Otberg, N.; Richter, H.; Jacobi, U.; Schaefer, H.; Blume-Peytavi, U.; Sterry, W. [Follicular penetration. An important pathway for topically applied substances]. *Hautarzt*, **2003**, *54*, 321-3.

[4] Lademann, J.; Otberg, N.; Richter, H.; Weigmann, H. J.; Lindemann, U.; Schaefer, H.; Sterry, W. Investigation of follicular penetration of topically applied substances. *Skin Pharmacol Appl Skin Physiol*, **2001**, *14 Suppl 1*, 17-22.

[5] Barry, B. W. Novel mechanisms and devices to enable successful transdermal drug delivery. *Eur J Pharm Sci*, **2001**, *14*, 101-14.

[6] Albery, W. J.; Hadgraft, J. Percutaneous absorption: in vivo experiments. *J Pharm Pharmacol*, **1979**, *31*, 140-7.

[7] Potts, R. O.; Guy, R. H. Predicting skin permeability. *Pharm Res*, **1992**, *9*, 663-9.

[8] Guy, R. H.; Hadgraft, J. Physicochemical aspects of percutaneous penetration and its enhancement. *Pharm Res*, **1988**, *5*, 753-8.

[9] Potts, R. O.; Guy, R. H. A predictive algorithm for skin permeability: the effects of molecular size and hydrogen bond activity. *Pharm Res*, **1995**, *12*, 1628-33.

[10] Pugh, W. J.; M.S., R.; J., H. Epidermal permeability — Penetrant structure relationships: 3. The effect of hydrogen bonding interactions and molecular size on diffusion across the stratum corneum. *Int J Pharm*, **1996**, *138*, 149-65.

[11] Williams, A. C.; Barry, B. W. Penetration enhancers. *Adv Drug Deliv Rev*, **2004**, *56*, 603-18.

[12] Barry, B. W. Lipid-Protein-Partitioning theory of skin penetration enhancement. *Journal of Controlled Release*, **1991**, *15*, 237-48.

[13] Moser, K.; Kriwet, K.; Naik, A.; Kalia, Y. N.; Guy, R. H. Passive skin penetration enhancement and its quantification in vitro. *Eur J Pharm Biopharm*, **2001**, *52*, 103-12.

[14] Suhonen, P.; Jarvinen, T.; Rytkonen, P.; Peura, P.; Urtti, A. Improved corneal pilocarpine permeability with O,O'-(1,4-xylylene) bispilocarpic acid ester double prodrugs. *Pharm Res*, **1991**, *8*, 1539-42.

[15] Menczel, E. Assessment of delipidization as an enhancing factor in percutaneous penetration. *Curr Probl Dermatol*, **1995**, *22*, 189-94.

[16] Menon, G. K.; Lee, S. H.; Roberts, M. S. *Ultrastructural effects of some solvents and vehicules on the stratum corneum and other skin components: evidence for an 'extended mosaic-partitioning model of the skin barrier'*,, Marcel Dekker: New York **1998**.

[17] Chien, Y. W.; Xu, H. L.; Chiang, C. C.; Huang, Y. C. Transdermal controlled administration of indomethacin. I. Enhancement of skin permeability. *Pharm Res*, **1988**, *5*, 103-6.

[18] Friend, D.; Catz, P.; Heller, J.; Reid, J.; Baker, R. Transdermal delivery of levonorgestrel I: Alkanols as permeation enhancers in vitro. *J Controlled Release*, **1988**, *7*, 243-50.

[19] Junginger, H. E.; Verhoef, J. C. Macromolecules as safe penetration enhancers for hydrophilic drugs – a fiction? *J Pharm Sci Technol Today*, **1998**, *1*, 370-76.

[20] Aungst, B. J. Structure/effect studies of fatty acid isomers as skin penetration enhancers and skin irritants. *Pharm Res*, **1989**, *6*, 244-7.

[21] Aungst, B. J.; Rogers, N. J.; Shefter, E. Enhancement of naloxone penetration through human skin in vitro using fatty acids, fatty alcohols, surfactants, sulfoxides and amides. *Int J Pharm* **1986**, *33*, 225-34.

[22] Friend, D.; Catz, P.; Heller, J. Simple alkyl esters as skin permeation enhancers. *J Controlled Release*, **1989**, *9*, 33-41.

[23] Sato, K.; Sugibayashi, K.; Morimoto, Y. Effect and mode of action of aliphatic esters on the in vitro skin permeation of nicorandil. *Int J Pharm*, **1988**, *43*, 31-40.

[24] Purdon, C. H.; Azzi, C. G.; Zhang, J.; Smith, E. W.; Maibach, H. I. Penetration enhancement of transdermal delivery--current permutations and limitations. *Crit Rev Ther Drug Carrier Syst*, **2004**, *21*, 97-132.

[25] Kim, N.; El-Khalili, M.; Henary, M. M.; Strekowski, L.; Michniak, B. B. Percutaneous penetration enhancement activity of aromatic S, S-dimethyliminosulfuranes. *Int J Pharm*, **1999**, *187*, 219-29.

[26] Kim, C. K.; Kim, J.-J.; Chi, S.-C.; Shim, C.-K. Effect of fatty acids and urea on the penetration of ketoprofen through rat skin. *Int J Pharm*, **1993**, *99*, 109-18.

[27] Godwin, D. A.; Player, M. R.; Sowell, J. W.; Michniak, B. B. Synthesis and investigation of urea compounds as transdermal penetration enhancers. *Int J Pharm*, **1998**, *167*, 165-75.

[28] Trommer, H.; Neubert, R. H. Overcoming the stratum corneum: the modulation of skin penetration. A review. *Skin Pharmacol Physiol*, **2006**, *19*, 106-21.

[29] Michniak, B. B.; Player, M. R.; Sowell, J. W., Sr. Synthesis and in vitro transdermal penetration enhancing activity of lactam N-acetic acid esters. *J Pharm Sci*, **1996**, *85*, 150-4.

[30] Farsa O. Potenciální akceleranty transdermální penetrace na bázi derivátů 6-aminohexanových kyselin se sekundární a terciární aminoskupinou. *Disertační práce*. Univerzita Karlova v Praze, Farmaceutická fakulta v Hradci Králové, 2000.

[31] Hrabalek, A.; Dolezal, P.; Farsa, O.; Sklubalova, Z.; Kunes, J. Esters of 6-dimethylaminohexanoic acid as skin penetration enhancers. *Pharmazie*, **2000**, *55*, 759-61.

[32] Kontturi, K.; Murtomaki, L.; Hirvonen, J.; Paronen, P.; Urtti, A. Electrochemical characterization of human skin by impedance spectroscopy: the effect of penetration enhancers. *Pharm Res*, **1993**, *10*, 381-5.

[33] Fincher, T. K.; Yoo, S. D.; Player, M. R.; Sowell, J. W., Sr.; Michniak, B. B. In vitro evaluation of a series of N-dodecanoyl-L-amino acid methyl esters as dermal penetration enhancers. *J Pharm Sci*, **1996**, *85*, 920-3.

[34] Vávrová, K.; Hrabálek, A.; Doležal, P.; Holas, T.; Zbytovská, J. L-Serine and glycine based ceramide analogues as transdermal permeation enhancers: polar head size and hydrogen bonding. *Bioorg Med Chem Lett*, **2003**, *13*, 2351-53.

[35] Hrabalek, A.; Dolezal, P.; Vavrova, K.; Zbytovska, J.; Holas, T.; Klimentova, J.; Novotny, J. Synthesis and enhancing effect of transkarbam 12 on the transdermal delivery of theophylline, clotrimazole, flobufen, and griseofulvin. *Pharm Res*, **2006**, *23*, 912-9.

[36] Klimentova, J.; Hrabalek, A.; Vavrova, K.; Holas, T.; Kroutil, A. Synthesis and transdermal penetration-enhancing activity of carbonic and carbamic acid esters--comparison with transkarbam 12. *Bioorg Med Chem Lett*, **2006**, *16*, 1981-4.

[37] Seth, B. Transdermal delivery using decyloxazolidin-2-one. *Arzneim Forsch Drug Res*, **1999**, *42*, 120-22.

[38] Barrie C. Finnin, T. M. M. Transdermal penetration enhancers: Applications, limitations, and potential. *J Pharm Sci*, **1999**, *88*, 955-58.

[39] Thong, H. Y.; Zhai, H.; Maibach, H. I. Percutaneous penetration enhancers: an overview. *Skin Pharmacol Physiol*, **2007**, *20*, 272-82.

[40] Vavrova, K.; Zbytovska, J.; Hrabalek, A. Amphiphilic Transdermal Permeation Enhancers: Structure-Activity Relationships *Curr Med Chem* **2005**, *12*, 2273-91.

2. Synthesis and Structure-Activity Relationships of Skin Ceramides

(submitted)

Jakub Novotný, Alexandr Hrabálek, Kateřina Vávrová

ABSTRACT

Ceramides are a complex group of lipids that has gained much attention as cell signaling molecules and skin barrier constituents. In the skin, these sphingolipids form a major part of the stratum corneum intercellular lipid matrix, which is the barrier for penetration of most compounds. The development of such a protective layer was a critical step in the evolution of life on a dry land. Moreover, prominent skin diseases such as psoriasis and atopic dermatitis are associated with diminished ceramide levels and may be effectively improved by exogenous ceramides or their analogues. Since ceramides are not obtained from natural sources in pure form, they are of synthetic interest since 1950's. In this review, we describe sphingosine syntheses from 1998 until 2008, and the synthetic approaches to the unique epidermal ceramides, including the 6-hydroxysphingosine-based ones, the alpha- and omega-hydroxy forms and the omega-acyloxy species. Moreover, the structural requirements of ceramides for a competent skin barrier are discussed, including acyl chain length, *trans* double bond, acyl alpha-hydroxyl, stereochemistry, omega-linoleyloxy species and ceramide conformation.

INTRODUCTION

The primary function of the skin is to protect the body from the loss of water and other physiologically important components and to prevent or limit the penetration of potential toxic compounds, allergens, irritants and microbes. The principal barrier for penetration of most compounds resides is the stratum corneum (SC), the uppermost layer of the skin, which consists of flattened dead cells, corneocytes, and intercellular lipid lamellae. The intercellular lipids are considered as the only continuous domain through the SC to be the most important pathway for the diffusion of substances into the body. This lipidic matrix is composed of an approximately equimolar mixture of ceramides, cholesterol and free fatty acids. The unusual composition of the SC lipids with high ceramide content and, particularly, their exceptional organization seems to be essential for maintaining the skin barrier function. This is supported by the observation that prominent skin diseases, such as atopic dermatitis and psoriasis, have diminished ceramide levels. On the other hand, administration of drugs across the skin is a delivery route with great potential; however, only a limited number of drug are able to cross the skin barrier to reach therapeutically active plasma levels. For recent reviews on the skin barrier formation, physiology and pathology, see [1-6].

SKIN CERAMIDE STRUCTURES

Ceramides, i.e. *N*-acylsphingosines, belong to the class of sphingolipids, which are a complex group of lipids that gained much attention as cell signaling molecules and skin barrier constituents. The role of sphingolipids in cell signaling has been covered in many recent reviews, for example [7-10]. Ceramides are among the most hydrophobic lipids in membranes, which may explain their abundance in SC. Their solubility in water is negligible. Thus, free natural long-chain ceramides cannot exist in solution in biological fluids or in cytosol. In addition, they belong to the category of non-swelling amphiphiles [11], implying

that they cannot even give rise to micelles or other aggregates in aqueous suspension, as do, for example phospholipids and short-chain ceramides [12].

Table 1. Structure and nomenclature of skin ceramides

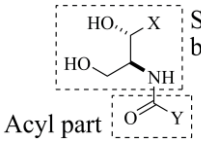	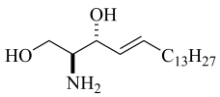 Sphingosine (S) **1**	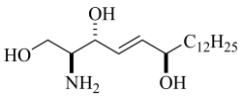 6-Hydroxy-sphingosine (H) **2**	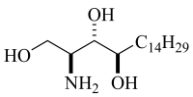 Phyto-sphingosine (P) **3**	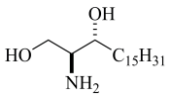 Dihydro-sphingosine (DS) **4**
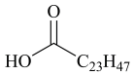 Lignoceric acid (N) **5**	Ceramide NS (Ceramide 2)	Ceramide NH (Ceramide 8)	Ceramide NP (Ceramide 3)	Ceramide NDS
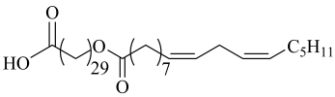 30-(Linoleyloxy)-triacontanoic acid (EO) **6**	Ceramide EOS (Ceramide 1)	Ceramide EOH (Ceramide 4)	Ceramide EOP (Ceramide 9)	
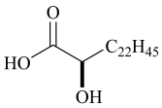 (*R*)-2-Hydroxytetracosanoic acid (A) **7**	Ceramide AS (Ceramide 5)	Ceramide AH (Ceramide 7)	Ceramide AP (Ceramide 6)	Ceramide ADS

In the human SC, eleven major ceramide subclasses have been identified (Table 1) [13]. These compounds consist of a sphingoid base – sphingosine (**1**) (designated as S), 6-hydroxysphingosine (**2**) (H), phytosphingosine (**3**) (P) or dihydrosphingosine (**4**) (DS), which is N-acylated by a long-chain saturated fatty acid (N, $C_{16\text{-}30}$, mostly lignoceric acid (**5**)), α-hydroxy acid (A, $C_{16\text{-}30}$, mostly 2-hydroxylignoceric acid (**7**)) or ω-hydroxy acid (O, $C_{28\text{-}32}$). The ω-hydroxyl is further esterified with linoleic acid (**6**) (E) or attached to carboxyl side chains on the outer surface of the corneocyte to form a monolayer of covalently bound lipids. The letters in parentheses refer to the Motta's nomenclature [14]; for example, non-hydroxy acyl sphingosine, the most abundant SC ceramide formerly known as ceramide 2, is designated ceramide NS, the phytosphingosine acylated with ω-linoleyloxy acid would be ceramide EOP, etc. For an extensive overview of the biodiversity of the sphingoid bases, both naturally occurring and synthetic, see [15].

STRUCTURE-ACTIVITY RELATIONSHIPS IN SKIN CERAMIDES

Although the physiological and pathological role of ceramides in the skin, their biosynthesis and physicochemical behavior has been widely investigated, little is known about their structure-activity relationships. In order for the epidermal lipid barrier to protect the body from external insult and internal water loss, the lipids of the SC must be highly ordered. At the same time, the lipid matrix must remain plastic enough to withstand the stress

and shear forces routinely encountered by the skin [16]. It is generally accepted, that the relatively small polar head of ceramides in contrast to phospholipids, their ability to create an extensive hydrogen bonding network, their exceptionally long saturated chains allowing for strong hydrophobic attraction and the heterogeneity in their structure are the basic prerequisites of a competent skin barrier. The available data are summarized in the following sections.

ω-Acyloxy- and ω-hydroxy ceramides

The linoleate and ω-hydroxyacid-containing ceramides are the most unusual of the SC ceramides Ceramide EOS was proved to influence dominantly the formation of the long periodicity phase and lateral lipid packing [17], which is essential for skin barrier function. It has been postulated that the ω-hydroxyacyl portion of the ceramide EOS completely spans a bilayer while the linoleate tail inserts into an adjacent bilayer, thus riveting the two together at a molecular level. In essential fatty acid deficiency, oleate replaces linoleate in ceramide EOS, and this is accompanied by a decreased barrier function [18]. While it seems likely that ceramide EOP and EOH have similar role, there are presently no data on this point. The only exception is an X-ray diffraction study on the phase behavior of synthetic lipid mixtures containing ceramide EOS and EOP. It was shown that complete substitution of ceramide EOS with EOP reduces the formation of the long periodicity phase and results in phase separation of ceramide EOP [19]. This may well be connected with smaller polar head of sphingosine ceramides allowing for a tighter chain packing, see below.

During the formation of the skin lipid barrier, linoleate is removed from a part of EO-type ceramides and recycled and the resulting ω-hydroxy ceramide becomes ester-linked through the ω-hydroxyl group to carboxyl side groups at the corneocyte surface [20-22]. These covalently bound ceramides may function as a template that provides for orientation of the initially extruded lamellar granule contents [23] and this lipid envelope is sometimes regarded as the least permeable part of the skin barrier [24]. Further details on covalently bound SC lipids can be found in [25, 26].

Recently, it has been found that the loss of very long-chain fatty acids (C_{28} and more) and ω-acyloxyceramides in the skin was incompatible with survival in desiccating environment leading to neonatal death [27].

Acyl chain length

In order to increase their aqueous solubility in various experiments, native long-chain ceramides are often replaced by synthetic derivatives with short-chain fatty acids like acetyl- or hexanoylsphingosine. However, many substantial differences between naturally occurring long-chain ceramides and their short-chain analogues were described recently (for a review, see Goñi and Alonso [28] and van Blitterswijk [29] and references therein). In the skin ceramides, the acyl chain length was found to be crucial for their barrier properties [30]. Ceramides with C_{4-8} acyl chain were able to increase skin permeability for two model drugs up to 10.8 times with maximum effect at C_6 acyl. No increase in permeability was found for ceramide analogues with C_2 and C_{12} acyl and ceramide NS. Those relationship between ceramide acyl chain length and its ability to perturb skin barrier showed striking similarity to the behavior of short-chain ceramides in sphingomyelin/phospholipid membranes [31-34] and confirmed that short-chain ceramides do not act as natural ceramides. Thus, their use as experimental tools should be cautious.

Moreover, examples of the effects of the chain length on the skin permeability of fatty acids and other amphiphiles may be found in transdermal permeation enhancers, i.e. compounds that promote transdermal drug delivery by decreasing skin barrier resistance. The most promising enhancers are believed to interact with SC ceramides; thus, their structure-activity relationships may be relevant to those of ceramides. For a review, see [35].

C4 trans double bond

The C4 *trans* double bond seems to be essential in most ceramide biological actions [36-38]. Moreover, the importance of the allylic alcohol moiety in ceramide-induced apoptosis and anticancer drugs has been widely discussed by Radin [39, 40]. In the skin, the significance of the C4 *trans* double bond has not been established to date. Due to physiological occurrence of sphingoid bases lacking this structural feature in human SC, i.e. phytosphingosine and dihydrosphingosine; it may not seem important. Moreover pseudoceramides without this double bond effectively repair skin barrier disrupted by various insults, for example L-serine ester 14S24 [41, 42]. However, the C4 *trans* double bond was found to promote tight water association through internal hydrogen bonding and closer packing of ceramides in interfaces relative to comparable dihydroceramides. Moreover, the sphingosine-based ceramides exhibited dipole potentials as much as 150-250 mV higher that the saturated species [43]. Conformational characterization of ceramides by NMR pointed to a network of cooperative hydrogen bonds that involves the NH and OH groups as well as two molecules of water. This structural motif was distorted when the *trans* double bond was absent [44]. This could contribute to ceramide phase behavior in membranes and may also be relevant to their SC packing.

Ceramides containing C4 *cis* double bond form different internal hydrogen bonding network, they insert more easily than the *trans* isomers in lipid monolayers, but they are less effective in inducing flip-flop motion (unpublished results, in [12]). Recently, long-chain dicarboxylic acids with *cis* double bond in their headgroup have been shown to increase intact skin permeability while their *trans* isomers were less active [45].

From the comparison of the sphingosine and phytosphingosine ceramides, Rerek concluded that the driving force for molecular self-assembly in the sphingosine-based ceramides is the orthorhombic chain packing, while in the phytosphingosines it appears to be headgroup hydrogen bonding [46]. The finding that phytoceramides pack less tightly than the corresponding ceramides is consistent with the monolayer study of Lofgren and Pascher [47]. Moreover, the lesser importance of hydrogen bonding in comparison to chain length of sphingosine-based ceramides for their barrier properties was shown by Novotný [30]. Thus, these two types of ceramides act by different mechanisms: the sphingosine ceramides form separate domains while ceramides NP and AP help join the mosaic domains together through H-bond connection. Acting together, a structure that is relatively water impermeable, yet flexible can result in agreement with the domain mosaic model of the skin barrier [48]. However, the role of 6-hydroxysphingosine and dihydrosphingosine remains unresolved.

α-Hydroxyl

It has been demonstrated that model SC lipid systems have quite different physical properties depending on whether they contain ceramide NS or AS [16, 49]. While both ceramide species were packed in highly ordered crystalline phases at physiological temperatures, the interactions of the headgroups were different. A transverse organization via

hydrogen bonding between ceramide NS molecules, which collapsed with the melting of the chains, was described. In contrast, strong lateral hydrogen bonding was maintained between headgroups of ceramide AS even after conformational disordering of the chains. Similar differences in hydrogen bonding between ceramide NP and AP were also described implicating that the water permeability barrier is smaller for ceramide AP compared to ceramide NP [50]. It seems that the additional hydroxyl, either in phytosphingosine or next to amide carbonyl, prevents tight association of the lipid chains via hydrophobic interactions but allows for more extensive hydrogen bonding between the headgroups.

Stereochemistry

Despite their structural diversity, sphingoid bases share a common D-*erythro* (2*S*,3*R*) amino alcohol moiety. This stereochemistry of sphingosine, isolated first in 1884 [51], was established in 1950's (reviewed in [52]). Phytosphingosine was first isolated from mushroom *Amanita muscaria* in 1911 [53] and its configuration was assigned as D-*ribo* or 2*S*,3*S*,4*R*. The 6-hydroxysphingosine, which seem to be unique to the epidermis, was identified first in 1994 [54] and its stereochemistry was assigned to 2*S*,3*R*,6*R* in 2005 [55].

The importance of ceramide stereochemistry in the skin is not known at present. Lofgren and Pascher [47] showed that acyl α-hydroxyl group in natural *R* configuration [56] promoted the condensation of ceramide monolayers to a close packed crystalline state with a small molecular area whereas the reverse effect was observed for a hydroxyl in unnatural *S* configuration. Stereoselective interaction of ephedrine enantiomers with ceramide AS monolayer was shown [57]; however, further studies with permeation of chiral drugs (see [58, 59] and references therein) and chiral permeation enhancers [59, 60] did not confirm these findings.

Ceramide conformation

Two conformations of the ceramide molecule were described: a hairpin conformation, i.e. with the two chains pointing in the same direction and a splayed chain (or extended) conformation, i.e. with the chains pointing in opposite direction [61]. During the preliminary stages of skin barrier morphogenesis the ceramide precursors, glucosylceramides, should be in the hairpin conformation [62]. During the formation of the SC lipid matrix, however, a transition of the ceramides from hairpin to extended conformation is possible. The existence of the fully extended conformation of ceramide AP in a model SC lipid system was shown by Kiselev [63]. This conformation seems to be advantageous since it allows higher cohesion of the lamellae interconnected by the ceramide chains and the absence of water-swelling hydrophilic interfaces [64]. Interestingly, the extended ceramide conformation has also been proposed as one of the mechanisms how ceramide in plasma membranes interact with proteins [65].

SYNTHESIS OF SKIN CERAMIDES

The key step in ceramide synthesis is the preparation of the sphingoid base. Ceramides are then prepared by conventional acylation including the use of succinimidyl esters, *p*-

nitrophenyl esters, carbodiimide coupling, acyl halogenides and anhydrides. The major synthetic problems are associated with surfactant-like properties of amphiphilic intermediates or low solubility at low temperatures. Moreover, the allylic hydroxyl moiety of sphingosine is prone to epimerization. The preparation of ceramides of the EO and A type is more complicated due to difficult handling of its poorly soluble parts and introduction of another chiral centre, respectively.

In this review, we will focus on the syntheses of ceramides that were not covered by earlier reports with special attention to epidermal ceramides, including the 6-hydroxysphingosine-based ones, the α- and ω-hydroxy forms and the ω-acyloxy species. The procedures for the synthesis of the most abundant sphingoid base, sphingosine, will be reported since 1998; the earlier publications were summarized by Koskinen [52] and Devant [66]. Likewise, the synthesis of phytosphingosine [67] and dihydrosphingosine (sphinganine) [68] has been carefully reviewed recently.

Synthesis of sphingoid bases of naturally occurring skin ceramides

Synthesis of sphingosine

Since sphingosine is not readily obtained from natural sources in homogeneous form, great effort has been devoted to development of a simple and low cost synthetic method, starting with the first racemic one in 1954 [69]. Due to the presence of two stereogenic centers and *trans* double bond in the target molecule, several synthetic strategies based on chiral starting compounds (in particular serine, carbohydrates or tartaric acid) or asymmetric reactions have been used. When chiral substrates are used as starting material, the characteristic *trans* double bond is often generated by Wittig reaction, Julia olefination, Horner-Wadsworth-Emmons reaction or by alkynylation of the chiral substrate and subsequent selective reduction of triple bond. Recently, methods using olefin cross-metathesis have been described, see below. Other syntheses have employed asymmetric introduction of the chiral centres, including Sharpless asymmetric epoxidation, asymmetric aldol or other stereoselective reactions. Additionally, strategies based on Diels-Alder reaction, iodolactonization, enzymatic approach etc. have been reported.

From the earlier methods reviewed by Koskinen [52] and Devant [66] we would like to mention several representative ones, which are widely applied in sphingosine synthesis for sphingolipid studies. Two characteristic methods using carbohydrate approach are the syntheses published by Schmidt and Zimmermann [70] and Kiso [71]. The sphingosine synthesis relying on the Sharpless asymmetric epoxidation are well illustrated in the work of Julina [72]. Method of Nicolaou relies on the aldol reaction of boron enolate of *N*-acyloxazolidinone with hexadecenal to construct the sphingosine carbon skeleton. The methods of Garner [73] and Herold [74] are based on alkynylation of protected serinal known as Garner aldehyde [75].

In comparison with the methods published between 1991 and 1997, asymmetric syntheses are the most abundant, followed by the preparations from serine. Monosaccharides as precursors of sphingosine partially lost their attraction for synthetic chemists but phytosphingosine became a frequent starting material. The recent syntheses are described here in chronological order.

In 1998, Kobayashi reported synthesis of sphingosine and its derivatives including sphingofungines B and F using heterocycles as chiral ligands and auxiliaries via 1,3-dioxane (**12**) as a key intermediate (Scheme 1) [76]. Trimethylsilylpropynal (**8**) and (*Z*)-2-benzyloxy-1-phenoxy-1-trimethylsiloxyethen (**9**) were used as starting compouns for tin(II) triflate and (*R*)-methyl-2-[(N-1-naphtylamino)methyl]pyrrolidone catalyzed asymmetric aldol reaction (*syn*/*anti* = 97/3, 91% ee for *syn*). Resulting phenyl ester (**10**) was reduced with DIBAL to give diol, which was protected as acetonide (**11**). Sphingosine and its derivatives were then prepared from (**11**) according to standard transformations. The removal of trimethylsilyl group was followed by alkylation and removal of benzyl group by lithium in liquid ammonia. Azide group was introduced by Sn2 process by successive treatment of alcohol by triflic anhydride/pyridine and sodium azide. The removal of acetal and reduction of azido group yielded 2-amino-1,3-hydroxy alkyne (**15**) as a second key intermediate for preparation of D-*erythro*-sphingosine (**1**), cis-sphingosine and dihydrosphingosine by various reduction procedures. D-*erythro*-sphingosine was prepared in 10 steps and 19% overall yield.

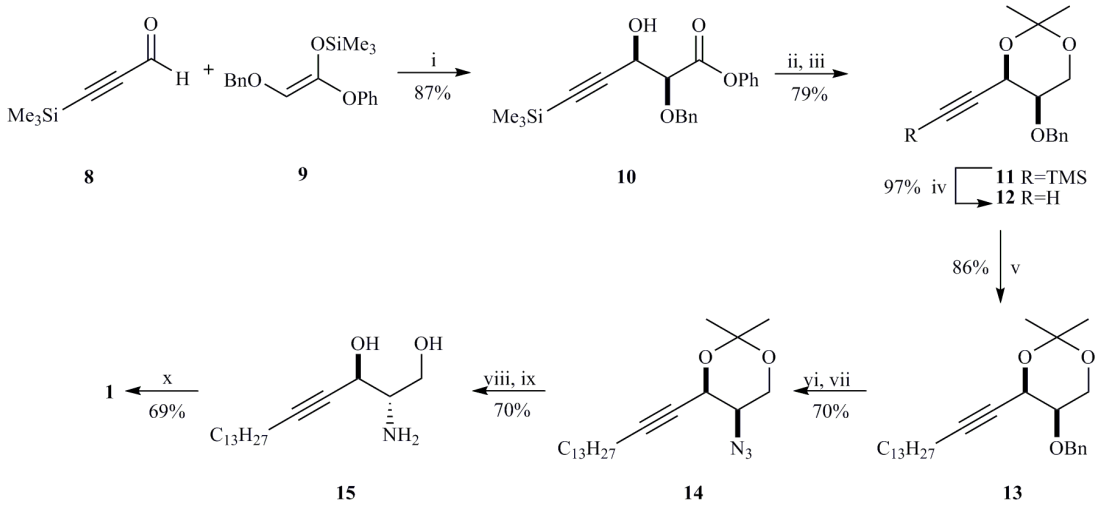

Scheme 1. Reagents and conditions: (i) $Sn(OTf)_2$/SnO/(*R*)-methyl-2-[(N-1-naphtylamino)methyl]pyrrolidone/ propionitrile; (ii) DIBAL; (iii) DMP/TsOH; (iv) Bn_4NF; (v) BuLi/$C_{13}H_{27}Br$; (vi) Li/liq. NH_3; (vii) Tf_2O/pyridine/NaN_3; (viii) AcOH-H_2O; (ix) Ph_3P/H_2O-pyridine; (x) Red-Al.

Synthesis D-*erythro*-sphingosine, L-*threo*-sphingosine and sphinganine diastereomers from commercially available *N*-Boc-L-serine methyl ester (**16**) via its biological intermediate 3-ketosphinganine (**20**) as a key synthetic intermediate was published in the same year (Scheme 2) [77]. The strategy sets the stereochemistry of the allylic hydroxyl in the last stage of the synthesis and allows attachment of diverse tails as triflate electrophiles derived from alcohols. The starting compound was protected by cyclization with DMP. Conversion to β-ketoester (**17**) with CDI and lithium allyl acetate followed a standard procedure published by Harris [78]. The subsequent alkylation of (**17**) with sodium hydride and 1-tetradecyl triflate allowed for using milder conditions than the procedure employing 1-bromotetradecane, HMPE and sodium iodide, and minimized the chances of epimerization. Deallylation and decarboxylation achieved with $Pd(PPh_3)_4$ and morpholine yielded the desired oxazolidinone derivative (**18**). The utilization of Pd[0] enabled to use mild and neutral conditions for the removal of allylic group and following decarboxylation. This was a significant improvement over the previous method using *t*-butyl ester [79]. Treatment of the 3-ketosphinganine with NaHMDS followed by TMSCl gave TMS-enol ether, which was oxidized with $Pd(OAc)_2$ to unsaturated ketone (**20**). The crude (**20**) was reduced with $NaBH_4$/$CeCl_3$ to D-*erythro*-sphingosine derivative (**21**). $CeCl_3$ suppressed conjugate reduction, which occurred in its

absence. The straightforward deprotection of sphingosine was achieved with 1M HCl. The synthesis proceeded in approximately 26% overall yield in six steps with a good stereocontrol (>91% de, >95% ee).

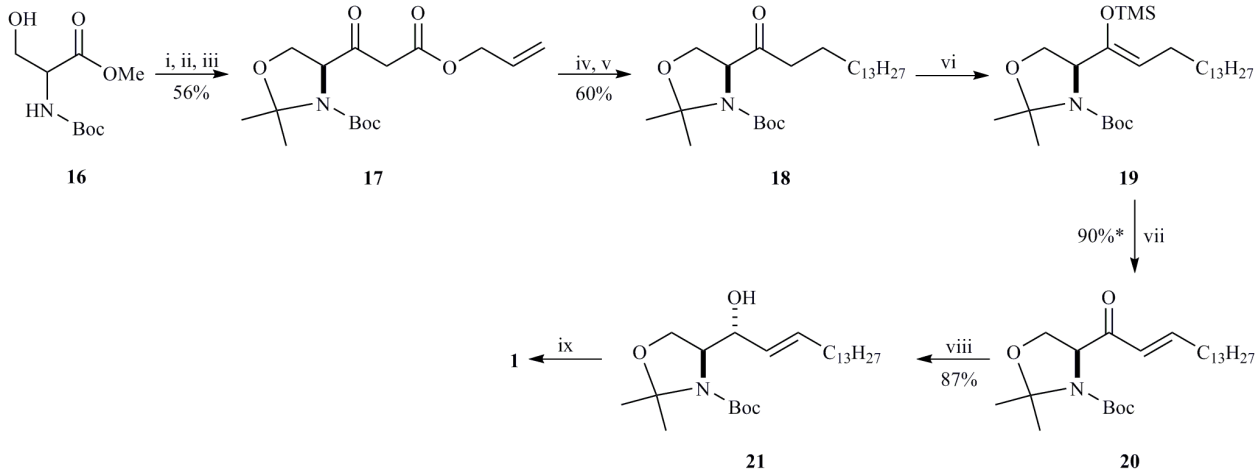

Scheme 2. Reagents and conditions: (i) DMP/TsOH; (ii) LiOH; (iii) a) CDI, (b) lithium allyl acetate; (iv) NaH/1-tetradecyl triflate; (v) $Pd(Ph_3)_4$/morpholine; (vi) a) NaHMDS, b) TMSCl; (vii) $Pd(OAc)_2/CHCN_3$; (viii) $NaBH_4/CeCl_3$; (ix) 1M HCl. * - in two steps.

An alternative approach using sulfoxide as a chiral auxiliary in the reduction of β-ketosulfoxide precursor in the syntheses of D-*erythro* and L-*threo*-sphingosine was published by Khiar (Scheme 3) [80]. β-Ketosulfoxide (**23**) was prepared by the condensation of protected L-serine methyl ester with (*R*)-(+)-methyl-4-tolyl sulfoxide carbanion (**22**) [81]. The key step in this synthetic sequence was the quantitative DIBAL reduction of compound (**23**) to β-hydroxysulfoxide (**24**) as a single isomer. Interestingly, the addition of one equivalent of $ZnCl_2$ to the reaction caused the change in the spatial arrangement of C3 hydroxyl, giving thus epimer of (**24**) also quantitatively as a single isomer. Protection of the secondary alcohol with MOMCl in the presence of NaH yielding (**25**) and subsequent one-pot Pummerer rearrangement using trifluoroacetic anhydride and $NaBH_4$ reduction led to optically pure primary alcohol (**26**). Its oxidation was followed by the Schlosser modification of Wittig olefination using tetradecyltriphenylphosphonium bromide, which afforded the protected sphingosine (**28**) as the only isomer. The deprotection with aqueous acetic and aqueous TFA resulted in the desired sphingosine. The synthesis gave D-*erythro*-sphingosine in nine steps from protected serine and may be used for preparation of other three sphingosine stereoisomers, depending on the starting material and the conditions of β-ketosulfoxide reduction. Unfortunately, the authors did not publish the yields of the Wittig olefination.

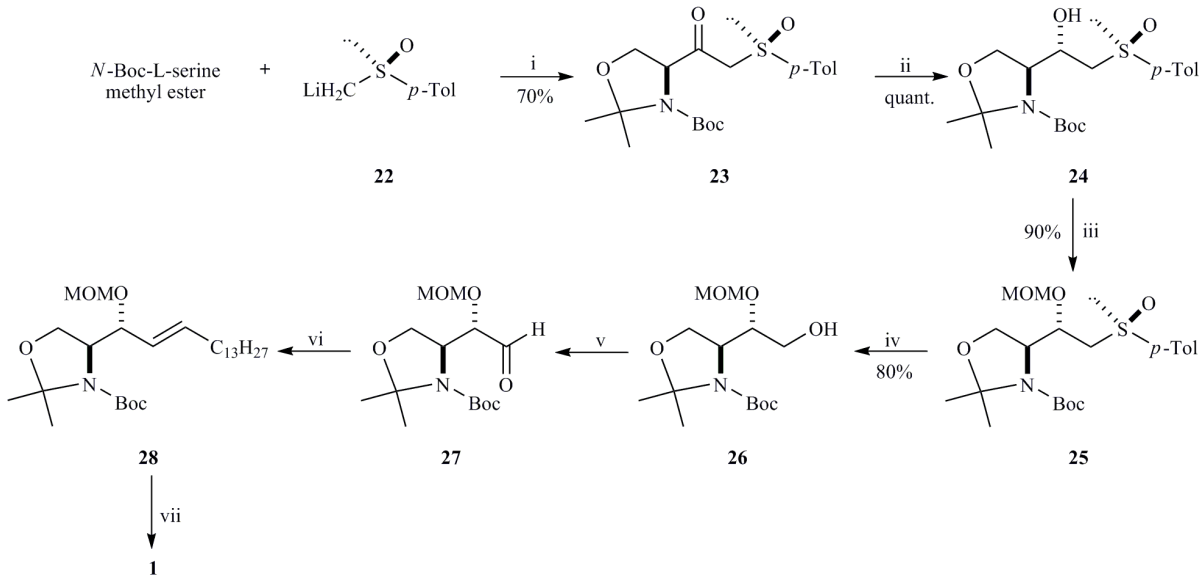

Scheme 3. Reagents and conditions: (i) Condensation; (ii) DIBAL; (iii) NaH/MOMCl; (iv) a) $(CF_3CO)_2O$/Collidine, b) $NaBH_4/H_2O$; (v) $(COCl)_2$/ Et_3N; (vi) $H_{31}C_{14}PPh_3Br$/PhLi/LiBr; (vii) a) $AcOH/H_2O$, b) TFA/H_2O.

Hertweck and Boland introduced a synthetic strategy based on α-chloroallylation of Garner aldehyde (**29**), followed by base mediated cyclization of the originating chlorohydrine (**30**) and reaction of the resulting vinyloxirane (**31**) with an organocuprate (Scheme 4) [82]. Serinal (**29**) was treated with γ-(Z)-chloroallylboranes prepared *in situ* from $^{D}Ipc_2BOME$, allylchloride and lithium dicyclohexylamide. Since the chloroallylation is largely substrate controlled, the 9-OMe-9-BBN can be used as an inexpensive alternative to the pinene-based borane with only slightly decreased diastereo- and E/Z selectivity. Nevertheless, the recrystallization of halohydrines (or epoxides obtained by their cyclization) afforded isomerically pure material. The treatment of halohydrine (**30**) with DBU furnished vinyloxirane (**30**) under mild conditions and without isomerization. The allylation/epoxidation sequence can be conducted as one pot procedure. Copper assisted Sn2 alkylation of the epoxide was achieved by its simple addition into the solution of organocuprate prepared *in situ* from CuCN and carbon nucleophile (RLi, RMgCl) with exclusive formation of *trans*-double bond (**32**). Sphingosine (**1**) can be received from (**32**) by hydrolysis with 1M HCl/THF or aqueous TFA.

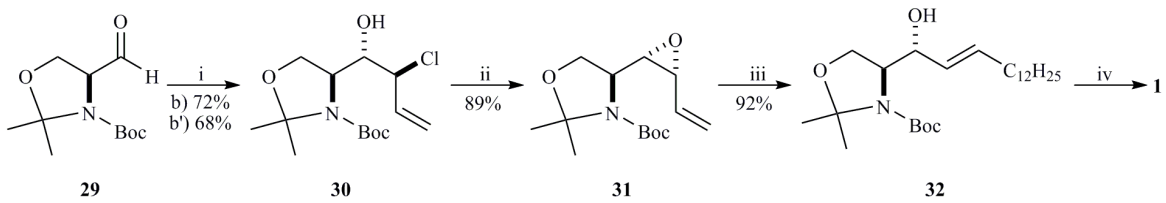

Scheme 4. Reagents and conditions: (i) a) $^{l}IpcBOMe/LiN(^{c}Hex)_2/n$-BuLi, b) 8-hydroxyquinoline or $NaHCO_3/H_2O_2$; (ii) DBU; (iii) $BrC_{12}H_{25}/t$-BuLi/CuCN; (iv) acidic hydrolysis.

Johnson presented a total synthesis of the L-*threo*-isomer of sphingosine and formal synthesis of the other three isomers employing a chemoenzymatic approach [83]. The general strategy was based on the use of enantiocomplementary hydroxynitrile lyases to yield an enantiomeric pair of starting compounds. This method yields L-*threo*-sphingosine in 14 steps

in 12% overall yield. The sequence employing hydroxynitrile lyase from *Prunus amygdalus* should allow the preparation of D-*erythro*-sphingosine as well.

He reported asymmetric synthesis of ceramide and sphingosine analogues from pentadecyne via cyclic thionocarbonate intermediate (**36**) (Scheme 5) [84]. Their strategy involved three key reactions including asymmetric dihydroxylation of an (*E*)-α,β-unsaturated ester (**34**) as the chiral induction stage, regioselective induction of the azido group at the α-position with inversion via cyclic thionocarbonate intermediate, and selective reduction of the ester. Substrate for asymmetric dihydroxylation was prepared by Horner-Wadsworth-Emmons reaction via coupling of hexadec-2-ynal with a phosphonate reagent. To the authors disappointment the optimized Sharpless conditions for dihydroxylation of enyne ester have brought the product very slowly and in a low yield, probably due to the electron deficient double bond placed between triple bond and ester function. Nevertheless, they were able to overcome the problem by addition of more osmium reagent ($K_2OsO_4.2H_2O$) and chiral ligand ($(DHDQ)_2$-PHAL or $(DHQ)_2$-PHAL) to the commercial AD-mix-β/α and thus receive (**35**) in high yield and 98% ee. Diastereoselective α-azidation of the diol ester via a cyclic sulfate was unsuccessful due to parallel oxidation of the triple bond. Direct regioselective Mitsunobu monoazidation also furnished unwanted β-azido ester. Finally, α-azido ester (**37**) was prepared via cyclic thionocarbonate intermediate by reaction with thiophosgene in the presence of DMAP. The ring opening of the crude was achieved by NaN_3. Although the monoazidation (**36**) was achieved in high yield, only poor degree of regioselectivity (α/β 2.4:1) was encountered. The simultaneous reduction of ester and azido group together with triple bond was performed using $LiAlH_4$. The final product was obtained in five steps and 25% overall yield.

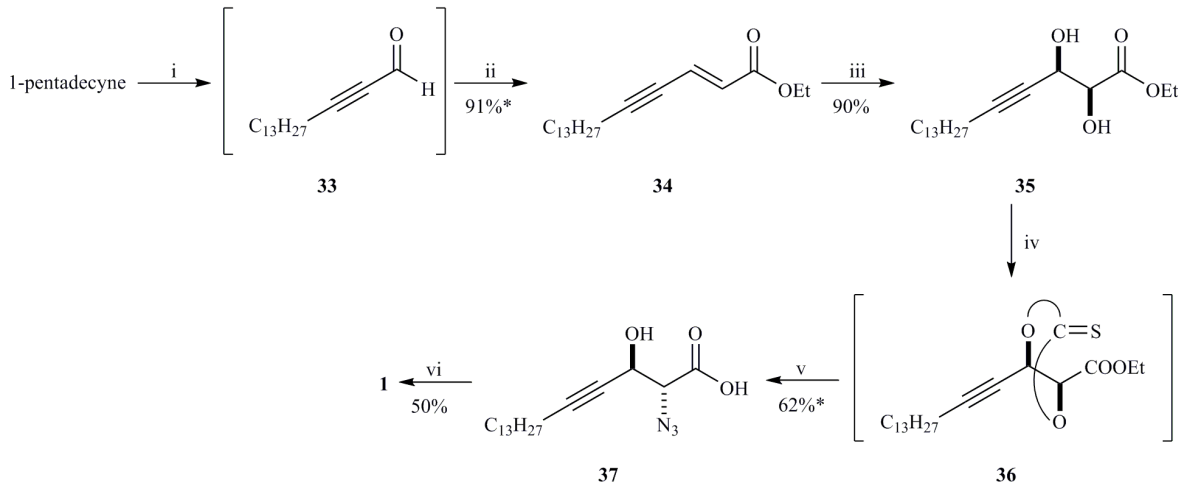

Scheme 5. Reagents and conditions: (i) *n*-BuLi/1-formylpiperidine; (ii) $(i\text{-PrO})_2P(O)CH_2CO_2Et/LiBr/Et_3N$; (iii) AD mix β, $CH_3SO_2NH_2$; (iv) Cl_2CS/pyridine/DMAP; (v) NaN_3/PPTS; (vi) $LiAlH_4$.

Chiral β-lactam (**38**) obtained from D-(-)-tartaric acid [85], was used as a basic building block for the synthesis of sphingosine and phytosphingosine in the work of Nakamura (Scheme 6) [86]. First, the ester group was reduced to alcohol and protected as triisopropylsilyl ether. The lactam nitrogen was protected by di-*t*-butyl dicarbonate to yield compound (**40**). The alkylation of the lactam (**40**) with carbanion of n-tetradecyl-*p*-toluensulfone yielded a mixture of diastereomers of (**41**). Elimination of *p*-toluensulfonyl moiety with lithium naphthalenide and subsequent deprotonation and sulfonylation with *N*-phenyltrifluoromethanesulfonimide afforded *Z*-enoltriflate (**42**) exclusively. The reductive elimination of triflate group by formic acid and Et_3N using palladium catalyst and the successive deprotection of the remaining silyl groups by tetrabutylammonium fluoride yielded in *E*-olefin (**43**). The Boc-derivative can be easily converted into sphingosine by deprotection according to known methods. The authors claim approximately 35% yield in six steps. However, the practical use of this synthesis is hampered by the use of commercially unavailable starting material.

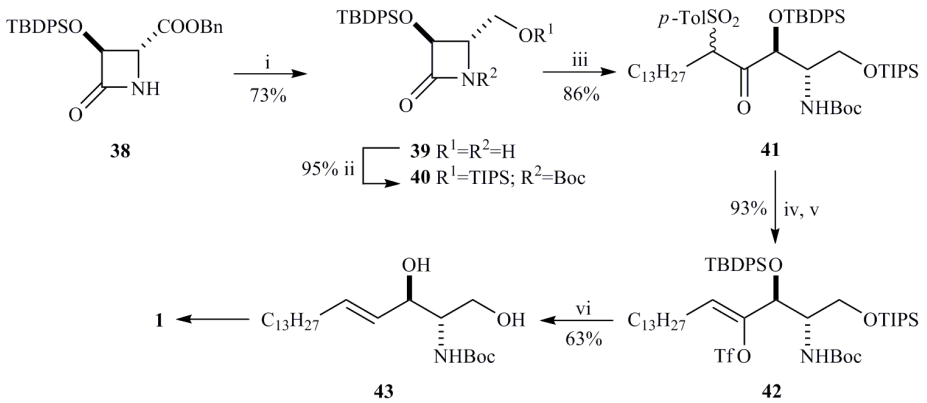

Scheme 6. Reagents and conditions: (i) $NaBH_4$/EtOH; (ii) a) TIPSCl/imidazole, b) $(Boc)_2O/Et_3N$/DMAP; (iii) *p*-Tol-SO_2-$C_{13}H_{27}$/*n*-BuLi; (iv) lithium naphthalenide; (v) $KN(SiMe_3)_2/(CF_3SO_2)_2NPh$; (vi) a) HCOOH/ $Pd(OAc)_2(PPh_3)_2/Et_3N$, b) *n*-Bu_4NF.

The total sphingosine synthesis from D-galactose via an azidosphingosine using Wittig olefination, and determination of its optical purity by new method using Mosher's acid was presented by Duclos [87]. The synthesis is rather a combination of previously published sequences, e.g. [70, 71], but it resolves their discrepancies in synthetic procedures and characterizations.

Milne reported synthesis of sphingosine from D-xylose via 1,2-metallate rearrangement of higher order cuprate (Scheme 7) [88]. The crucial α-lithiated glycal intermediate (**46**) may be prepared by two different ways. The shorter one used 1-thio-β-D-xylopyranoside, protected as its tris(*t*-butyldimethylsilyl) ether (**44**), which was oxidized to the corresponding sulfoxide. β-Elimination of TBSOLi with LDA gave stable α-phenylsulfinyl glycal (**45**). Its reaction with *t*-BuLi resulted in phenylsulfinyl-lithium exchange and generation of α-lithiated glycal (**46**). The reaction of the glycal with $CuBr.SMe_2$ and *n*-tridecyllithium caused a 1,2-metallate rearrangement of higher order cuprate (**47**) connected with inversion of configuration and O-C-O silicon shuttle. The 1,3-diol (**49**) was protected as its benzylidene acetal derivative and the remaining *O*-TBS group was cleaved with Bu_4NF to yield compound (**50**). The *C*-TBS group was transferred back to oxygen by Brooks rearrangement and resulting mixture of alcohol and its *O*-TBS ether was treated with Bu_4NF again, giving the alcohol (**51**) only. Mitsunobu reaction with diphenylphosphoryl azide afforded inverted azide (**52**), which was reduced with zinc and ammonium chloride to give sphingosine. The synthesis

is very interesting from a chemical point of view but it consists of 12 steps and gives sphingosine in a poor overall yield (9-12% from D-xylose).

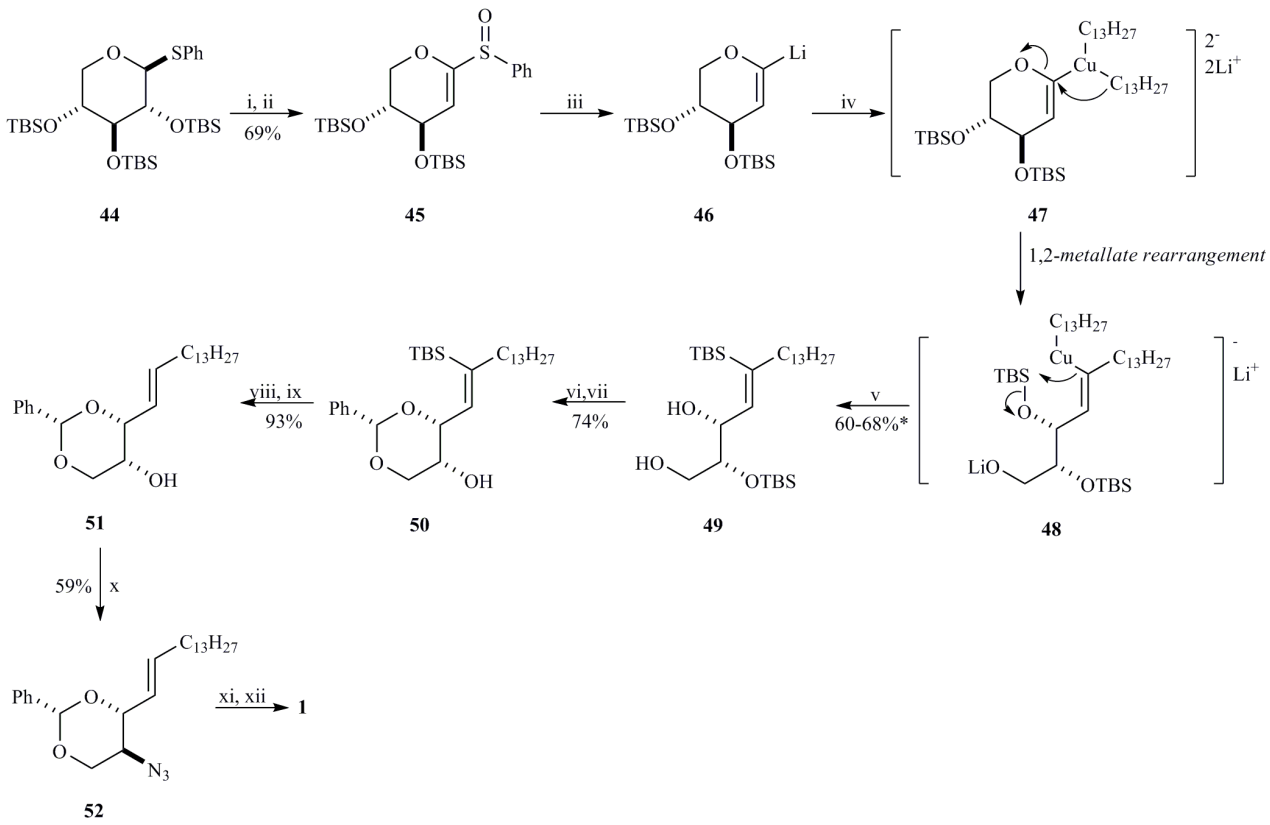

Scheme 7. Reagents and conditions: (i) $H_2O_2/(NH_4)_2MoO_4$; (ii) LDA; (iii) *t*-BuLi; (iv) $C_{13}H_{27}Li/CuBr.SMe_2/Et_2O\text{-}SMe_2$; (v) H_2O; (vi) $PhCH(OMe)_2$/*p*-TsOH; (vii) Bu_4NF; (viii) NaH/15-crown-5; (ix) Bu_4NF; (x) diphenylphosphoryl azide/DIAD/Ph_3P; (xi) *p*-TsOH; (xii) Zn/NH_4Cl. * - from (**47**).

Lee described convenient, stereoselective synthesis of all four diastereoisomers of sphingosine from L-serine methyl ester (Scheme 8) [89]. Protected L-serine methylester (**53**) was quantitatively converted to β-ketophosphonate (**54**) by treatment with excess lithium dimethyl methylphosphonate. The Horner-Wadsworth-Emmons olefination with tetradecylaldehyde under Masamune conditions provided the corresponding enone (**55**), which was deprotected to give 3-ketosphingosine hydrochloride (**56**). The chelation-controlled reduction of free amino enone, presumably via a cyclic Felkin-Anh transition state, gave D-*erytro*-sphingosine in satisfactory 90% *de*. Sphingosine was obtained by this practical synthetic route in 51% overall yield in six steps. Similar procedure using serine-derived β-ketophosphonates was also described previously by Koskinen [52].

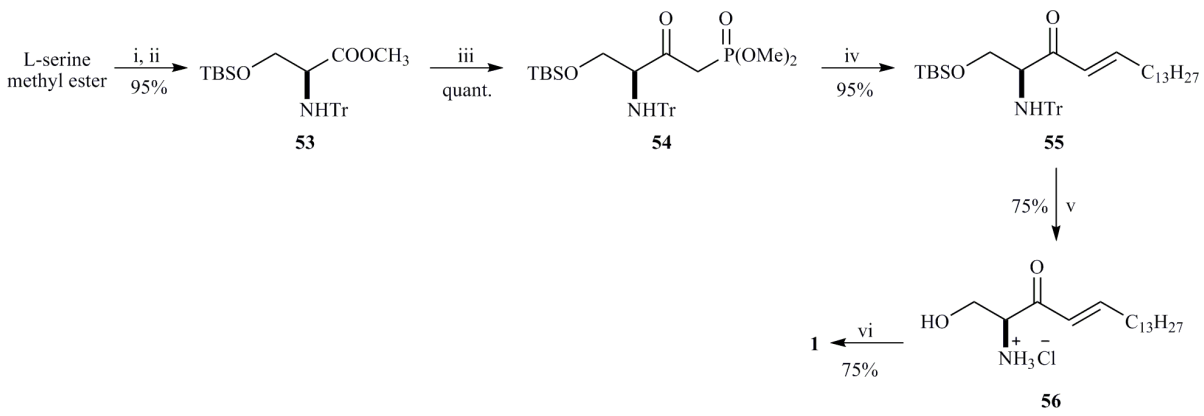

Scheme 8. Reagents and conditions: (i) $TBSCl/Et_3N$; (ii) $TrCl/Et_3N$; (iii) $LiCH_2PO(OMe)_2$; (iv) $C_{13}H_{27}CHO/DBU/LiCl$; (v) 2M HCl; (vi) $Zn(BH_4)_2$.

The experience with the preparation of *syn*- and *anti*-β-amino alcohols accessible through electrophile-promoted intramolecular amidation of allylic and homoallylic trichloroacetimidates was used by Kang for the establishing of D-*erythro*-sphingosine and D-*ribo*-phytosphingosine synthetic route [90] (Scheme 9). The disilylation of the starting triol (**57**) was followed by chemoselective monodesilylation and monoimidate formation in the presence of Cl_3CCN, sodium hydride and *n*-Bu_4NF. Iodoamidation of the resulting silyloxy homoallylic imidate by IBr afforded dihydro-1,3-oxazine (**58**). The eliminative reduction of the iodohydrine functionality, hydrolysis of the alkene and protection of the amino group furnished dihydroxycarbamate (**59**). The ozonolysis of the olefinic bond, formation of 1,3-dioxane and subsequent Swern oxidation of primary hydroxyl group provided a substrate for the attachment of the aliphatic chain by Julia olefination. Unfortunately, the alkene (**61**) was formed with rather poor stereoselectivity as 2.8:1 mixture of *trans*- and *cis*-isomer. D-*erythro*-sphingosine (**1**) was received from trans-alkene after its chromatographic isolation and acidic hydrolysis of the benzylidene ring. The procedure provides sphingosine in 21% overall yield.

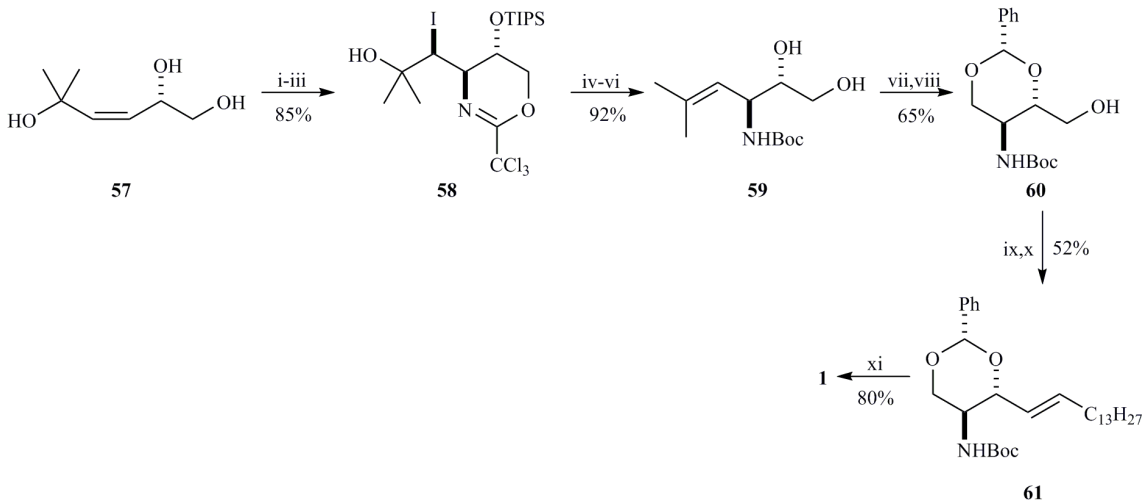

Scheme 9. Reagents and conditions: (i) $TIPSOTf/Et_3N$; (ii) a) Cl_3CCN/NaH, b) *n*-Bu_4NF; (iii) IBr/K_2CO_3; (iv) a) $(CF_3CO)_2O/Et_3N$, b) NaI; (v) 6N HCl; (vi) Boc_2O/K_2CO_3; (vii) a) O_3, b) $NaBH_4$; (viii) *p*-TsOH/PhCHO; (ix) Swern oxid.; (x) 1-phenyl-5-(tetradecylsulfonyl)-1*H*-tetrazole/ KHMDS; (xi) CF_3COOH.

Olofsson and Somfai published an asymmetric, divergent route from a common starting material, vinyl epoxide, toward all possible regio- and stereoisomers of sphingosine (Scheme

10) [91]. The starting dienol was prepared from 1-tetradecanol by modified Horner-Emmons reaction and reduction of crude ester (**62**) with DIBAL, and protected as its benzyl ether (**63**). Though Shi's epoxidation on protected dienols proceeds on the most electron-rich double bond, 2,3- (**64**) and 4,5-epoxides were formed in equimolar ratios, probably due to the lipid chain shielding of 4,5-double bond. As the vinyl epoxides are unstable on silica, their mixture was subjected to stereoselective ring opening (>20:1) in the presence of ammonium hydroxide. Because only the 2,3 isomer reacts under the described reaction conditions, resulting *anti*-amino alcohol (**65**) and unreacted epoxide isomer were separated on silica. The authors continued the synthesis by regioselective ring opening of *N*-H vinylaziridine (**66**), which was obtained from *anti*-amino alcohol (**65**) by ring closure under Mitsunobu conditions. The crude aziridine was treated with TFA and amino alcohol (**67**) was obtained with high diastereo- and regioselectivity (>20:1). Sphingosine was obtained by removal of the benzyl group with sodium in liquid ammonia in less than 16% overall yield.

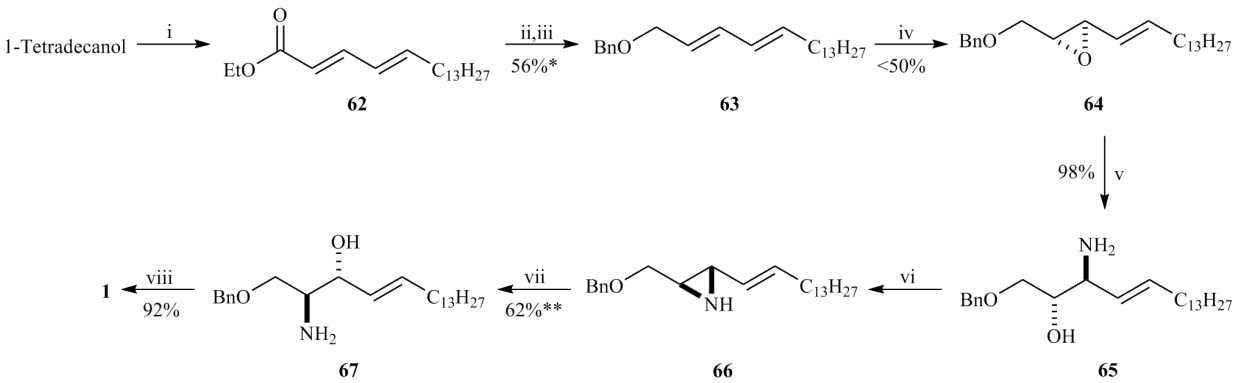

Scheme 10. Reagents and conditions: (i) a) IBX, b) triethyl phosphonocrotonate/LiOH; (ii) DIBAL; (iii) BnBr/NaH/Bu_4NI; (iv) Shi's reagent/Oxone; (v) NH_4OH/THF; (vi) DIAD/PhP_3; (vii) TFA; (viii) Na/NH_3. * - from 1-tetradecanol. ** - two steps.

An elegant and short three-step synthesis of sphingosine and C10 sphingosine from protected L-serine methyl ester (**68**) involving β-ketosulfoxide or sulfone intermediates was published recently (Scheme 11) [92]. Alkyl phenyl sulfoxide was prepared in high yield by the reaction of thiophenol with *n*-alkyl bromides and subsequent treatment of the resulting sulfide with MCPBA. Nucleophilic addition of the sulfoxide anion to the L-serine ester (**68**) afforded sulfoxide intermediate (**69**). Its overnight heating in tetrachloromethane gave the desired enone (**70**). A lower yield of the long-chain derivative in comparison with the short-chain one was observed. The requisite configuration at C(3) was reached by diastereoselective reduction of (**70** by $NaBH_4$ with addition of $CeCl_3$. Regrettably, the authors did not report diastereoselective excess of this reaction. Hydrolysis of alcohol (**71**) provided D-*erythro*-sphingosine in three steps and 26% overall yield from the starting ester. Another method of sphingosine synthesis described in the same article was based on sulfone derivatives of L-serine [92]. Since the reaction of pentadecyl phenyl sulfone with L-serine ester (**68**) produced low yields, the sulfone intermediate (**75**) was acquired by reaction with aldehyde (**73**) and subsequent oxidation of secondary hydroxyl. The intermediate β-ketosulfon (**75**) can also be received from ester (**68**) by reaction with methyl phenyl sulfone and alkylation with tetradecyl iodide. Desulfonylation of (**75**) was done by aluminum amalgam. The ketone (**76**) was selectively reduced to enone (**70**) according to Hoffman [77]. The synthesis was finished as described above.

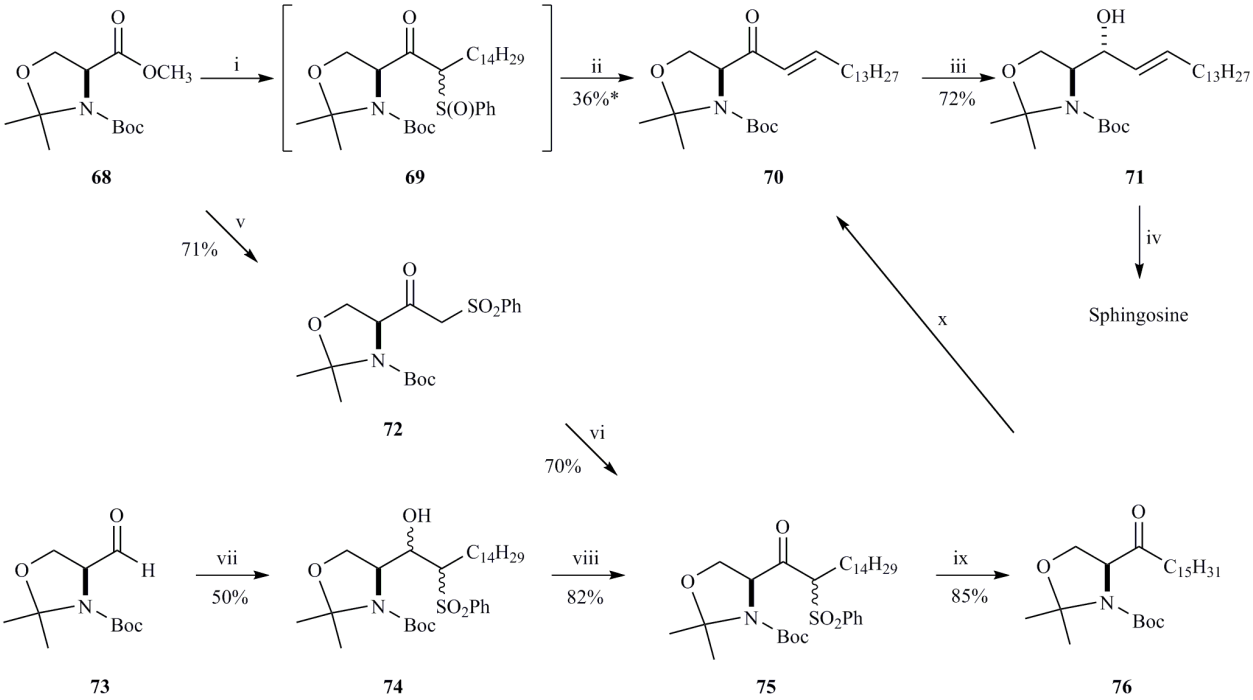

Scheme 11. Reagents and conditions: (i) LDA/PhS(O)$C_{14}H_{29}$; (ii) CCl_4; (iii) $NaBH_4/CeCl_3$; (iv) 1M HCl; (v) $MeSO_2Ph$/*n*-BuLi; (vi) DBU/$C_{14}H_{29}I$; (vii) $C_{15}H_{31}SO_2Ph$/*n*-BuLi; (viii) PCC; (ix) Al(Hg); (x) see scheme 2 [77]. * - from (**68**).

Phytosphingosine, as a relatively inexpensive and commercially available sphingoid base with both sphingosine chiral centers established, was used for synthesis of sphingosine in 2002 [93]. The authors utilized the introduction of the requisite *E*-alkene moiety by two different ways. First strategy dealt with transformation of protected 4-oxo derivative with a high degree of stereoselectivity (Scheme 12), as showed previously by Nakamura [86]. Commencing with phytosphingosine (**3**), amino group and 1,3 hydroxy groups had to be protected. The amino group was protected by treatment with di-*t*-butyl dicarbonate. In order to avoid an inseparable mixture caused by protection of 1 and 3 hydroxyl with benzylidene group, the regioselective protection was accomplished by silylation with di-*t*-butyl silyl ditriflate. The oxidation of protected phytosphingosine derivative (**78**) to 4-ketone (**79**) and its *in situ* conversion into enolate was followed by sulfonylation with *N*-phenyl-bis(trifluoromethanesulfonimide) furnishing *Z*-enol triflate (**80**). The regiospecific reductive elimination of the enol triflate function, desilylation and acidolysis of *N*-Boc moiety led to sphingosine in 58% overall yield.

Second approach was based upon the procedure published by Wild [94], which envisaged the conversion of protected 2-azido-4-nitrophenylsulfonate derivative into azidosphingosine (Scheme 13). Phytosphingosine was subjected to Wong's diazo transfer to furnish azido derivative (**83**), which was silylated to protect 1,3-hydroxy groups. Disappointingly, the nitrophenylsulfonylation under Schmid's conditions led to intractable mixture of products. In contrast, nosylation with *in situ* prepared mixed anhydride provided nitrophenylsulfonyl derivative in a high yield. However, the elimination of the product led to (**85**) in unsatisfactory yield. Surprisingly, the triflation of alcohol (**84**) with triflic anhydride in the presence of pyridine gave directly the *E*-olefin (**85**), instead of expected triflate ester. The following Staudinger reduction and desilylation afforded sphingosine in 58% overall yield.

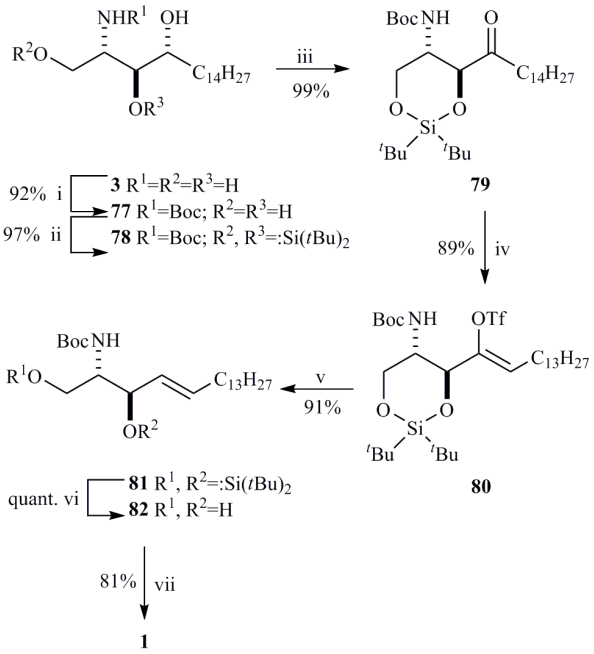

Scheme 12. Reagents and conditions: (i) Boc_2O/Et_3N; (ii) $(t\text{-}Bu)_2Si(OTf)_2$/pyridine; (iii) $(Ac)_2O$; (iv) KHMDS/N-phenyl-bis(trifluoromethanesulfonimide); (v) $Pd(OAc)_2(PhP_3)_2/HCOOH/Et_3N$; (vi) $n\text{-}Bu_4NF$/AcOH; (vii) TFA.

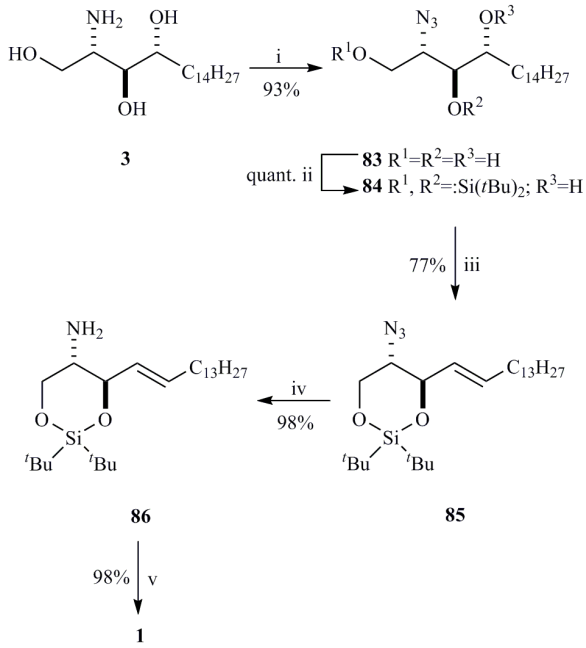

Scheme 13. Reagens and conditions: (i) $TfN_3/K_2CO_3/CuSO_4$; (ii) $(t\text{-}Bu)_2Si(OTf)_2$/pyridine; (iii) Tf_2O/ pyridine; (iv) Me_3P; (v) $n\text{-}Bu_4NF$/AcOH.

The same authors succeeded in the development of even more economical approach based on phytosphingosine as a starting material, trying to avoid the use of expensive chemicals (Scheme 14) [95]. 1,2-aminoalcohol moiety of phytosphingosine was protected in one step as 2-phenyl-1,3-oxazoline derivative (**87**) with ethyl benzimidate hydrochloride. The key events of the procedure were the stereospecific transformation of the vicinal diol into oxirane derivative (**89**) followed by regio- and stereoselective transformation of the epoxide into allylic hydroxyl functionality of sphingosine. After the failure of the oxirane formation by the methods reviewed by Kolb and Sharpless [96] (decomposition of the starting material) and Szejas phase transfer epoxidation [97] (inseparable diastereomeric mixture), the conversion of (**87**) into (**89**) was finally achieved by tosylation of vicinal diol and treatment with potassium *t*-butoxide in methanol. The regioselective eliminative opening of oxirane using TMSI and DBN led to a high yield formation of *E*-allyl silyl ether (**90**). Acidic deprotection of trimethylsilyl and phenyloxazoline protecting groups followed by base hydrolysis of *in situ* formed 1-*O*-benzoate sphingosine furnished (**1**). It is worth to note that this two pot multigram synthesis can be accomplished under mild conditions and with a minimal number of column chromatography purifications in an overall yield of 70%.

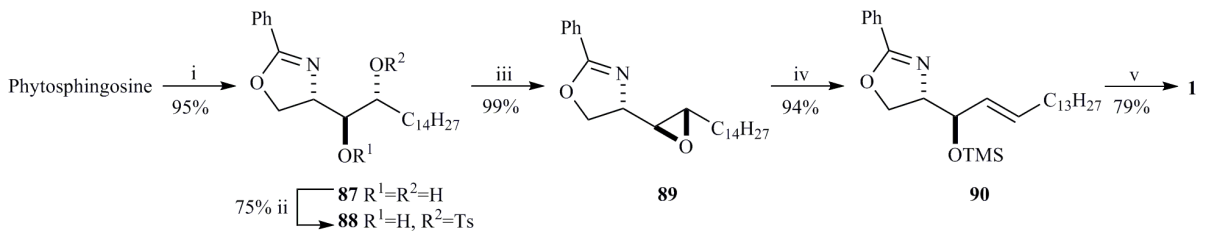

Scheme 14. Reagents and conditions: (i) ethyl benzimidate hydrochloride; (ii) TsCl/pyridineDMAP; (iii) *t*-BuOK; (iv) TMSI/DBN; (v) a) 2N HCl, b) NaOH/MeOH.

Raghavan and Rajender described a procedure using β-hydroxy-γ,δ-unsaturated sulfoxide for the synthesis of L-*erythro*-sphingosine [98]. The stereochemistry of the polar head was established by transformation of the double bond into bromohydrine which utilizes the sulfinyl moiety as an intramolecular nucleophile. The sequence continues with conversion of bromodiol into epoxide and its regio- and stereoselective opening to azidodiol according to Sharpless protocol. The aliphatic chain was introduced by the Pummerer ene reaction. The authors claim the preparation to be flexible and permit the synthesis of D-*erythro*-sphingosine by following an identical reaction sequence. The synthesis is relatively inovative, but complicated with rather low overall yield and with commercially unavailable starting material.

The first synthesis employing *E*-selective cross metathesis for the formation of double bond and connection of aliphatic chain appeared in 2004 (Scheme 15) [99]. The polar head spatial arrangement was introduced via a stereoselective epoxide opening. Dienol (**91**) was transformed by Sharpless epoxidation and base induced Payne rearrangement to vinyl epoxide (**92**) (>99% ee) [100]. To circumvent the preferential ring opening at the allylic position, the alcohol was converted to benzyl carbamate (**93**). Carbamate, as a nitrogen nucleophile, provided regioselective attack at C2 position in the presence of NaHMDS causing intramolecular ring opening and thus giving oxazolidinone (**94**). Protected sphingosine derivative (**95**) was synthesized in 17:1 *E*/*Z* selectivity by coupling allylic alcohol with 1-pentadecene using Grubbs' phosphine-free ruthenium catalyst C. The benzyl group was removed with sodium in liquid ammonia and resulting oxazolidinone was then hydrolyzed with KOH to afford (**1**). Sphingosine was obtained in 51% overall yield over five steps from (**92**). The introduction of the aliphatic chain in the later phase of the synthesis enables to avoid problems with surfactant like properties of amphiphilic intermediates e.g. aggregation of the material on silica during the purification or low solubility at low temperatures. Another advantage lies in the low formation of byproducts during the cross metathesis process and the possibility to introduce different aliphatic chains. Unfortunately, the commercially available catalysts are relatively costly.

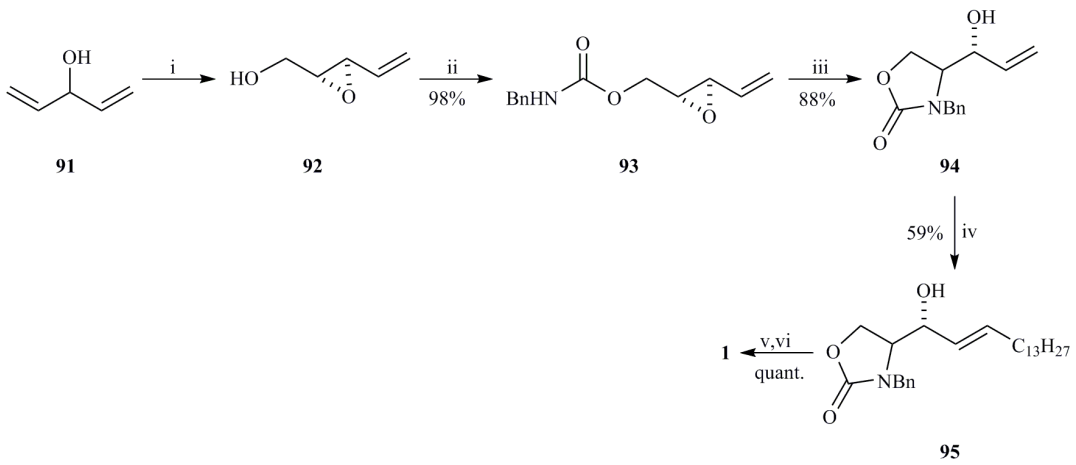

Scheme 15. Reagents and conditions: (i) Ref [100]; (ii) BnNCO/Et_3N; (iii) NaHMDS; (iv) 1-pentadecene/ Grubbs' catalyst C; (v) Na/NH_3; (vi) 1M KOH.

Rai and Basu described the preparation of glycosphingolipids and differentially protected building blocks starting with diethyl tartrate and mesylate diol (Scheme 16), respectively [101, 102]. Assembling of the *E*-double bond provided intermediates of natural ceramides. Mesylate diol (**96**), requisite for the latter, improved synthesis, was prepared in five steps without chromatographic purification following a patented procedure [103]. The primary alcohol was protected as silyl ether. Protection of the secondary alcohol was followed by azide displacement of the sulfonate to receive (**98**). Because its cross-metathesis suffered from low yields and undesirable side reactions, probably due to the interaction of the phosphine ligands with the azide group and/or metal-mediated nitrene process, the azido group was reduced to amine and protected as an Fmoc carbamate. The orthogonally protected alkene (**99**) was obtained in 21% yield from the diol (**96**). Reaction of (**99**) with 1-pentadecene catalyzed by Grubbs' catalyst A delivered protected sphingosine (**100**) as a precursor for the synthesis of glycosphingolipids.

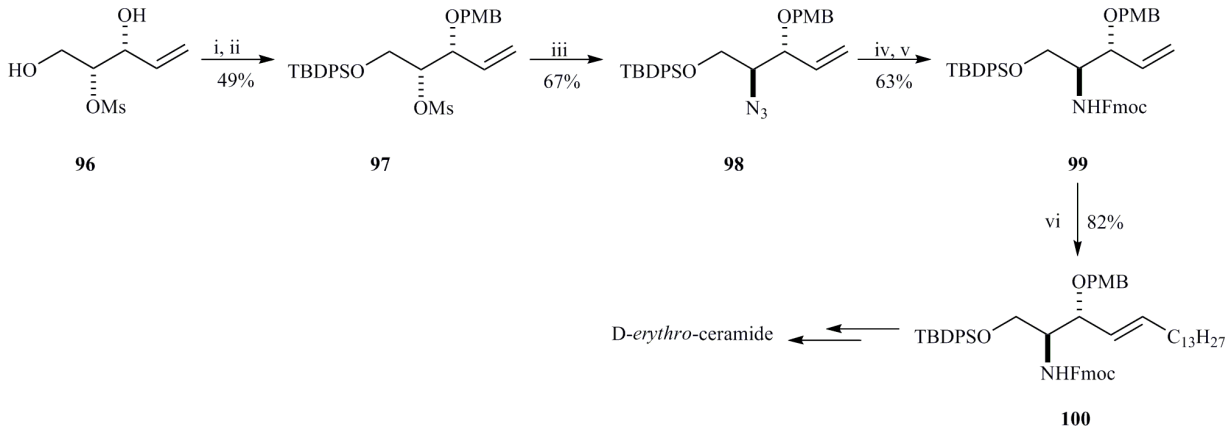

Scheme 16. Reagents and conditions: (i) *t*-BuPh2SiCl/imidazole; (ii) *p*-MeO-benzyl trichloroacetimidate/La$(OTf)_3$; (iii) a) NaN_3/Bu_4NCl, b) TBDPSCl/imidazole; (iv) Zn/NH_4Cl; (v) Fmoc-Cl/Hunig's base; (vi) Grubbs' cat. A/1-pentadecene.

The synthesis of sphingosine by the sequence including Horner-Wadsworth-Emmons olefination and copper-mediated Grignard coupling was described by Lu (Scheme 17) [104]. Pentylidene-protected D-threitol derivative (**101**) was used as a starting material due to its lower acid sensitivity than the corresponding isopropylidene acetal. Its oxidation to aldehyde (**102**) was followed by formation of double bond with diisopropyl (ethoxycarbonylmethyl)phosphonate and conversion of the resulting ester (**103**) to allylic acetate (**105**) via alcohol (**104**). Regioselective coupling of (**105**) with dodecylmagnesium bromide afforded intermediate (**107**) exclusively. The conversion of secondary hydroxyl group to an azido group after deprotection was achieved with DIAD, triphenylphosphine and trimethylsilylazide. Resulting *O*-silyl ether was hydrolyzed by tetrabutylammonium fluoride. The reduction of azide (**108**) was accomplished by Staudinger reaction and benzyl group was removed by Birch reduction to give (**1**) in nine steps and 17% yield from (**101**).

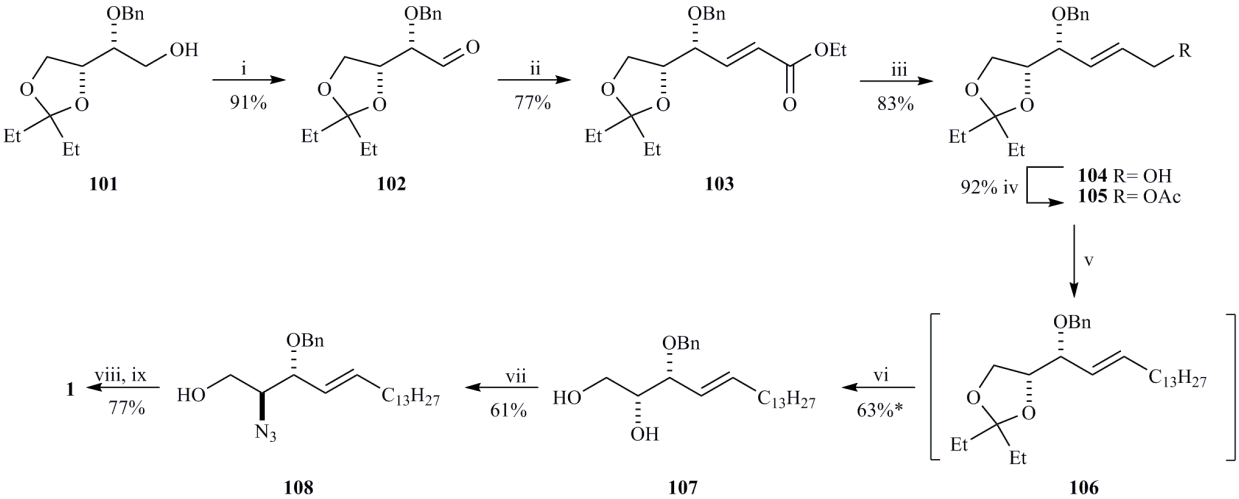

Scheme 17. Reagents and conditions: (i) PCC/NaOAc; (ii) $(i\text{-PrO})_2P(O)CH_2CO_2Et/Et_3N/LiBr$; (iii) DIBAL; (iv) $AcCl/i\text{-}Pr_2NEt$; (v) $C_{12}H_{25}MgBr/Li_2CuCl_4$; (vi) 5% H_2SO_4; (vii) a) $PPh_3/DIAD/TMSN_3$, b) $n\text{-}Bu_4NF$; (viii) PPh_3/H_2O; (ix) Na/NH_3.

Disadee and Ishikawa utilized alkenyl aziridines as key intermediates in the preparation of D-*erythro*-sphingosine (Scheme 18) [105]. Treatment of (*S*,*S*)-guanidinium salt (**109**) with (*E*)-hexadec-2-enal in the presence of TMG yielded in the formation of *cis*- and *trans*-isomers with a good combined yield and enantioselectivity. The ring opening of *trans*-isomer (**111**) and methanolysis of acetyl derivative (**113**) produced allylic alcohol (**114**) (Scheme 17). The protection of hydroxyl as a silyl ether was followed by reduction of carboxyl group with lithium aluminium hydride. (**116**) was converted to oxazolidinone (**117**) and the subsequent debenzylation was carried out under Birch conditions affording *N*-deprotected oxazolidinone as a substrate for further removal of TIPS function and alkaline hydrolysis. Sphingosine was thus received in eight steps and 62% overall yield starting with *trans*-aziridine (**111**). Similarly, *cis*-aziridine derivative (**112**) was used for the synthesis of sphingosine with aziridine ring opening as a crucial step (Scheme not shown). The required configuration of sphingosine was achieved by inversion of stereochemistry at C3 and the desired product was obtained in 27% overall yield in eight steps from (**112**).

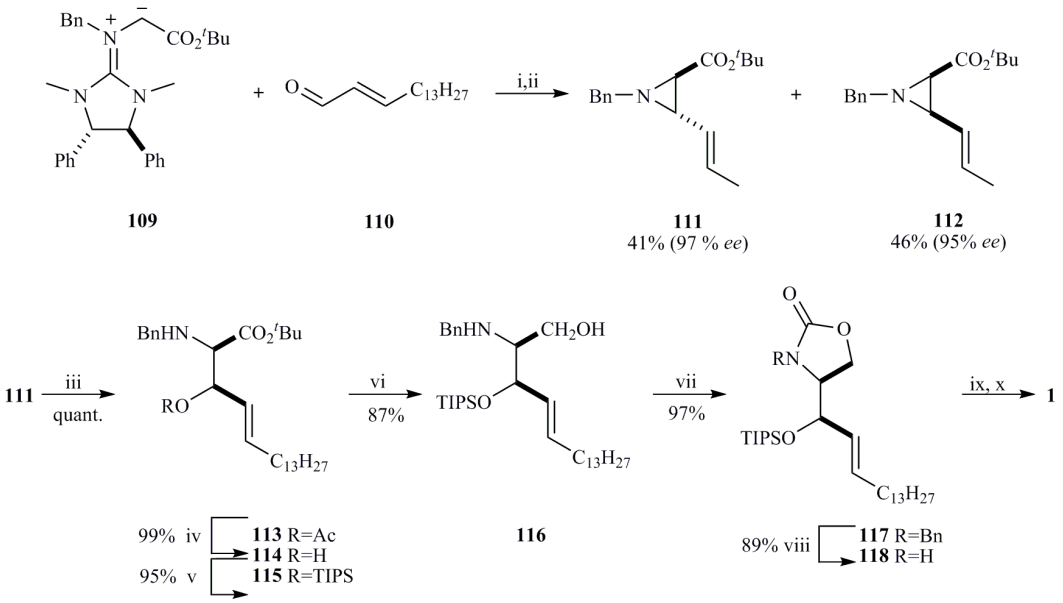

Scheme 18. Reagents and conditions: (i) TMG/THF; (ii) $SiO_2/CHCl_3$; (iii) AcOH; (iv) KOH/THF/MeOH; (v) $TIPSOTf/Et_3N/CH_2Cl_2$; (vi) $LiAlH_4$/THF; (vii)CDI/CH_2Cl_2; (viii) Li/liq. NH_3/Et_2O; (ix) *n*-Bu_4NF/THF; (x) 2M NaOH/EtOH.

Another sequence exploiting olefin cross metathesis used a D-glucose-derived building block as the source of chirality for the synthesis of D-*erythro*- and D-*threo*-sphingosine(Scheme 19) [106]. The requisite azido-carbohydrate (**119**) was synthesized according to Gruner [107]. Despite the supposed failure of cross-metathesis olefination due to the presence of azide functionality, the authors succeeded in coupling of the sugar derivative and pentadecene in the presence of Grubbs' catalyst B. The cross-coupled product (**120**) was treated with TFA to afford an anomeric mixture of hemiacetal (**121**) that on sodium periodate cleavage and subsequent reduction afforded D-*erythro*-sphingosine. This strategy provides the product in nine steps and 52% overall yield from D-glucose.

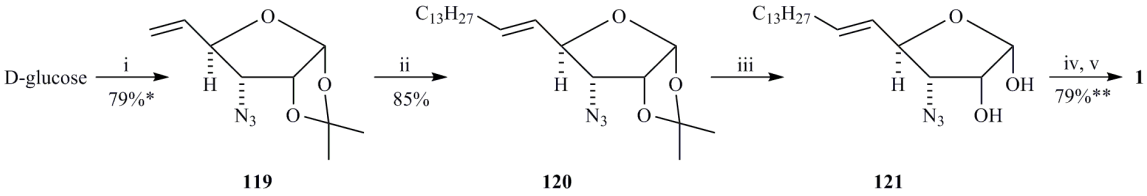

Scheme 19. Reagents and conditions: (i) Ref: [106]; (ii) 1-pentadecene/Grubbs' catalyst B; (iii) TFA/H_2O; (iv) $NaIO_4$; (v) $LiAlH_4$. * - multistep procedure. ** - three steps.

A nucleophilic addition of 2-silyloxy silylketene acetal (**123**) to *N*-benzyl-2,3-O-isopropylidene-D-glyceraldehyde nitron (**122**) (Mannich type reaction) gave adducts, which may be further converted into suitable orthogonally protected enantiomeric D- and L-*erythro*-sphingosines (Scheme 20) [108]. Nitron was chosen because it is an excellent equivalent of several chiral units, containing both amino- and oxygen functionalities. Furthermore, its activity can be modulated by the use of different Lewis acids due to the presence of reactive oxygen atom. Both the nitron and silyl ketene acetal are readily available [109, 110]. Several Lewis acids were evaluated in this work, with $Zn(OTf)_2$ furnishing the best diastereoselectivity and yields of *O*-silylhydroxylamine (**124**). Its hydrolysis provided free hydroxylamine (**125**), which was transformed into *N*-Boc protected ester (**126**). Reduction to

aldehyde (**127**) and Schlosser modification of the Wittig condensation with tetradecenylphosphorane afforded alkene (**128**). The dioxolane ring was transformed to orthogonally protected sphingosine (**130**) which was treated with Bu_4NF and TFA to give D-*erythro*-sphingosine (**1**). The synthesis was accomplished in 28% overall yield from the starting nitron.

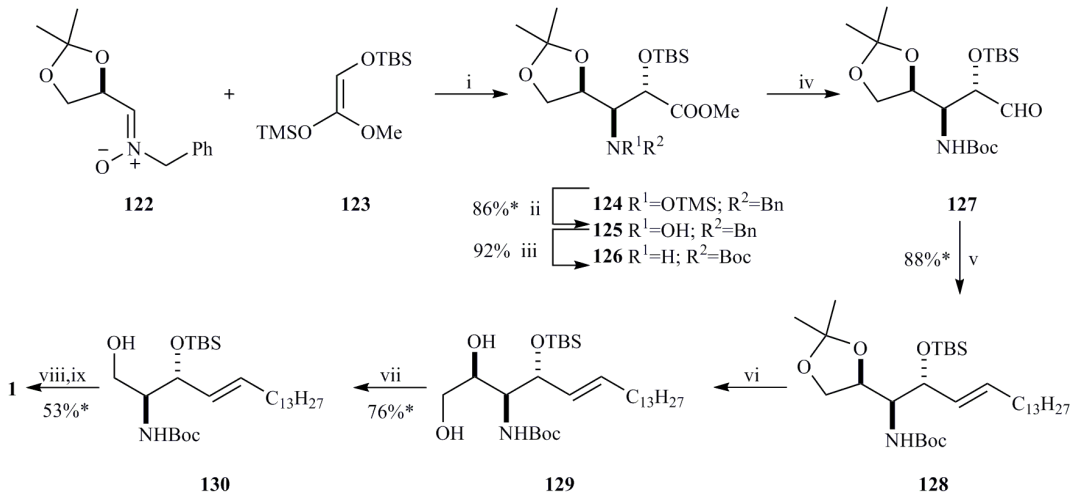

Scheme 20. Reagents and conditions: (i) $Zn(OTf)_2$; (ii) citric acid; (iii) $H_2/Pd(OH)_2$-C/Boc_2O; (iv) DIBAL; (v) $C_{14}H_{28}PPh_3$; (vi) *p*-TsOH; (vii) a) $NaIO_4$, b) $NaBH_4$; (viii) *n*-Bu_4NF; (ix) TFA. * - two steps.

A synthesis of sphingosine from phytosphingosine (**3)** via a cyclic sulfate intermediate (**132**) (Scheme 21) [111] offers a complementary transformation to the eliminative epoxide opening used for the introduction of *E*-allylic alcohol. The authors presented two synthetic pathways and claimed avoiding some drawbacks of the previous methods [86] (Schemes 12 and 13), including the use of rather expensive reagents, low temperature manipulations and unwanted side products. Their approach started with the protection of amino function as azide and primary hydroxyl group as silyl ether. The treatment of silylated 3,4-vicinal diol (**131**) with thionyl chloride in the presence of triethylamine followed by oxidation with ruthenium chloride provided cyclic sulfate (**132**). The next step included one-pot opening of the sulfate by iodide and dehydrohalogenation with DBU, which furnished the desired *E*-allylic alcohol (**134**) as the only isomer. The silyl group was removed with Bu_4NF and azido group was reduced to amine by $NaBH_4$ in 2-propanol. Alternatively, the primary hydroxyl group can be blocked as a trityl ether. Tritylated azido sphingosine obtained by the procedure described above is than hydrolyzed with HCl to azidosphingosine and reduced to sphingosine. This preparative route affords D-*erythro*-sphingosine in approximately 60% overall yield.

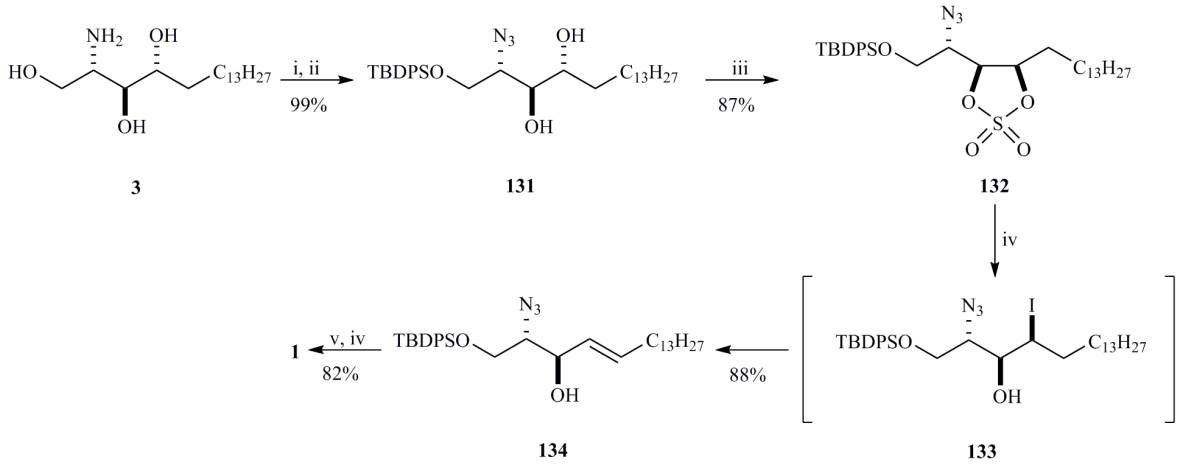

Scheme 21. Reagents and conditions: (i) $TfN_3/K_2CO_3/CuSO_4$; (ii) $TBDPSCl/Et_3N/DMAP$; (iii) a) $SOCl_2/Et_3N$, b) $RuCl_3.3H_2O/NaIO_4$; (iv) a) Bu_4NI/DBU, b) H_2SO_4; (v) *n*-Bu_4NF; (vi) $NaBH_4$.

An asymmetric synthesis of sphingosine and phytosphingosine isomers from commercially available *Z*-4-benzyloxybut-2-en-1-ol via a common oxazolidine derivative for the preparation was published by Righi (Scheme 22) [112]. The chiral epoxide (**135**), obtained by Sharpless asymmetric epoxidation was regioselectively opened to give bromohydrine (**136**). The one pot sequence of azidation, reduction of azide to amine group, Boc protection of amino group and formation of oxazolidine gave ester (**139**). The key intermediate for the synthesis of sphingoid bases was prepared from (**139**) by reduction of ester group to hydroxyl, its subsequent silylation and transformation of benzyl-protected group to aldehyde (**142**). The aldehyde (**142**) was transformed to D-*erythro*-sphingosine by an already reported sequence of olefination, izomerization and deprotection [113]. In spite of the versatility of the presented synthesis regarding the preparation of stereoisomers of both bases, the synthesis is somewhat complicated. The isomerization of double bond in the synthesis of sphingosine proceeds in 70/30 *E*/*Z* selectivity; being thus more useful for parallel preparation of *cis*- and *trans*-isomers. The overall yield for preparation of D-*erythro*-sphingosine is 24%.

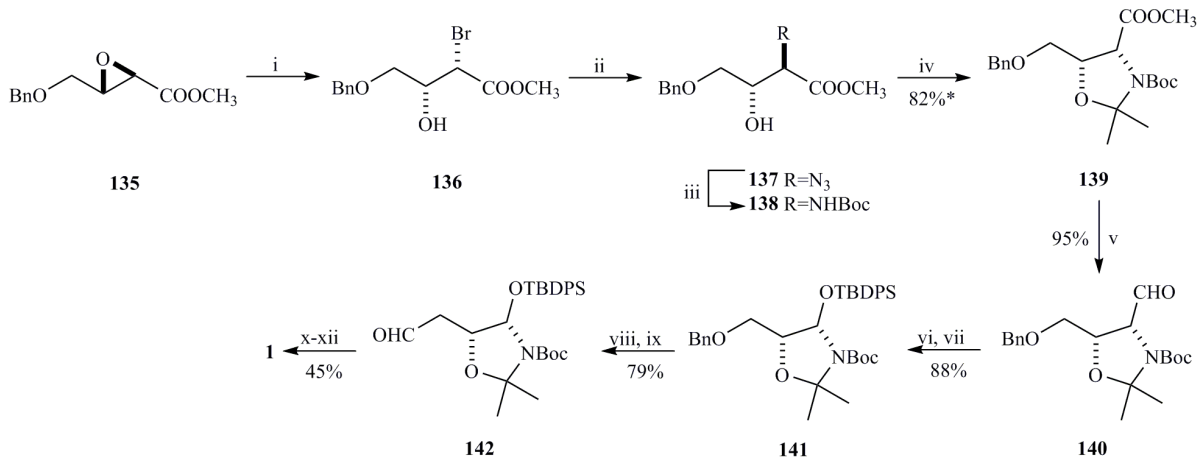

Scheme 22. Reagents and conditions: (i) Amberlyst 15/NaBr; (ii) NaN_3; (iii) $H_2/Pd/Boc_2O$; (iv) 2,2-DMP/*p*-TsOH; (v) DIBAL; (vi) $NaBH_4$; (vii) $TBDPSCl/Et_3N/DMAP$; (viii) H_2/Pd; (ix) Py/SO_3; (x) $C_{14}H_{29}PPh_3Br$/n-BuLi; (xi) hν/Ph_2S_2; (xii) TFA. * from epoxide (**131**).

Preparation of sphingosine, sphingomyelin, ceramide, sphingosine 1-phosphate and functionalized sphingosine derivatives from L-serine by cross-metathesis olefination were

reported by Yamamoto. (Scheme 23) [114]. The Boc protection of serine was followed by Weinreb amide formation and the protection of the primary hydroxyl group by TBSCl without column chromatography. The reaction with vinylmagnesium bromide provided vinyl ketone (**144**). Then, the carbonyl was selectively reduced with lithium tri-*t*-butoxyaluminohydride and primary hydroxyl deprotected to yield (**146**). Cross-metathesis and following deprotection of (**147**) produced D-*erythro*-sphingosine (**1**) in 37% overall yield. Similar synthesis via Weinreb amide was also described by Pham. [115].

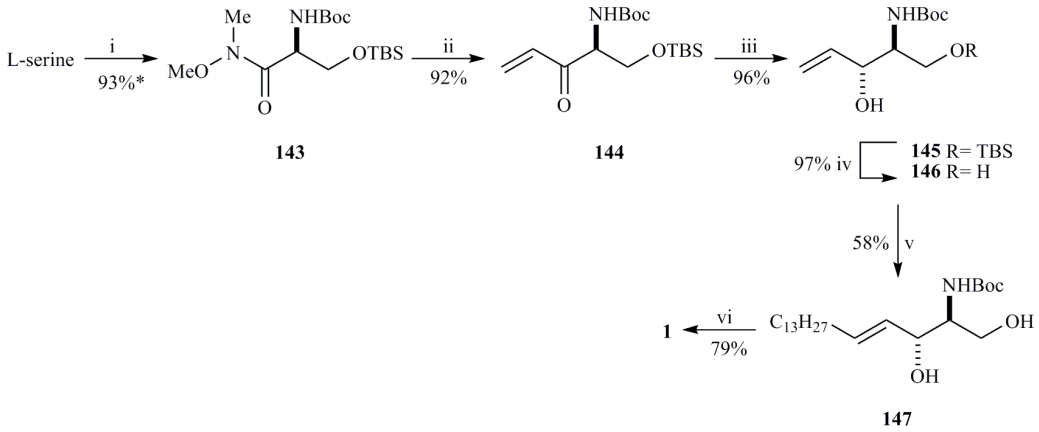

Scheme 23. Reagents and conditions: (i) a) Boc_2O/Et_3N, b) Me(MeO)NH.HCl/NMM, c) TBSCl/imidazole; (ii) vinylmagnesium bromide; (iii) $LiAl(O\text{-}tBu)_3H$; (iv) 2M HCl/MeOH; (v) 1-pentadecene/ Grubbs' catalyst B; (vi) TFA. * - three steps.

A novel approach for the synthesis of sphingosine was reported by Yang and Liebeskind (Scheme 24) [116]. The sequence started with *N*-Boc-L-serine and the key steps were palladium catalyzed, copper(I)-mediated, non-basic coupling of the thiophenyl ester of *N*-Boc-*O*-TBS L-serine (**150**) with *E*-1-pentadecenyl boronic acid and highly diastereoselective reduction of the resulting peptidyl ketone. Thiophenyl ester (**149**) was prepared by common dehydration conditions using DCC and DMAP. The primary hydroxyl group was than protected as *O*-silylether employing *N*-methyl morpholine as a base. Boronic acid requisite for the cross-coupling was obtained by hydroboration of 1-pentadecyne with $HBBr_2.SMe_2$ followed by hydrolysis on ice-water. Its reaction with protected thiophenyl ester (**150**) delivered ketone (**151**) with no *E*/*Z* isomerization. Racemization-free asymmetric reduction of enone by LiAl(*t*-BuO)$_3$H generated alcohol (**152**). The synthesis was ended up by desilylation and *N*-deprotection. Sphingosine was received in 71% overall yield from *N*-Boc-L-serine in six steps. The synthesis is characterized by high enantio- and diastereoselectivity (*ee*>99%, *de* up to 99%).

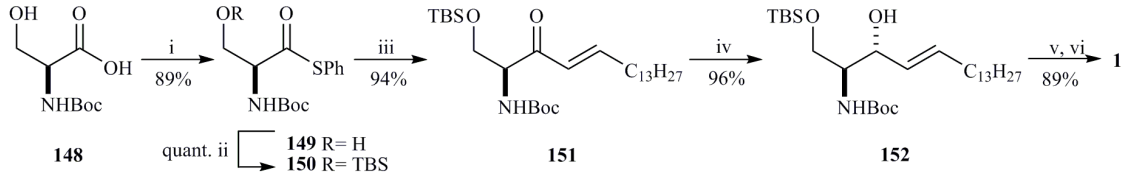

Scheme 24. Reagents and conditions: (i) PhSH/DCC/HOBt; (ii) TBSCl/NMM/DMAP; (iii)$Pd_2(dba)_3$/P(OEt)$_3$/CuTC/$C_{13}H_{27}CH{=}CHB(OH)_2$; (iv) LiAl(*t*-BuO)$_3$H; (v) 1M HCl; (vi) TFA.

Synthesis of 6-hydroxysphingosine

Because 6-hydroxysphingosine occurs mainly in human skin (as a structural part of ceramide EOH, AH, NH and protein-bound ceramide OH) and it does not play an important role in cell processes, there was not so much attention paid to its synthesis up to date. Since 1994 and 1999, when Downing reported the isolation of several new ceramides containing this base [54, 117], only three methods for its preparation were reported. All of them are based on the coupling of lithiated propargylic ethers and L-serine-derived Garner aldehyde. Because the spatial arrangement at C2 and C3 is introduced via L-serine derivative, the main task envisaged by the authors was the enantioselective preparation of the propargylic alcohol synthon. It is worth to mention that the 6*R* configuration of 6-hydroxysphingosine skin ceramides was determined by Masuda and Mori in 2005 [55].

Chun applied two different synthetic approaches to obtain both enantiomers of the intermediate (**155**) [118]. The asymmetric reduction of α,β-ynones neither with lithium aluminum hydride in the presence of Darvon alcohol nor with *B*-(3-pinanyl)-9-borabicyclo[3.3.1]nonane proved to give the desired product in satisfactory enantioselectivity. The alternative method consisted of base-mediated double elimination of 4-(chloromethyl)-1,3-dioxolane (**157**) (Scheme 25). Diol ester (**154**) was prepared by Horner-Wadsworth-Emmons reaction of tridecanal with ethyl 2-(diisopropoxyphosphoryl)acetate and asymmetric dihydroxylation of resulting α,β-unsaturated ester (**153**) with AD-mix-β (96% *ee*). Protection of vicinal hydroxy groups and reduction of ester with DIBAL furnished alcohol (**156**), which was converted to chloride (**157**) under Mitsunobu conditions. (*R*)-pentadec-1-yn-3-ol (**158**) was obtained in high enantioselectivity (96% *ee*) by treatment of chloride (**157**) with butyl lithium and HMPA. Its silylation and coupling with Garner aldehyde provided the protected

6-hydroxysphingosine (**160**). The removal of TBS group, Birch reduction of triple bond, acidic hydrolysis of oxazolidine cycle and subsequent acylation gave ceramide analogue without the separation of 6-hydroxysphingosine intermediate. To authors disappointment this method provided the ceramide in 42% yield only from (**161**). The changed sequence of the reactions (acidic hydrolysis of the oxazolidine, acylation and Birch reduction) gave *N*-octanoyl 6-hydroxysphingosine in good 73% yield from (**161**).

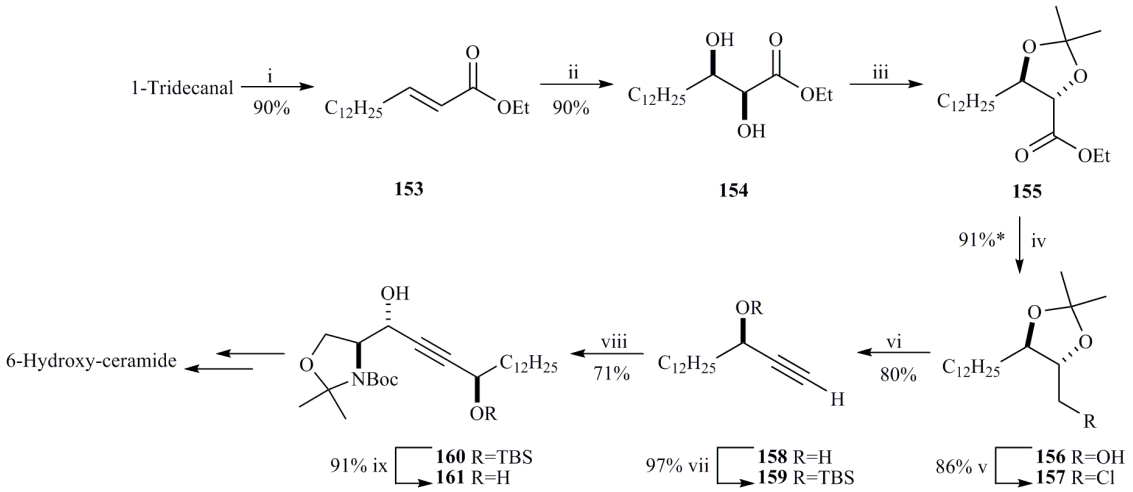

Scheme 25. Reagents and conditions: (i) $(i\text{-PrO})_2P(O)CH_2CO_2Et/Et_3N/LiBr$; (ii) AD-mix-β/$MeSO_2NH_2$; (iii) DMP/*p*-TsOH; (iv) DIBAL; (v) NCS/PhP_3; (vi) *n*-BuLi/HMPA; (vii) TBSCl/imidazole; (viii) Garner aldehyde/ *n*-BuLi; (ix) $n\text{-Bu}_4NF$. *- two steps.

Yadav used Sharpless asymmetric epoxidation of *E*-allyl alcohol and subsequent elimination of 2,3-epoxy chloride as the key reactions for the preparation of the propargyl alcohol intermediate (**167**) (Scheme 26) [119]. Reaction of propargyl alcohol (**162**) with dodecyl bromide gave pentadecynol (**163**), which was treated with $LiAlH_4$ to provide *E*-allylic alcohol (**164**). Its Sharpless asymmetric epoxidation using titanium tetraisopropoxide, (-)-DET and TBHP yielded epoxy alcohol (**165**), which was converted to epoxy chloride (**166**). The triple bond was introduced by treatment of 2,3-epoxy chloride (**166**) with $LiNH_2$ in liquid ammonia. The protection of secondary hydroxyl functionality was followed by coupling with Garner aldehyde. The removal of Boc, acetonide and TBS protecting groups was achieved by treatment with 1M HCl/THF. The final reduction of triple bond with $LiAlH_4$ led to 6-hydroxysphingosine (**2**).

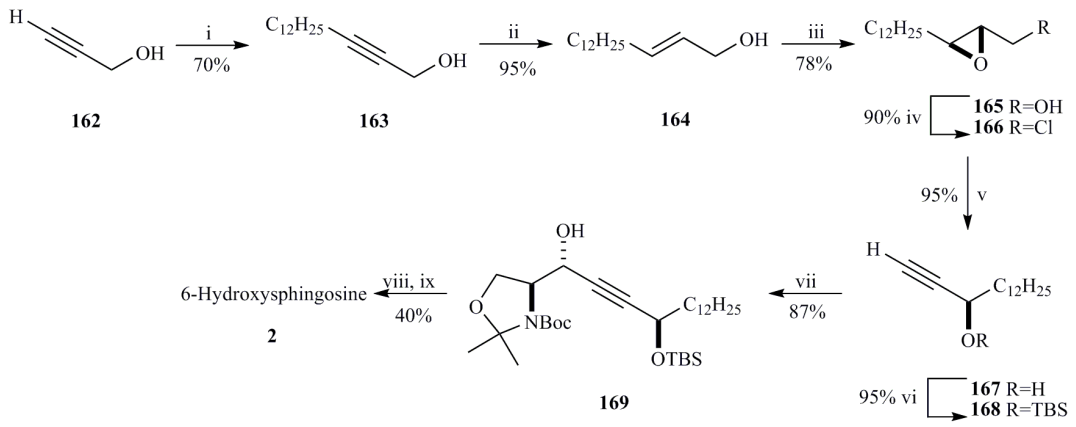

Scheme 26. Reagents and conditions: (i) $C_{12}H_{25}Br/LiNH_2/NH_3$; (ii) $LiAlH_4$; (iii) (-)-DET/Ti(O-*i*-Pr)$_4$/TBHP; (iv) $PPh_3/CCl_4/NaHCO_3$; (v) $LiNH_2/NH_3$; (vi) TBSCl/imidazole; (vii) Garner aldehyde/ *n*-BuLi/HMPA; (viii) 1M HCl; (ix) $LiAlH_4$.

Masuda and Mori used similar reaction of Garner aldehyde and protected (*R*)-pentadec-1-yn-3-ol for the preparation of skin ceramides derived from 6-hydroxysphingosine (Scheme 27) [55, 120]. Treatment of tridecanal with lithium trimethylsilylacetylide furnished racemic alkynol (**170**). Asymmetric acetylation of the latter with vinyl acetate in the presence of lipase PS on Celite and subsequent HPLC separation afforded acetylated (*R*)-enantiomer (**171**) in 49% yield and 99% *ee*, while (*S*)-enantiomer of (**170**) was recovered. Intermediate (**171**) was converted to acetylenic alcohol (**172**) and the secondary hydroxyl functionality was protected as silyl ether (**173**). Silylation improved diastereoselectivity of the coupling with Garner aldehyde.

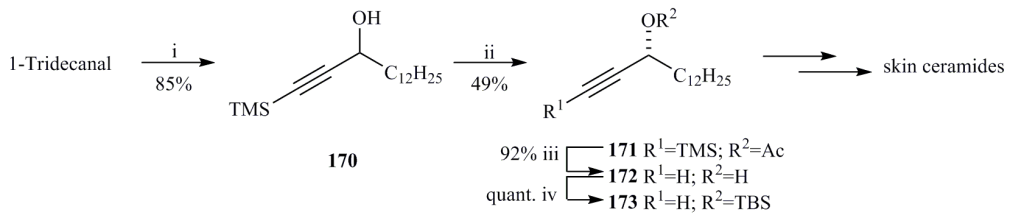

Scheme 27. Reagents and conditions: (i) lithium trimethylsilylacetylide/*n*-BuLi; (ii) lipase PS on Celite/vinyl acetate; (iii) K_2CO_3/MeOH; (iv) TBSCl/imidazole.

Synthesis of acid part of skin ceramides

Synthesis of ω-acyloxy fatty acid (EO)

The procedure for the preparation of skin-identical cerebroside containing ceramide EOS was published by Matsuda and Mori in 1991 [121] (Scheme 28). The synthesis of the 30-(linoleyloxy)triacontanoic acid segment started from pentadecan-15-olide (**174**). Its methanolysis and oxidation with PCC gave aldehyde (**176**). The second bifunctional intermediate (**179**) required for the subsequent Wittig coupling was obtained by treatment of (**175**) with TBDPSCl, reduction of the resulting ester and halogenation with tetrabromomethane and triphenylphosphine. Wittig reaction of aldehyde (**176**) and ylide derived from the bromide (**179**) provided a mixture of geometrical isomers (**180**). Their hydrogenation followed by ester hydrolysis, activation of the carboxyl with *p*-nitrophenyl

trifluoroacetate and mild desilylation achieved with Et_2O-BF_3 yielded the ω-hydroxy ester (**184**). Acylation of (**184**) with linoleyl chloride afforded the desired *p*-nitrophenyl 30-(linoleyloxy)triacontanoate (**185**) in 59% yield based on (**181**).

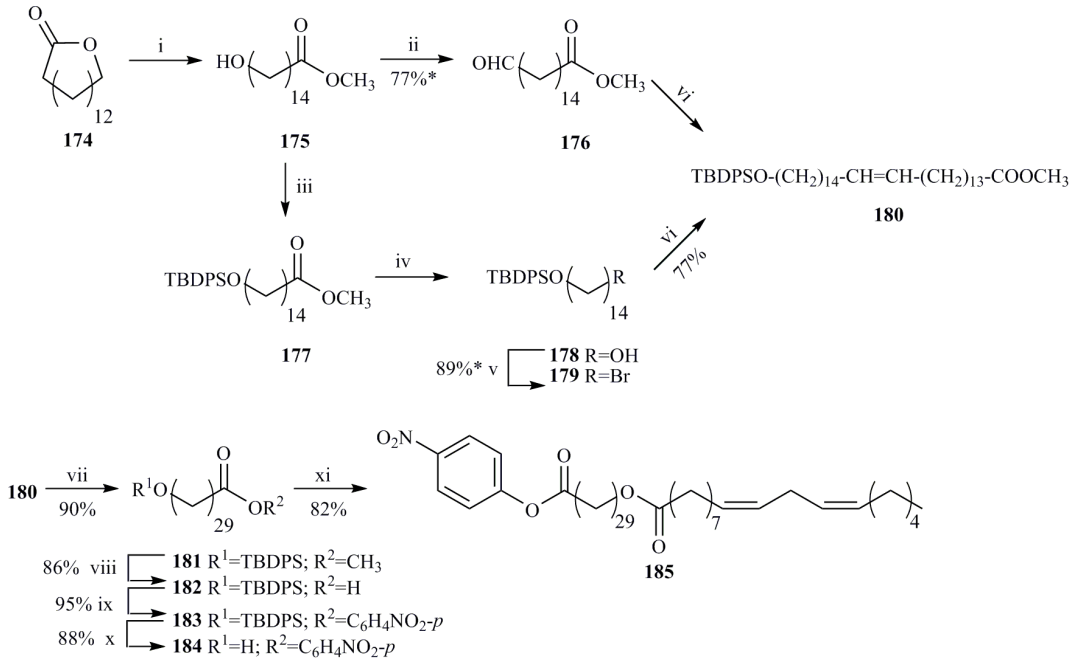

Scheme 28. Reagents and conditions: (i) *p*-TsOH/MeOH; (ii) PCC/powdered molecular sieves 4Å; (iii) TBDPSOCl/imidazole; (iv) $LiAlH_4$; (v) CBr_4/PhP_3; (vi) PhP_3/n-BuLi; (vii) Pd-C/H_2; (viii) KOH/EtOH; (ix) $CF_3COOC_6H_5NO_2$-*p*/pyridine; (x) Et_2O-BF_3; (xi) linoleoyl chloride/pyridine.

Another preparation of ceramide EOS and ceramide EOS-derived cerebroside was described by Müller and Schmidt (Scheme 29) [122]. The synthetic sequence involved three coupling steps to obtain 30-hydroxytriacontanoic acid (**199**), including the reaction of 11-bromoundecan-1-ol (**186**) with diethyl malonate to introduce the carboxylic function, coupling of Grignard compound obtained from (**193**) and chloromagnesium salt of (**190**) with Li_2CuCl_4 catalysis to yield (**194**), and Wittig reaction to connect the building blocks A and B (**188** and **195**) (Scheme 29). The activation of linoleic acid with 2-chloro-1-pyridinium iodide was necessary for esterification with almost insoluble saturated ω-hydroxy acid. *N*-acylation of sphingosine with resulting *O*-acyl fatty (**200**) acid in the presence of EEDQ furnished ceramide EOS in 60% yield.

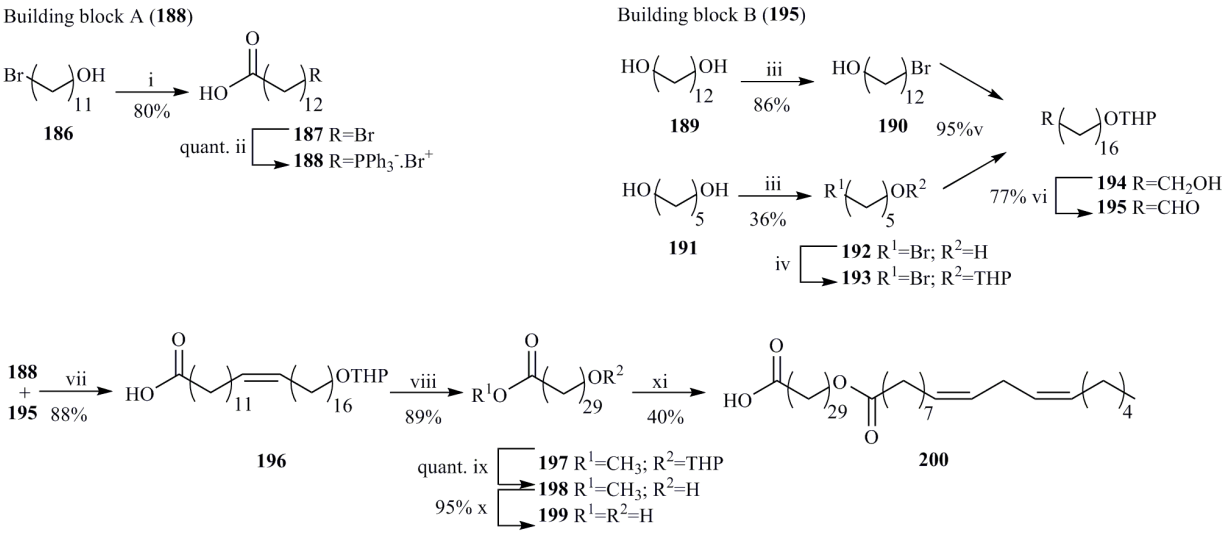

Scheme 29. Reagents and conditions: (i) a) diethyl malonate/NaOEt, b) $HBr/CH_3COOH/H_2SO_4$; (ii) PPh_3; (iii) HBr; (iv) DHP/H^+; (v) Mg/CH_3MgCl $/Li_2CuCl_4$; (vi) PCC; (vii) a) $NaN(SiMe_3)_2$, b) CH_2N_2; (viii) $Pd\text{-}C/H_2$; (ix) H^+; (x) NaOH; (xi) linoleic acid/CMPI/ $(C_4H_9)_3N$/pyridine.

Synthesis of α-hydroxy fatty acid (A)

α-Hydroxytetracosanoic acid was synthesized as an intermediate for the preparation of cerebrosides based on ceramide AS by Koike (Scheme 30) [123]. The ethyl (*S*)-2-acetoxytetracosanoate, necessary for the synthesis, was obtained by Horn and Pretorius procedure from (S)-(-)-malic acid [124]. The silylated α-hydroxytetracosanoic acid (**206**) was prepared from (**202**) in four steps including the inversion of configuration according to Eguchi and Mitsunobu [125]. The hydrolysis of the resulting benzoate (**203**), silylation of secondary hydroxyl and deprotection of the carboxylic group gave compound (**206**) in a good stereoselectivity.

An enzymatic approach was published in 2005 (Scheme 31) [55]. Tetracosanoic acid (**207**) reacted with bromine in the presence of phosphorus. The resulting racemic 2-bromo acid (**208**) was treated with aqueous sodium hydroxide to give (±)-2-hydroxy acid (**209**). Its enzymatic kinetic resolution was achieved with lipase PS and vinyl acetate to give (*S*)-acetoxy acid (**211**). The natural (*R*)-2-hydroxy acid (**210**) was recovered, its hydroxyl group protected and used for the preparation of ceramide AH.

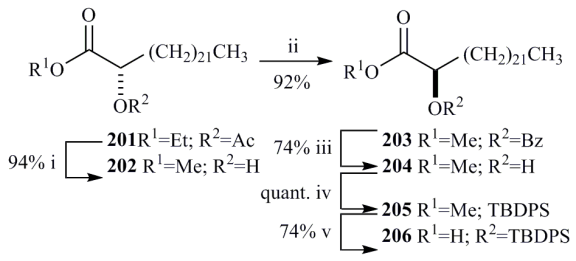

Scheme 30. Reagents and conditions: (i) MeONa/MeOH/Amberlyst 15; (ii) Ph_3P/DIAD/benzoic acid; (iii) MeONa/MeOH/Amberlyst 15; (iv) TBDPSCl/imidazole; (v) NaOH/MeOH/Amberlyst 15.

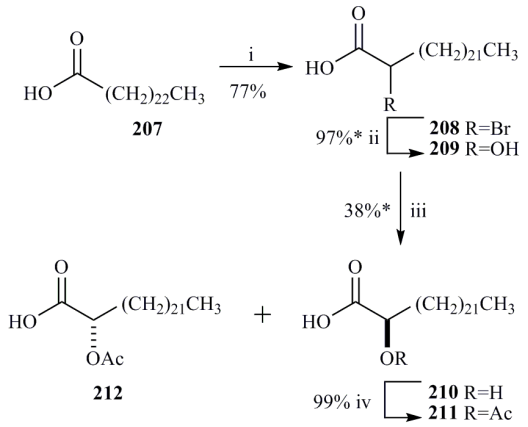

Scheme 31. Reagents and conditions: (i) Br_2/P; (ii) NaOH/H_2O; (iii) lipase PS/vinyl acetate/BHT; (iv) Ac_2O/pyridine. * - yield for (*R*)-hydroxy acid.

CONCLUSION

Synthesis of ceramides and their analogues in pure form is essential for elucidation of their biological functions and structure-activity relationships, which are still poorly understood. In the last decade, significant progress has been achieved in both the synthetic methodologies and the functional elucidation of epidermal ceramides. Since the last review in 1998 [52], many interesting syntheses of sphingosine emerged. Asymmetric syntheses together with the preparations from L-serine are the most abundant while monosaccharides have partially lost their attractiveness as starting material. Synthesis using serine-derived β-ketophosphonates (Scheme 8) is convenient and high yielding with satisfactory selectivity. The use of phytosphingosine as a relatively inexpensive starting material has been explored since 2002 (Schemes 12-14 and 21). These procedures are economical, suitable for large-scale preparations, but somewhat less versatile for the synthesis of ceramide analogues. It is worth to mention that a process to identify microorganisms that are capable of converting exogenous phytosphingosine to sphingosine was patented in 2007 [126]. First in 2004, olefin cross metathesis was used for the formation of double bond and attachment of the lipophilic chain. These syntheses are versatile, high yielding and highly stereoselective, e.g. Schemes 19 and 23. Another high yielding, scalable and highly stereoselective synthesis used thiol ester-boronic acid cross-coupling (Scheme 24). Nevertheless, the early synthesis using alkynylation of Garner aldehyde [73, 74] is still very common for the preparation of sphingosine and its analogues for biological studies.

In addition, methods for the preparation of the unique epidermal ceramides and their structural fragments including 6-hydroxysphingosine, α-hydroxy- and ω-hydroxy- and ω-linoleyloxy acids are described in this paper.

The current data on the structure-activity relationships of ceramides in the skin barrier are summarized in this review. Although these data are not conclusive and many may be model system-dependent, it seems that the exceptionally long hydrophobic chains, hydrogen bonding ability and the presence of the ω-linoleyloxy- and protein-bound ceramides are the basic prerequisites for a competent skin barrier. In general, the most important feature seems to be the structural heterogeneity of the epidermal lipids. Particularly interesting is the suggestion about the complementary mechanisms of lamellar self-assembly of sphingosine and phytosphingosine based ceramides [46].

For a deeper understanding of the role of the individual ceramide species and their structural moieties in the skin, and in order to design better ceramide analogues for the treatment of skin diseases and better permeation enhancers for transdermal drug delivery, further studies are needed. Synthetic lipid models are an excellent tool to investigate the behavior of the individual ceramides on a molecular level (reviewed recently in [127]). However, it should be confirmed by permeability studies that the changes in ceramide packing/chain order/hydrogen bonding strength, etc. observed by physicochemical methods result in the suggested changes in skin barrier function. Indeed, a direct effect of exogenous short-chain ceramides on skin permeability for two model drugs was described recently [30].

When regarding the SC lipid models as tools to study the role of SC ceramides, the model recently described by Bouwstra's group [128-132] seems to be well suited for such experiments since the lipid lamellae reconstituted on a filter support may be used for both the physicochemical characterization and permeation studies. Alteration of the lipid content of this or similar model or replacement of selected species by their synthetic analogues may be a reasonably simplified tool to obtain information on the function of this unique class of lipids.

In conclusion, although impressive progress has been made in elucidating the role of ceramides in the skin barrier, the essential information is still missing. Possibly, lessons could be learned from the studies on the behavior of ceramides in phospholipid/sphingomyelin

membranes and those on the structure-activity relationships of transdermal permeation enhancers.

ACKNOWLEDGEMENTS

This work was supported by the Centre for New Antivirals and Antineoplastics (1M0508) and the Ministry of Education of the Czech Republic (MSM0021620822).

ABBREVIATIONS

BHT	butylated hydroxy toluene
Boc	*t*-butyloxycarbonyl
CDI	1,1'-carbonyldiimidazole
CMPI	2-chloro-1-methyl-pyridinium iodide
CuTC	copper(I) thiophene-2-carboxylate
DBN	1,5-diazabicyclo[5.4.0]undec-5-ene
DBU	1,8-diazabicyclo[5.4.0]undec-7-ene
DCC	dicyclohexylcarbodiimide
de	diastereomeric excess
DET	diethyltryptamine
DHP	dihydropyrane
DIAD	diisopropyl azodicarboxylate
DIBAL	diisobutylaluminium hydride
DMAP	4-dimethylaminopyridine
DMSO	dimethylsulfoxide
DMP	2,2-dimethoxypropane
EDCl	1-ethyl-3-(3-dimethylaminopropyl) carbodiimide hydrochloride
ee	enantiomeric excess
EEDQ	ethyl 1,2-dihydro-2-ethoxyquinoline-1-carboxylate
Fmoc	9-fluorenylmethyl
HMPA	hexamethylphosphoramide
IBX	2-iodoxybenzoic acid
Ipc2BOMe	*B*-methoxydiisopinocampheylborane
KHMDS	potassium bis(trimethylsilyl)amide
MCPBA	3-chloroperoxybenzoic acid
9-MeO-9-BBN	9-methoxy-9-Borabicyclo[3.3.1]nonane
MOM	methoxymethyl
Ms	mesylate
NaHMDS	bistrimethylsilyl amide
NCS	*N*-chlorosuccinimide
NMM	*N*-methylmaleimide
Oxone	potassium peroxomonosulfate
PCC	pyridinium chlorochromate
Pd2(bda)3	tris(dibenzylideneacetone)dipalladium(0))
PMB	*p*-methoxybenzyl
PPTS	pyridinium 4-toluensulfonate
SC	stratum corneum
TBDPS	*t*-butyldiphenylsilyl
TBHP	*t*-butyl hydroperoxide
TBS	*t*-butyldimethylsilyl
Tf	trifluoromethylsulfonyl
TFA	trifluoroacetic acid
TIPS	triisopropylsilyl
TMG	1,1,3,3-tetramethyl guanidine
TMS	trimethylsilyl
Tr	trityl
TsOH	toluensulfonic acid

REFERENCES

[1] Holleran, W. M.; Takagi, Y.; Uchida, Y. Epidermal sphingolipids: metabolism, function, and roles in skin disorders. *FEBS Lett*, **2006**, *580*, 5456-66.

[2] Bouwstra, J. A.; Ponec, M. The skin barrier in healthy and diseased state. *Biochim. Biophys. Acta*, **2006**, *1758*, 2080-95.

[3] Choi, M. J.; Maibach, H. I. Role of ceramides in barrier function of healthy and diseased skin. *Am. J. Clin. Dermatol.*, **2005**, *6*, 215-23.

[4] Feingold, K. R. Thematic review series: skin lipids. The role of epidermal lipids in cutaneous permeability barrier homeostasis. *J. Lipid Res.*, **2007**, *48*, 2531-46.

[5] Wertz, P. W. Lipids and barrier function of the skin. *Acta Derm Venereol Suppl (Stockh)*, **2000**, *208*, 7-11.

[6] Elias, P. M.; Feingold, K. R. *Skin Barrier* CRC Press: NY **2006**.

[7] Ogretmen, B.; Hannun, Y. A. Biologically active sphingolipids in cancer pathogenesis and treatment. *Nat. Rev. Cancer*, **2004**, *4*, 604-16.

[8] Goni, F. M.; Contreras, F. X.; Montes, L. R.; Sot, J.; Alonso, A. Biophysics (and sociology) of ceramides. *Biochem. Soc. Symp.*, **2005**, 177-88.

[9] Morales, A.; Fernandez-Checa, J. C. Pharmacological modulation of sphingolipids and role in disease and cancer cell biology. *Mini Rev. Med. Chem.*, **2007**, *7*, 371-82.

[10] van Blitterswijk, W. J.; van der Luit, A. H.; Veldman, R. J.; Verheij, M.; Borst, J. Ceramide: second messenger or modulator of membrane structure and dynamics? *Biochem. J.*, **2003**, *369*, 199-211.

[11] Small, D. M. Surface and bulk interactions of lipids and water with a classification of biologically active lipids based on these interactions. *Fed. Proc.*, **1970**, *29*, 1320-6.

[12] Goni, F. M.; Alonso, A. Biophysics of sphingolipids I. Membrane properties of sphingosine, ceramides and other simple sphingolipids. *Biochim. Biophys. Acta*, **2006**, *1758*, 1902-21.

[13] Masukawa, Y.; Narita, H.; Shimizu, E.; Kondo, N.; Sugai, Y.; Oba, T.; Homma, R.; Ishikawa, J.; Takagi, Y.; Kitahara, T.; Takema, Y.; Kita, K. Characterization of overall ceramide species in human stratum corneum. *J. Lipid. Res.*, **2008**, *49*, 1466-76.

[14] Motta, S.; Monti, M.; Sesana, S.; Caputo, R.; Carelli, S.; Ghidoni, R. Ceramide composition of the psoriatic scale. *Biochim. Biophys. Acta*, **1993**, *1182*, 147-51.

[15] Pruett, S. T.; Bushnev, A.; Hagedorn, K.; Adiga, M.; Haynes, C. A.; Sullards, M. C.; Liotta, D. C.; Merrill, A. H., Jr. Biodiversity of sphingoid bases ("sphingosines") and related amino alcohols. *J. Lipid Res.*, **2008**, *49*, 1621-39.

[16] Moore, D. J.; Rerek, M. E.; Mendelsohn, R. Role of ceramides 2 and 5 in the structure of the stratum corneum lipid barrier. *Int. J. Cosmet. Sci.*, **1999**, *21*, 353-68.

[17] Bouwstra, J. A.; Gooris, G. S.; Dubbelaar, F. E.; Weerheim, A. M.; Ijzerman, A. P.; Ponec, M. Role of ceramide 1 in the molecular organization of the stratum corneum lipids. *J Lipid Res*, **1998**, *39*, 186-96.

[18] Wertz, P. W.; Cho, E. S.; Downing, D. T. Effect of essential fatty acid deficiency on the epidermal sphingolipids of the rat. *Biochim Biophys Acta*, **1983**, *753*, 350-5.

[19] de Jager, M.; Gooris, G.; Ponec, M.; Bouwstra, J. Acylceramide head group architecture affects lipid organization in synthetic ceramide mixtures. *J. Invest. Dermatol.*, **2004**, *123*, 911-6.

[20] Swartzendruber, D. C.; Wertz, P. W.; Madison, K. C.; Downing, D. T. Evidence that the corneocyte has a chemically bound lipid envelope. *J. Invest. Dermatol.*, **1987**, *88*, 709-13.

[21] Wertz, P. W.; Downing, D. T. Covalently bound omega-hydroxyacylsphingosine in the stratum corneum. *Biochim. Biophys. Acta*, **1987**, *917*, 108-11.

[22] Stewart, M. E.; Downing, D. T. The omega-hydroxyceramides of pig epidermis are attached to corneocytes solely through omega-hydroxyl groups. *J. Lipid Res.*, **2001**, *42*, 1105-10.

[23] Wertz, P. W.; van den Bergh, B. The physical, chemical and functional properties of lipids in the skin and other biological barriers. *Chem. Phys. Lipids*, **1998**, *91*, 85-96.

[24] Alonso, A.; Meirelles, N. C.; Tabak, M. Lipid chain dynamics in stratum corneum studied by spin label electron paramagnetic resonance. *Chem. Phys. Lipids*, **2000**, *104*, 101-11.

[25] Uchida, Y.; Holleran, W. M. Omega-O-acylceramide, a lipid essential for mammalian survival. *J. Dermatol. Sci.*, **2008**, *51*, 77-87.

[26] Lopez, O.; Cocera, M.; Wertz, P. W.; Lopez-Iglesias, C.; de la Maza, A. New arrangement of proteins and lipids in the stratum corneum cornified envelope. *Biochim. Biophys. Acta*, **2007**, *1768*, 521-9.

[27] Vasireddy, V.; Uchida, Y.; Salem, N., Jr.; Kim, S. Y.; Mandal, M. N.; Reddy, G. B.; Bodepudi, R.; Alderson, N. L.; Brown, J. C.; Hama, H.; Dlugosz, A.; Elias, P. M.; Holleran, W. M.; Ayyagari, R. Loss of functional ELOVL4 depletes very long-chain fatty acids (> or =C28) and the unique omega-O-acylceramides in skin leading to neonatal death. *Hum Mol Genet*, **2007**, *16*, 471-82.

[28] Goni, F. M.; Alonso, A. Biophysics of sphingolipids I. Membrane properties of sphingosine, ceramides and other simple sphingolipids. *Biochim Biophys Acta*, **2006**, *1758*, 1902-21.

[29] van Blitterswijk, W. J.; van der Luit, A. H.; Veldman, R. J.; Verheij, M.; Borst, J. Ceramide: second messenger or modulator of membrane structure and dynamics? *Biochem J*, **2003**, *369*, 199-211.

[30] Novotny, J.; Janusova, B.; Novotny, M.; Hrabalek, A.; Vavrova, K. Short-Chain Ceramides Decrease Skin Barrier Properties. *Skin. Pharmacol. Physiol.*, **2008**, *22*, 22-30.

[31] Nybond, S.; Bjorkqvist, Y. J.; Ramstedt, B.; Slotte, J. P. Acyl chain length affects ceramide action on sterol/sphingomyelin-rich domains. *Biochim. Biophys. Acta*, **2005**, *1718*, 61-6.

[32] Megha; Sawatzki, P.; Kolter, T.; Bittman, R.; London, E. Effect of ceramide N-acyl chain and polar headgroup structure on the properties of ordered lipid domains (lipid rafts). *Biochim. Biophys. Acta*, **2007**, *1768*, 2205-12.

[33] Chiantia, S.; Kahya, N.; Schwille, P. Raft domain reorganization driven by short- and long-chain ceramide: a combined AFM and FCS study. *Langmuir*, **2007**, *23*, 7659-65.

[34] Gidwani, A.; Brown, H. A.; Holowka, D.; Baird, B. Disruption of lipid order by short-chain ceramides correlates with inhibition of phospholipase D and downstream signaling by FcepsilonRI. *J. Cell. Sci.*, **2003**, *116*, 3177-87.

[35] Vavrova, K.; Zbytovska, J.; Hrabalek, A. Amphiphilic transdermal permeation enhancers: structure-activity relationships. *Curr Med Chem*, **2005**, *12*, 2273-91.

[36] Obeid, L. M.; Linardic, C. M.; Karolak, L. A.; Hannun, Y. A. Programmed cell death induced by ceramide. *Science*, **1993**, *259*, 1769-71.

[37] Bielawska, A.; Crane, H. M.; Liotta, D.; Obeid, L. M.; Hannun, Y. A. Selectivity of ceramide-mediated biology. Lack of activity of erythro-dihydroceramide. *J. Biol. Chem.*, **1993**, *268*, 26226-32.

[38] Brodesser, S.; Sawatzki, P.; Kolter, T. Bioorganic Chemistry of Ceramide. *Eur. J. Org. Chem.*, **2003**, 2021 - 34.

[39] Radin, N. S. Designing anticancer drugs via the achilles heel: ceramide, allylic ketones, and mitochondria. *Bioorg Med Chem*, **2003**, *11*, 2123-42.

[40] Radin, N. S. Meta-analysis of anticancer drug structures--significance of their polar allylic moieties. *Anticancer Agents Med Chem*, **2007**, *7*, 209-22.

[41] Vavrova, K.; Hrabalek, A.; Mac-Mary, S.; Humbert, P.; Muret, P. Ceramide analogue 14S24 selectively recovers perturbed human skin barrier. *Br. J. Dermatol.*, **2007**, *157*, 704-12.

[42] Vavrova, K.; Zbytovska, J.; Palat, K.; Holas, T.; Klimentova, J.; Hrabalek, A.; Dolezal, P. Ceramide analogue 14S24 ((S)-2-tetracosanoylamino-3-hydroxypropionic acid tetradecyl ester) is effective in skin barrier repair in vitro. *Eur. J. Pharm. Sci.*, **2004**, *21*, 581-7.

[43] Brockman, H. L.; Momsen, M. M.; Brown, R. E.; He, L.; Chun, J.; Byun, H. S.; Bittman, R. The 4,5-double bond of ceramide regulates its dipole potential, elastic properties, and packing behavior. *Biophys. J.*, **2004**, *87*, 1722-31.

[44] Li, L.; Tang, X.; Taylor, K. G.; DuPre, D. B.; Yappert, M. C. Conformational characterization of ceramides by nuclear magnetic resonance spectroscopy. *Biophys. J.*, **2002**, *82*, 2067-80.

[45] Novotny, M.; Hrabalek, A.; Janusova, B.; Novotny, J.; Vavrova, K. Dicarboxylic acid esters as transdermal permeation enhancers: effects of chain number and geometric isomers. *Bioorg Med Chem Lett*, **2009**, *19*, 344-7.

[46] Rerek, M. E.; Chen; Markovic, B.; Van Wyck, D.; Garidel, P.; Mendelsohn, R.; Moore, D. J. Phytosphingosine and Sphingosine Ceramide Headgroup Hydrogen Bonding: Structural Insights through Thermotropic Hydrogen/Deuterium Exchange. *J. Phys. Chem. B*, **2001**, *105*, 9355-62.

[47] Lofgren, H.; Pascher, I. Molecular arrangements of sphingolipids. The monolayer behaviour of ceramides. *Chem. Phys. Lipids*, **1977**, *20*, 273-84.

[48] Forslind, B. A domain mosaic model of the skin barrier. *Acta Derm. Venereol.*, **1994**, *74*, 1-6.

[49] Moore, D. J.; Rerek, M. E. Insights into the molecular organization of lipids in the skin barrier from infrared spectroscopy studies of stratum corneum lipid models. *Acta. Derm. Venereol. Suppl. (Stockh)*, **2000**, *208*, 16-22.

[50] Garidel, P. Calorimetric and spectroscopic investigations of phytosphingosine ceramide membrane organisation. *Phys. Chem. Chem. Phys.*, **2002**, *4*, 1934-42.

[51] Thudichum, J. L. W. *A Treatise on the Chemical Constitution of the Brain*, Tindall and Cox: London, Bailliere **1884**.

[52] Koskinen, P. i. M.; Koskinen, A. M. P. Sphingosine, an Enigmatic Lipid: A Review of Recent Literature Syntheses. *Synthesis*, **1998**, *1998*, 1075-91.

[53] Zellner, J. Zur Chemie des Fliegenpilzes (Amanita muscaria L.). *Monatshefte für Chemie / Chemical Monthly*, **1911**, *32*, 133-42.

[54] Robson, K. J.; Stewart, M. E.; Michelsen, S.; Lazo, N. D.; Downing, D. T. 6-Hydroxy-4-sphingenine in human epidermal ceramides. *J. Lipid. Res.*, **1994**, *35*, 2060-8.

[55] Masuda, Y.; Mori, K. Synthesis and Absolute Configuration of 6-Hydroxylated New Ceramides in Human Skin, Ceramides B, 4, 7 and 8. *Eur. J. Org. Chem.*, **2005**, *2005*, 4789-800.

[56] Karlsson, K. A.; Pascher, I. Resolution and chromatographic configuration analysis of 2-hydroxy fatty acids. *Chem. Phys. Lipids*, **1974**, *12*, 65-74.

[57] Heard, C. M.; Brain, K. R. Does solute stereochemistry influence percutaneous penetration? *Chirality*, **1995**, *7*, 305-9.

[58] Reddy, I. K.; Kommuru, T. R.; Zaghloul, A. A.; Khan, M. A. Chirality and its implications in transdermal drug development. *Crit. Rev. Ther. Drug Carrier Syst.*, **2000**, *17*, 285-325.

[59] Vavrova, K.; Hrabalek, A.; Dolezal, P. Enhancement effects of (R) and (S) enantiomers and the racemate of a model enhancer on permeation of theophylline through human skin. *Arch. Dermatol. Res.*, **2002**, *294*, 383-5.

[60] Novotny, J.; Kovarikova, P.; Novotny, M.; Janusova, B.; Hrabalek, A.; Vavrova, K. Dimethylamino Acid Esters as Biodegradable and Reversible Transdermal Permeation Enhancers: Effects of Linking Chain Length, Chirality and Polyfluorination. *Pharm. Res.*, **2008**.

[61] Norlen, L. Skin barrier structure and function: the single gel phase model. *J Invest Dermatol*, **2001**, *117*, 830-6.

[62] Corkery, R. W.; Hyde, S. T. On the Swelling of Amphiphiles in Water. *Langmuir*, **1996**, *12*, 5528-29.

[63] Kiselev, M. A.; Ryabova, N. Y.; Balagurov, A. M.; Dante, S.; Hauss, T.; Zbytovska, J.; Wartewig, S.; Neubert, R. H. New insights into the structure and hydration of a stratum corneum lipid model membrane by neutron diffraction. *Eur Biophys J*, **2005**, *34*, 1030-40.

[64] Corkery, R. W. The anti-parallel, extended or splayed-chain conformation of amphiphilic lipids. *Colloid. Surf. B: Biointerfaces*, **2002**, *26*, 3-20.

[65] Kronke, M. Biophysics of ceramide signaling: interaction with proteins and phase transition of membranes. *Chem Phys Lipids*, **1999**, *101*, 109-21.

[66] Devant, R. M. Chemische Totalsynthese von Sphingosin, dem zentralen Baustein der Sphingolipide. *Kontakte*, **1992**, *3*, 11-28.

[67] Howell, A. R.; Ndakala, A. J. The Preparation and Biological Significance of Phytosphingosines. *Curr. Org. Chem.*, **2002**, *6*, 365-91.

[68] Howell, A. R.; So, R. C.; Richardson, S. K. Approaches to the preparation of sphinganines. *Tetrahedron*, **2004**, *60*, 11327-47.

[69] Shapiro, D.; Segal, K. The synthesis of sphingosine. *J. Am. Chem. Soc.*, **1954**, *76*, 5894-95.

[70] Schmidt, R. R.; Zimmermann, P. Synthesis of d-erythro-sphingosines. *Tetrahedron Lett.*, **1986**, *27*, 481-84.

[71] Kiso, M.; Nakamura, A.; Nakamura, J.; Tomita, Y.; Hasegawa, A. A Convenient Synthesis of Sphingosine and Ceramide from D-Xylose or D-Galactose. *J. Carbohydr. Chem.*, **1986**, *5*, 335-40.

[72] Julina, R.; Herzig, T.; Bernet, B.; Vasella, A. Enantioselective Synthesis of D-erythro-Sphingosine and of Ceramide. *Helv. Chim. Acta*, **1986**, *69*, 368-73.

[73] Garner, P.; Park, J. M.; Malecki, E. A stereodivergent synthesis of D-erythro-sphingosine and D-threo-sphingosine from L-serine. *J. Org. Chem.*, **1988**, *53*, 4395 - 98.

[74] Herold, P. Synthesis of D-Erythro- and D-Threo-Sphingosine Derivatives From L-Serine. *Helv. Chim. Acta*, **1988**, *71*, 354-62.

[75] Garner, P.; Park, J. M. 1,1,-Dimethylethyl (*S*)- or (*R*)-4-Formyl-2,2-Dimethyl-3-Ooxazolidinecarboxylate: A Useful Serinal Derivative. *Org. Synth.*, **1992**, *9*, 300.

[76] Kobayashi, S.; Furuta, T. Use of heterocycles as chiral ligands and auxiliaries in asymmetric syntheses of sphingosine, sphingofungins B and F. *Tetrahedron*, **1998**, *54*, 10275-94.

[77] Hoffman, R. V.; Tao, J. A Synthesis of d-erythro- and l-threo-Sphingosine and Sphinganine Diastereomers via the Biomimetic Precursor 3-Ketosphinganine. *J. Org. Chem.*, **1998**, *63*, 3979-85.

[78] Harris, B. D.; Joullié, M. M. Synthetic studies of didemnins. III : Syntheses of statine and isostatine stereoisomers. *Tetrahedron*, **1988**, *44*, 3489-500.

[79] Hoffman, R. V.; Tao, J. An Improved Enantiospecific Synthesis of Statine and Statine Analogs via 4-(N,N-Dibenzylamino)-3-keto Esters. *J. Org. Chem.*, **1997**, *62*, 2292-97.

[80] Khiar, N.; Singh, K.; García, M.; Martín-Lomas, M. A short enantiodivergent synthesis of d-erythro and l-threo sphingosine. *Tetrahedron Lett.*, **1999**, *40*, 5779-82.

[81] Solladie, G.; Hutt, J.; Girardin, A. Improved Preparation of Optically Active Methyl p-Tolyl Sulfoxide. *Synthesis*, **1987**, *1987*, 173-73.

[82] Hertweck, C.; Boland, W. Asymmetric alpha-Chloroallylboration of Amino Aldehydes: A Novel and Highly Versatile Route to d- and l-erythro-Sphingoid Bases. *J. Org. Chem.*, **1999**, *64*, 4426-30.

[83] Johnson, D. V.; Felfer, U.; Griengl, H. A Chemoenzymatic Access to D - and L -Sphingosines Employing Hydroxynitrile Lyases. *Tetrahedron*, **2000**, *56*, 781-90.

[84] He, L.; Byun, H.-S.; Bittman, R. Stereoselective Preparation of Ceramide and Its Skeleton Backbone Modified Analogues via Cyclic Thionocarbonate Intermediates Derived by Catalytic Asymmetric Dihydroxylation of ,-Unsaturated Ester *J. Org. Chem.*, **2000**, *65*, 7627-33.

[85] Barrett, A. G. M.; Sakadarat, S. Total syntheses of penicillanic acid S,S-dioxide and 6-aminopenicillanic acid using (benzyloxy)nitromethane. *J. Org. Chem.*, **1990**, *55*, 5110-17.

[86] Nakamura, T.; Shiozaki, M. Stereoselective synthesis of D-erythro-sphingosine and L-lyxo-phytosphingosine. *Tetrahedron*, **2001**, *57*, 9087-92.

[87] Duclos, R. I. The total syntheses of D-erythro-sphingosine, N-palmitoylsphingosine (ceramide), and glucosylceramide (cerebroside) via an azidosphingosine analog. *Chem. Phys. Lipids*, **2001**, *111*, 111-38.

[88] Milne, J. E.; Jarowicki, K.; Kocienski, P. J.; Alonso, J. Synthesis of D-erythro-sphingosine and D-erythro-ceramide. *Chem. Commun.*, **2002**, 426-7.

[89] Lee, J.-M.; Lim, H.-S.; Chung, S.-K. A short and efficient stereoselective synthesis of all four diastereomers of sphingosine. *Tetrahedron Asymmetry*, **2002**, *13*, 343-47.

[90] Kang, S. H.; Hwang, Y. S.; Lee, H. S. A Stereocontrolled Synthesis of D-erythro-Sphingosine and D-ribo-Phytosphingsine. *Bull. Korean Chem. Soc.*, **2002**, *23*, 1195-96.

[91] Olofsson, B.; Somfai, P. Divergent Synthesis of D-erythro-Sphingosine, L-threo-Sphingosine, and Their Regioisomers. *J. Org. Chem.*, **2003**, *68*, 2514-17.

[92] Chun, J.; Li, G.; Byun, H.-S.; Bittman, R. A concise route to d-erythro-sphingosine from N-Boc-l-serine derivatives via sulfoxide or sulfone intermediates. *Tetrahedron Lett.*, **2002**, *43*, 375-77.

[93] van den Berg, R. J. B. H. N.; Korevaar, C. G. N.; van der Marel, G. A.; Overkleeft, H. S.; van Boom, J. H. A simple and low cost synthesis of d-erythro-sphingosine and d-erythro-azidosphingosine from d-ribo-phytosphingosine: glycosphingolipid precursors. *Tetrahedron Lett.*, **2002**, *43*, 8409-12.

[94] Wild, R.; Schmidt, R. R. Sphingosine and phytosphingosine from D-threose synthesis of a 4-keto-ceramide. *Tetrahedron Asymmetry*, **1994**, *5*, 2195-208.

[95] van den Berg, R. J.; Korevaar, C. G.; Overkleeft, H. S.; van der Marel, G. A.; van Boom, J. H. Effective, high-yielding, and stereospecific total synthesis of D-erythro-(2R,3S)-sphingosine from D-ribo-(2S,3S,4R)-phytosphingosine. *J Org Chem*, **2004**, *69*, 5699-704.

[96] Kolb, H. C.; Sharpless, K. B. A simplified procedure for the stereospecific transformation of 1,2-diols into epoxides *Tetrahedron*, **1992**, *48*, 10515-30.

[97] Szeja, W. Phase Transfer-Catalyzed Preparation of Oxiranes. *Synthesis*, **1985**, 983-85.

[98] Raghavan, S.; Rajender, A. Novel, short, stereospecific synthesis of lyxo-(2R,3R,4R)-phytosphingosine and erythro-(2R,3S)-sphingosine. *J Org Chem*, **2003**, *68*, 7094-7.

[99] Torssell, S.; Somfai, P. A practical synthesis of D-erythro-sphingosine using a cross-metathesis approach. *Org. Biomol. Chem.*, **2004**, *2*, 1643-46.

[100] Romero, A.; Wong, C.-H. Chemo-Enzymatic Total Synthesis of 3-Epiaustraline, Australine, and 7-Epialexine. *J. Org. Chem.*, **2000**, *65*, 8264-68.

[101] Rai, A. N.; Basu, A. Synthesis of the Glycosphingolipid β-Galactosyl Ceramide and Analogues via Olefin Cross Metathesis. *J. Org. Chem.*, **2005**, *70*, 8228-30.

[102] Rai, A. N.; Basu, A. Sphingolipid Synthesis via Olefin Cross Metathesis: Preparation of a Differentially Protected Building Block and Application to the Synthesis of D-erythro-Ceramide. *Org. Lett.*, **2004**, *6*, 2861-63.

[103] Bundle, D.; Ling, C. C. Synthetic Methods for the Large Scale Production from Glucose of Analogs of Sphingosine, Azidosphingosine, Ceramides, Lactosyl Ceramides, and Glycosyl Phytosphingosine **2003**, *WO/2003/101937*.

[104] Lu, X.; Bittman, R. Efficient and versatile synthesis of (2S,3R)-sphingosine and its 2-azido-3-O-benzylsphingosine analogue. *Tetrahedron Lett.*, **2005**, *46*, 1873-75.

[105] Disadee, W.; Ishikawa, T. Chirality transfer from guanidinium ylides to 3-alkenyl (or 3-alkynyl) aziridine-2-carboxylates and application to the syntheses of (2R,3S)-3-hydroxyleucinate and D-erythro-sphingosine. *J Org Chem*, **2005**, *70*, 9399-406.

[106] Chaudhari, V. D.; Kumar, K. S. A.; Dhavale, D. D. An Efficient Synthesis of D-erythro- and D-threo-Sphingosine from D-Glucose: Olefin Cross-Metathesis Approach. *Org. Lett.*, **2005**, *7*, 5805-07.

[107] Gruner, S. A. W.; Kéri, G.; Schwab, R.; Venetianer, A.; Kessler, H. Sugar Amino Acid Containing Somatostatin Analogues that Induce Apoptosis in Both Drug-Sensitive and Multidrug-Resistant Tumor Cells. *Org. Lett.*, **2001**, *6*, 3723-25.

[108] Merino, P.; Jimenez, P.; Tejero, T. Enantiodivergent Synthesis of D- and L-erythro-Sphingosines through Mannich-Type Reactions of N-Benzyl-2,3-O-isopropylidene-D-glyceraldehyde Nitrone. *J. Org. Chem.*, **2006**, *71*, 4685-88.

[109] Merino, P.; Franco, S.; Merchan, F. L.; Tejero, T. Diastereoselective nucleophilic addition of acetylide to N-benzyl-2,3-O-isopropylidene-D-glyceraldehyde nitrone (BIGN). Stereodivergent synthesis of 13-hydroxy-oc-(hydroxyamino)- and 13-hydroxy- o -amino acids. *Tetrahedron Asymmetry*, **1997**, *8*, 3489-96.

[110] Hamura, T.; Hosoya, T.; Yamaguchi, H.; Kuriyama, Y.; Tanabe, M.; Miyamoto, M.; Yasui, Y.; Matsumoto, T.; Suzuki, K. Facile Access to Versatile Polyaromatic Building Blocks: Selectively Protected Benzocyclobutenedione Derivatives via Regioselective [2+2] Cycloaddition of -Alkoxybenzyne and Ketene Silyl Acetal. *Tetrahedron Asymmetry*, **2002**, *85*, 3589-604.

[111] Kim, S.; Lee, S.; Lee, T.; Ko, H.; Kim, D. Efficient Synthesis of D-erythro-Sphingosine and D-erythro-Azidosphingosine from D-ribo-Phytosphingosine via a Cyclic Sulfate Intermediate. *J. Org. Chem.*, **2006**, *71*, 8661-64.

[112] Righi, G.; Ciambrone, S.; D'Achille, C.; Leonelli, A.; Bonini, C. Highly efficient stereoselective synthesis of d-erythro-sphingosine and d-lyxo-phytosphingosine. *Tetrahedron*, **2006**, *62*, 11821-26.

[113] Tuch, A.; Saniere, M.; Le Merrer, Y.; Depezay, J.-C. Enantiopure Aminotriol from D-Isoascorbic Acid. Synthesis of D-Threo-C-18-Sphingosine. *Tetrahedron Asymmetry*, **1996**, *7*, 897-906.

[114] Yamamoto, T.; Hasegawa, H.; Hakogi, T.; Katsumura, S. Versatile synthetic method for sphingolipids and functionalized sphingosine derivatives via olefin cross metathesis. *Org. Lett.*, **2006**, *8*, 5569-72.

[115] Pham, V. T.; Joo, J. E.; Tian, Y. S.; Oh, C. Y.; Ham, W. H. A concise synthesis of a promising protein kinase C inhibitor: D-erythro-sphingosine. *Arch. Pharm. Res.*, **2007**, *30*, 22-7.

[116] Yang, H.; Liebeskind, L. S. A Concise and Scalable Synthesis of High Enantiopurity (-)-D-erythro-Sphingosine Using Peptidyl Thiol Ester-Boronic Acid Cross-Coupling. *Org. Lett.*, **2007**, *9*, 2993-95.

[117] Stewart, M. E.; Downing, D. T. A new 6-hydroxy-4-sphingenine-containing ceramide in human skin. *J. Lipid. Res.*, **1999**, *40*, 1434-9.

[118] Chun, J.; Byun, H.-S.; Bittman, R. First Asymmetric Synthesis of 6-Hydroxy-4-Sphingenine-Containing Ceramides. Use of Chiral Propargylic Alcohols To Prepare a Lipid Found in Human Skin. *J. Org. Chem.*, **2003**, *68*, 348-54.

[119] Yadav, J. S.; Geetha, V.; Krishnam, R. A.; Gnaneshwar, D.; Chandrasekhar, S. The first total synthesis of the 6-hydroxy-4E-sphingenines. *Tetrahedron Lett.*, **2003**, *44*, 2983-85.

[120] Mori, K.; Masuda, Y. Synthesis and stereochemistry of ceramide B, (2S,3R,4E,6R)-N-(30-hydroxytriacontanoyl)-6-hydroxy-4-sphingenine, a new ceramide in human epidermis. *Tetrahedron Lett.*, **2003**, *44*, 9193-96.

[121] Mori, K.; Matsuda, H. Synthesis of sphingosine relatives, X. Synthesis of (2S,3R,4E)-1-O-(β-D-glucopyranosyl)-N-[30'-(linoleoyloxy)triacontanoyl]-4-icosasphingenine, a new esterified cerebroside isolated from human and pig epidermis. *Liebigs Ann. Chem.*, **1991**, *1991*, 529-35.

[122] Müller, S.; Schmidt, R. R. Synthesis of two Unique Compounds, a Ceramide and a Cerebroside, Occurring in Human Stratum Corneum. *J. Prakt. Chem.*, **2000**, *342*, 779-84.

[123] Koike, K.; Sugimoto, M.; Nakahara, Y.; Ogawa, T. Total synthesis of cerebrosides: (2S, 3R, 4E)-1-O-β--galactopyranosyl-N-(2′R and 2′S)-2′-hydroxytetracosanoylsphingenine. *Carbohydr. Res.*, **1987**, *162*, 237-46.

[124] Horn, D. H. S.; Pretorius, Y. Y. Wool wax. Part VI. The synthesis and stereochemistry of the straight-chain α-hydroxy-acids. *J. Chem. Soc.*, **1954**, 1460-64.

[125] Mitsunobu, O.; Eguchi, M. Preparation of Carboxylic Esters and Phosphoric Esters by the Activation of Alcohols. *Bull. Chem. Soc. Jpn.*, **1971**, *44*, 237-46.

[126] Van den Berg, M. A.; Streekstra, H. Microbial Strains Producing Sphingosine **2007**, *EP1767644 (A1)*.

[127] Kessner, D.; Ruettinger, A.; Kiselev, M. A.; Wartewig, S.; Neubert, R. H. Properties of ceramides and their impact on the stratum corneum structure. Part 2: stratum corneum lipid model systems. *Skin. Pharmacol. Physiol.*, **2008**, *21*, 58-74.

[128] Gooris, G. S.; Bouwstra, J. A. Infrared spectroscopic study of stratum corneum model membranes prepared from human ceramides, cholesterol, and fatty acids. *Biophys. J.*, **2007**, *92*, 2785-95.

[129] de Jager, M.; Groenink, W.; Bielsa i Guivernau, R.; Andersson, E.; Angelova, N.; Ponec, M.; Bouwstra, J. A novel in vitro percutaneous penetration model: evaluation of barrier properties with p-aminobenzoic acid and two of its derivatives. *Pharm. Res.*, **2006**, *23*, 951-60.

[130] de Jager, M.; Groenink, W.; Bielsa, I. G. R.; Andersson, E.; Angelova, N.; Ponec, M.; Bouwstra, J. A Novel in Vitro Percutaneous Penetration Model: Evaluation of Barrier Properties with P-Aminobenzoic Acid and Two of Its Derivatives. *Pharm. Res.*, **2006**.

[131] de Jager, M.; Groenink, W.; van der Spek, J.; Janmaat, C.; Gooris, G.; Ponec, M.; Bouwstra, J. Preparation and characterization of a stratum corneum substitute for in vitro percutaneous penetration studies. *Biochim. Biophys. Acta*, **2006**, *1758*, 636-44.

[132] Groen, D.; Gooris, G. S.; Ponec, M.; Bouwstra, J. A. Two new methods for preparing a unique stratum corneum substitute. *Biochim. Biophys. Acta*, **2008**, *1778*, 2421-9.

3. Dimethylamino acid esters as biodegradable and reversible transdermal permeation enhancers: effects of linking chain length, chirality and polyfluorination

Pharm Res, **2008**, 26(4), 811-21

Jakub Novotný, Petra Kovaříková, Michal Novotný, Barbora Janůšová, Alexandr Hrabálek, Kateřina Vávrová

ABSTRACT

Purpose. Series of *N,N*-dimethylamino acid esters was synthesized to study their transdermal permeation-enhancing potency, biodegradability and reversibility of action. Effects of chirality, linking chain length and polyfluorination were investigated.
Methods. *In vitro* activities were evaluated using porcine skin and four model drugs – theophylline, hydrocortisone, adefovir and indomethacin. Biodegradability was determined using porcine esterase, reversibility was measured using electrical resistance.
Results. No differences in activity were found between (*R*), (*S*) and racemic dodecyl 2-(dimethylamino)propanoate (DDAIP). Substitution of hydrocarbon tail by fluorocarbon one resulted in loss of activity. Replacement of branched linking chain between nitrogen and ester of DDAIP by linear one markedly improved penetration-enhancing activity with optimum in 4-6C acid derivatives. Dodecyl 6-(dimethylamino)hexanoate (DDAK) was more potent than clinically used skin absorption enhancer DDAIP for theophylline (enhancement ratio of DDAK and DDAIP was 17.3 and 5.9, respectively), hydrocortisone (43.2 and 11.5) and adefovir (13.6 and 2.8), while DDAIP was better enhancer for indomethacin (8.7 and 22.8). DDAK was rapidly metabolized by porcine esterase, and displayed low acute toxicity. Electrical resistance of DDAK-treated skin barrier promptly recovered to control values.
Conclusion. DDAK, highly effective, broad-spectrum, biodegradable and reversible transdermal permeation enhancer, is promising candidate for future research.

INTRODUCTION

Transdermal drug delivery offers many advantages compared to the conventional routes of application including avoidance of the first pass effect, stable blood levels, easy application and higher compliance of the patient [1, 2]. However, physicochemical properties of the majority of clinically used drugs do not allow them to overcome the skin barrier, which is represented mainly by the uppermost epidermal layer, the stratum corneum (SC). One of the possibilities to temporarily decrease the skin barrier resistance is the use of permeation enhancers [3-5]. These compounds promote the permeation of topically applied drugs through SC to achieve the therapeutic concentrations necessary for local or systemic effect. Although hundreds of permeation enhancers have been identified to date, no ideal compound possessing high activity and low toxicity has been found, and the structure-activity relationships are still poorly understood.

Amino acid derivatives belong to the most promising groups of permeation enhancers. Dodecyl 2-(dimethylamino)propanoate (DDAIP, NexACT®, Figure 1), based on the amino acid alanine, is a clinically used biodegradable transdermal permeation enhancer [6]. It is effective in promoting the transdermal permeation of several types of drugs by mechanisms including disordering the lipid organization [7-9], keratin interaction [10] and drug complexation [11]. Moreover, DDAIP and its hydrochloride salt have low toxicity, are rapidly

metabolized by esterases, and are well tolerated on skin [12]. For a review on dimethylamino acid-based enhancers, see Ref. [10].

Being an alanine derivative, DDAIP bears a chiral centre within its polar head. Since the SC lipids, in particular the polar head groups of ceramides, represent a chiral environment, the interaction between DDAIP and skin lipids [7] may be of a stereoselective nature. For a review on chirality in skin permeation, see [5] and [13]. Previously, no difference in enhancing effect of (*R*), (*S*) and racemic 6-aminohexanoic acid 2-octyl ester was found [14]. However, those compounds are relatively weak enhancers with the chiral centre in the hydrophobic chain, not in the polar head, which is expected to interact with the chiral polar heads of ceramides. Therefore, we focused on DDAIP as a model chiral enhancer to evaluate the hypothesis that the enhancer action may be dependent on its configuration.

DDAIP is an amphiphilic substance possessing a bulky polar head and a 12C alkyl chain. The structure-activity relationships of enhancer hydrophobic chain(s) are well documented with the optimum usually at around 10-12 carbons in saturated chains [15, 16]. Nevertheless, there is no study concerned with the effect of polyfluorination of an enhancer. Fluorocarbon chains in general have exceptional chemical and biological inertness, unique hydro and lipophobicity, have greater cross-sectional area, are stiffer, and fluorocarbon surfactants are more surface-active than their hydrocarbon analogues [17, 18]. Highly fluorinated materials have potential as pulmonary, topical and ophthalmological drug delivery systems [19]. All of these properties may influence the enhancer behavior in the skin barrier.

Another structural feature of DDAIP is that the dimethylamino group is positioned on the α-carbon resulting in a sterically demanding polar head group. We have previously described dodecyl 6-(dimethylamino)hexanoate (DDAK, Figure 1) being even more active enhancer than DDAIP for theophylline [20] and adefovir [21, 22]. DDAK was designed by combining the 5-carbon linking group between the ionizable nitrogen and the enzymatically labile ester group of Transkarbam 12, a highly potent non-toxic permeation enhancer [21, 23], and the *N*,*N*-dimethylamino polar head from DDAIP. Based on these findings, we aimed to compare DDAIP and DDAK in a greater detail, particularly the linking chain structure.

The purpose of this study was to synthesize a series of DDAIP analogues to study the effects of chirality, polyfluorination and linking chain length on their transdermal permeation-enhancing potency. We aimed to evaluate their activity using four model drugs with distinct physicochemical properties, determine the biodegradability of the most potent compound by porcine esterase, and confirm the reversibility of its action by transdermal electrical resistance measurement.

MATERIALS AND METHODS

Chemicals and instrumentation

All chemicals were purchased from Sigma-Aldrich (Schnelldorf, Germany). Silica gel 60 (230-400 mesh) for column chromatography and TLC plates (silica gel 60 F_{254}, aluminum back) were obtained from Merck (Darmstadt, Germany). The structure and purity of the synthesized compounds were confirmed by FTIR (Nicolet Impact 400 spectrophotometer) and ^{1}H and ^{13}C NMR spectra (Varian Mercury-Vx BB 300 instrument, operating at 300 MHz for ^{1}H, 75 MHz for ^{13}C) and optically active compounds were characterized by their optical rotation (ADP Bellingham and Stanley Polarimeter; 1.0 dm cell). The melting points were measured with a Kofler apparatus, and are uncorrected.

Synthesis

General procedure for the preparation of the bromocarboxylic acid esters (**2a**, **2c-2g**). 9.8 mmol of a bromo acid, 9.8 mmol of an alcohol and 0.12 g (0.98 mmol) of 4-dimethylaminopyridine (DMAP) in 20 ml of ethyl acetate was cooled to 0°C and 2.22 g (10.8 mmol) of dicyclohexylcarbodiimide (DCC) in 15 ml of ethyl acetate was added. The reaction was allowed to reach room temperature, and then was stirred overnight. The unreacted DCC was removed by addition of a droplet of acetic acid. The resulting dicyclohexylurea was filtered off and washed with small amount of ethyl acetate. After a water/diethyl ether extraction work up, the pure product was obtained as a colorless liquid by column chromatography using ethyl acetate/hexane elution system.

Dodecyl 2-bromopropanoate (**2a**). Yield = 87%. ^{1}H NMR (300 MHz, $CHCl_3$): δ 4.36 (q; J=6.9 Hz; 1H), 4.09-4.22 (m; 2H), 1.82 (d; J=6.9; 3H), 1.61-1.71 (m; 2H), 1.26-1.38 (m; 18H), 0.88 (t; J=6.6 Hz; 3H); ^{13}C NMR (75 MHz, $CHCl_3$): δ 170.3, 66.1, 40.3, 31.9, 29.6, 29.5, 29.3, 29.2, 28.4, 25.7, 22.7, 21.7, 14.1; IR (ATR): ν_{max} 2922, 2853, 1739, 1219, 1157 cm^{-1}.

Dodecyl 4-bromobutanoate (**2c**). Yield = 72%. ^{1}H NMR (300 MHz, $CHCl_3$): δ 4.07 (t, J = 6.7 Hz, 2H), 3.46 (t, J = 6.5 Hz, 2H), 2.49 (t, J = 7.2 Hz, 2H), 2.12-2.21 (m, 2H), 1.57-1.67 (m, 2H), 1.25-1.41 (m; 18H), 0.87 (t, J = 6.7 Hz; 3H); ^{13}C NMR (75 MHz, $CHCl_3$): δ 170.3, 65.2, 37.8, 31.9, 29.6, 29.5, 29.4, 29.3, 29.2, 28.5, 25.8, 22.7, 21.7, 14.1; IR (ATR): ν_{max} 2922, 2853, 1734, 1198, 1170 cm^{-1}.

Dodecyl 5-bromopentanoate (**2d**). Yield = 84%. ^{1}H NMR (300 MHz, $CHCl_3$): δ 4.06 (t, J = 6.7 Hz, 2H), 3.41 (t, J = 6.5 Hz, 2H), 2.33 (t, J = 7.5 Hz, 2H), 1.74-1.94 (m, 4H), 1.56-1.69 (m, 2H), 1.25-1.41 (m; 18H), 0.87 (t, J = 6.7 Hz; 3H); ^{13}C NMR (75 MHz, $CHCl_3$): δ 173.2, 64.6, 33.3, 33.0, 31.0, 29.6, 29.5, 29.3, 29.2, 28.6, 25.9, 23.5, 22.7, 14.1; IR (ATR): ν_{max} 2922, 2853, 1731, 1458, 1253, 1170 cm^{-1}.

Dodecyl 6-bromohexanoate (**2e**). Yield = 83%. ^{1}H NMR (300 MHz, $CHCl_3$): δ 4.05 (t; J=6.7 Hz; 2H), 3.40 (t; J=6.7 Hz; 2H), 2.31 (t; J=7.4 Hz; 2H), 1.83-1.92 (m; 2H), 1.56-1.70 (m; 4H), 1.42-1.52 (m; 2H), 1.25-1.30 (m; 18H), 0.87 (t; J=6.7 Hz; 3H); ^{13}C NMR (75 MHz, $CHCl_3$): δ 173.5, 64.5, 34.1, 33.4, 32.4, 31.9, 29.6, 29.5, 29.3, 29.2, 28.6, 27.6, 25.9, 24.1, 22.7, 14.1; IR (ATR): ν_{max} 2923, 2853, 1734, 1463, 1253, 1173 cm^{-1}.

Dodecyl 8-bromooctanoate (**2f**). Yield = 56%. ^{1}H NMR (300 MHz, $CHCl_3$): δ 4.05 (t; J=6.9 Hz; 2H), 3.40 (t; J=6.9 Hz; 2H), 2.29 (t; J=7.5 Hz; 2H), 1.80-1.90 (m; 2H), 1.56-1.67 (m; 4H), 1.26-1.48 (m; 24H), 0.88 (t; J=6.6 Hz; 3H); ^{13}C NMR (75 MHz, $CHCl_3$): δ 173.9, 64.5, 34.3, 33.9, 32.7, 31.9, 29.6, 29.3, 29.2, 28.9, 28.6, 28.4, 27.9, 25.9, 24.9, 22.7, 14.1; IR (ATR): ν_{max} 2923, 2853, 1735, 1465, 1458, 1235, 1173 cm^{-1}.

1H,1H,2H,2H-Perfluorodecyl 2-bromopropanoate (**2g**). Yield = 88%. ^{1}H NMR (300 MHz, $CHCl_3$): δ 4.48 (t; J=6.4 Hz; 2H), 4.37 (q; J=6.9 Hz; 1H), 2.60-2.44 (m; 2H), 1.83 (d; J=7.0 Hz; 3H); ^{13}C NMR (75 MHz, $CHCl_3$): δ 169.8, 57.7, 39.3, 30.6, 30.3, 30.1, 21.4; IR (ATR): ν_{max} 2982, 2930, 1748, 1449, 1206, 1152 cm^{-1}.

Dodecyl 3-bromopropanoate (**2b**). 1.50 g (9.8 mmol) of 3-bromopropanoic acid was refluxed with 5 ml of thionyl chloride for two hours. Thionyl chloride was evaporated under vacuum, the residue dissolved in 5 ml of chloroform and added to the solution of 1.83 g (9.8 mmol) of dodecanol in 8 ml of chloroform. The mixture was kept under reflux for six hours. The product was purified on silica with hexane/ethyl acetate. Yield = 66%. ^{1}H NMR (300

MHz, $CHCl_3$): δ 4.12 (t; J = 6.7 Hz; 2H), 3.58 (t; J = 6.9 Hz; 2H), 2.91 (t; J = 6.9 Hz; 2H), 1.58-1.68 (m; 2H), 1.26-1.44 (m; 16H), 0.88 (t; J = 6.7 Hz; 3H); ^{13}C NMR (75 MHz, $CHCl_3$): δ 172.6, 64.8, 32.7, 32.5, 31.9, 29.6, 29.5, 29.3, 29.2, 28.6, 27.8, 25.9, 22.7, 14.1; IR (ATR): ν_{max} 2922, 2853, 1737, 1466, 1234, 1172 cm^{-1}.

General procedure for the preparation of *N,N*-dimethylaminoalkanoates (**3a-3g**). 4.67 mmol of the bromo ester **2a-2g** was dissolved in 10 ml of tetrahydrofurane (THF). 11 ml of 2.0M dimethylamine solution in THF was added by syringe and the mixture was stirred for 24 h at room temperature. The suspension was filtered and the filtrate was concentrated under vacuum. Compounds **3a, 3e, 3f** and **3g** were purified on silica column using hexane/ethyl acetate – ethyl acetate. The other compounds (**3b-d**) were dissolved in 50 ml of dry diethyl ether and gently bubbled with hydrogen chloride. White crystals of an ammonium salt appeared immediately and the mixture was bubbled with nitrogen to remove the unreacted hydrogen chloride. The solid was filtered off and recrystallized from chloroform/diethyl ether. The crystals were suspended in diethyl ether, corresponding amount of 5% solution of hydrogen carbonate was added and the free base was extracted. The organic phase was separated, treated with saturated solution of KBr, dried over sodium sulfate and concentrated in vacuum yielding colorless oily liquid.

Dodecyl 2-(dimethylamino)propanoate (**3a**, DDAIP). Yield = 96%. ^1H NMR (300 MHz, $CHCl_3$): δ 4.08-4.13 (m; 2H), 3.18-3.25 (q; J=7.0 Hz; 1H), 2.34 (s; 6H), 1.59-1.69 (m; 2H), 1.25-1.29 (m; 21H), 0.87 (t; J=6.9 Hz; 3H); ^{13}C NMR (75 MHz, $CHCl_3$): δ 173.3, 64.5, 62.9, 41.8, 31.9, 29.6, 29.5, 29.3, 29.2, 28.7, 25.9, 22.7, 15.1, 14.1; IR (ATR): ν_{max} 2923, 2853, 1731, 1454, 1167 cm^{-1}.

Dodecyl 3-(dimethylamino)propanoate (**3b**). Yield = 86%. ^1H NMR (300 MHz, $CHCl_3$): δ 4.06 (t; J=6.9 Hz; 2H), 2.61 (t; J=7.2 Hz; 2H), 2.47 (t; J=6.9 Hz; 2H), 2.24 (s; 6H), 1.56-1.65 (m; 2H), 1.25-1.35 (m; 18H), 0.87 (t; J=6.9 Hz; 3H); ^{13}C NMR (75 MHz, $CHCl_3$): δ 172.6, 64.6, 54.7, 45.2, 32.9, 31.9, 29.6, 29.5, 29.3, 29.2, 28.6, 25.9, 22.7, 14.1; IR (ATR): ν_{max} 2923, 2853, 1736, 1461, 1168 cm^{-1}.

Dodecyl 4-(dimethylamino)butanoate (**3c**). Yield = 71%. ^1H NMR (300 MHz, $CHCl_3$): δ 4.05 (t; J=6.9 Hz; 2H), 2.26-2.36 (m; 4H), 2.22 (s; 6H), 1.74-1.84 (m; 2H), 1.56-1.65 (m; 2H), 1.25-1.35 (m; 18H), 0.88 (t; J=6.9 Hz; 3H); ^{13}C NMR (75 MHz, $CHCl_3$): δ 173.6, 64.5, 58.5, 45.3, 32.1, 31.9, 29.6, 29.5, 29.3, 29.2, 28.6, 25.9, 22.9, 22.6, 14.1; IR (ATR): ν_{max} 2923, 2853, 1736, 1461, 1181 cm^{-1}.

Dodecyl 5-(dimethylamino)pentanoate (**3d**). Yield = 60%. ^1H NMR (300 MHz, $CHCl_3$): δ 4.04 (t; J=6.9 Hz; 2H), 2.31(t; J=7.2 Hz; 2H), 2.25 (t; J=7.2 Hz; 2H), 2.20 (s; 6H), 1.55-1.56 (m; 4H), 1.43-1.53 (m; 2H), 1.25-1.36 (m; 18H), 0.87 (t; J=6.9 Hz; 3H); ^{13}C NMR (75 MHz, $CHCl_3$): δ 173.7, 64.5, 59.3, 45.5, 34.2, 31.9, 29.6, 29.5, 29.3, 29.2, 28.6, 27.2, 25.9, 22.8, 22.7, 14.1; IR (ATR): ν_{max} 2923, 2853, 1736, 1459, 1174 cm^{-1}.

Dodecyl 6-(dimethylamino)hexanoate (**3e**, DDAK). Yield = 80%. ^1H NMR (300 MHz, $CHCl_3$): δ 4.04 (t; J=6.9 Hz; 2H), 2.29 (t; J=7.5 Hz; 2H), 2.23 (t; J=7.5 Hz; 2H), 2.20 (s; 6H), 1.55-1.68 (m; 4H), 1.42-1.52 (m; 2H), 1.25-1.37 (m; 20H), 0.87 (t; J=6.9 Hz; 3H); ^{13}C NMR (75 MHz, $CHCl_3$): δ 173.8, 64.4, 59.6, 45.5, 34.3, 31.9, 29.6, 29.5, 29.3, 29.2, 28.6, 27.4, 27.0, 25.9, 24.9, 22.7, 14.1; IR (ATR): ν_{max} 2923, 2853, 1736, 1459, 1170 cm^{-1}.

Dodecyl 8-(dimethylamino)octanoate (**3f**). Yield = 87%. ^{1}H NMR (300 MHz, $CHCl_3$): δ 4.05 (t; J=6.9 Hz; 2H), 2.28 (t; J=7.5 Hz; 2H), 2.22 (t; J=7.2 Hz; 2H), 2.20 (s; 6H), 1.56-1.66 (m; 4H), 1.39-1.49 (m; 2H), 1.25-1.31 (m; 24H), 0.87 (t; J=6.9 Hz; 3H); ^{13}C NMR (75 MHz, $CHCl_3$): δ 173.9, 64.4, 59.9, 45.5, 34.4, 31.9, 29.6, 29.5, 29.3, 29.2, 29.1, 28.6, 27.7, 27.3, 25.9, 25.0, 22.7; 14.1; IR (ATR): ν_{max} 2924, 2853, 1736, 1459, 1168 cm^{-1}.

1H,1H,2H,2H-Perfluorodecyl 2-(dimethylamino)propanoate (**3g**). Yield = 86%. ^{1}H NMR (300 MHz, $CHCl_3$): δ 4.42 (t; J=6.4 Hz; 2H), 3.26 (q; J=7.0 Hz; 1H), 2.41-2.58 (m; 2H), 2.34 (s; 6H), 1.29 (d; J=7.0 Hz; 3H); ^{13}C NMR (75 MHz, $CHCl_3$): δ 172.8, 62.7, 56.2, 41.6, 30.9, 30.6, 30.3, 14.7; IR (ATR): ν_{max} 2985, 2945, 2873, 2834, 2787, 1735, 1458 cm^{-1}.

Preparation of DDAIP enantiomers.

2-(*tert*-butoxycarbonylamino)propanoic acid (**4h**, **4i**). 1.47 g (6.74 mmol) of di-*tert*-butyl dicarbonate in 6 ml of dioxane was added to an ice cold solution of 0.5 g (5.61 mmol) of L- or D-alanine in 10 ml of 1M sodium hydroxide. The reaction was stirred for 0.5 h at 5 °C and subsequently for 3.5 h at room temperature. The mixture was concentrated to half of its volume on rotary evaporator, cooled to 0 °C, and acidified to pH 2-3 by slow addition of 1N $KHSO_4$. Product was extracted with ethyl acetate, dried over Na_2SO_4 and concentrated under vacuum providing white crystalline solid with melting point of 81-82°C. (*R*)-isomer (**4h).** Yield = 90 %. (*S*)-isomer (**4i**). Yield = 93 %. ^{1}H NMR (300 MHz, $CHCl_3$): δ 5.05 (d; J=5.7 Hz; 1H), 4.34 (m; 1H), 1.45 (s; 9H), 1.43 (s; 3H); ^{13}C NMR (75 MHz, $CHCl_3$): δ 177.9, 155.4, 80.3, 49.1, 28.3, 18.3.

Dodecyl 2-(tert-butoxycarbonylamino)propanoate (**5h**, **5i**). 1.00 g (5.29 mmol) of the protected acid **4h** or **4i**, 0.99 g (5.29 mmol) of dodecanol and 0.065 g (0.53 mmol) of DMAP was dissolved in 10 ml of ethyl acetate. The mixture was cooled to 0 °C and 1.20 g (5.82 mmol) of DCC in 10 ml of ethyl acetate was added. The mixture was allowed to warm to room temperature and stirred for additional 24h. Subsequently, the reaction was quenched by addition of a droplet of acetic acid and filtered. The filtrate was concentrated under vacuum, and purified on silica column using hexane/ethyl acetate 19:1. (*R*)-isomer (**5h).** Yield = 65 %. $[\alpha]_D^{22.7°C}$ = 2.77° (1.0, $CHCl_3$), (*S*)-isomer (**5i**). Yield = 68 %. $[\alpha]_D^{22.9°C}$ = -2.84° (1.0, $CHCl_3$). ^{1}H NMR (300 MHz, $CHCl_3$): δ 5.05 (d; J=5.7 Hz; 1H), 4.29 (m; 1H), 4.9-4.15 (m; 2H), 1.63 (m; 2H), 1.44 (s; 9H), 1.37 (d; J=7.2 Hz; 3H), 1.25-1.32 (m; 18H), 0.87 (t; J=6.7 Hz; 3H); ^{13}C NMR (75 MHz, $CHCl_3$): δ 173.4, 155.1, 79.7, 65.5, 49.2, 31.9, 29.6, 29.5, 29.3, 29.2, 28.5, 28.3, 25.8, 22.7, 18.8, 14.1.

Dodecyl 2-aminopropanoate. 5 ml of trifluoroacetic acid (TFA)/dichlomethane (1:1 v/v) mixture was added to 0.5 g (1.40 mmol) of the *N*-protected ester (**5h, 5i**). TLC (butanol/water/acetic acid 4:1:1, Rf = 0.79) indicated a full deprotection of the amino group in 30 min. The solvent was evaporated in vacuum, oily residue dissolved in 20 ml of dichloromethane, cooled on ice and neutralized with 25 ml of ice cold 2% solution of sodium bicarbonate. The aqueous phase was extracted with additional 2×20 ml of dichloromethane. The organic phase was dried over sodium sulfate, concentrated and used without further purification.

Dodecyl 2-(dimethylamino)propanoate (**6h**, **6i**). 0.35 g (1.35 mmol) of dodecyl 2-aminopropanoate was dissolved in 20 ml of dry dichloromethane and 214 µl of 35% formaldehyde solution was added. Then, 1.14 g (5.38 mmol) of sodium triacetoxyborohydride [24] was added and the mixture was stirred for two hours at room temperature. The reaction was cooled to 0 °C and extracted with 0.25M sodium bicarbonate. The products were

obtained after separation on silica using hexane/ethyl acetate 4:1 as a colorless liquid. (*R*)-isomer (**6h).** Yield = 82 %. $[\alpha]_D^{22°C}$ = 12.5° (1.0, $CHCl_3$), (*S*)-isomer (**6i).** Yield = 82 %. $[\alpha]_D^{22°C}$ = -12.8° (1.0, $CHCl_3$). The spectra were in accordance with racemic DDAIP (**3a**).

Donor samples

The composition of the donor samples is listed in Table I. The enhancers were added in 1% concentration (w/v). The suspension was stirred for 5 min at 50°C and then allowed to equilibrate at 37°C for 24h before the application on the skin. All the donor samples were saturated with the pertinent model drug at these concentrations.

For the determination of the effect of the studied enhancers on the solubility of the model drugs in the donor vehicle, the samples, either with or without the enhancer, were prepared in triplicate as described above. The samples were centrifuged at 10,000g for 5 min, the supernatant was withdrawn, diluted with the pertinent mobile phase and the concentration of the drug was determined by HPLC.

Table I. The properties of the model drugs and the composition of the donor samples used for the permeation experiments.

Model drug	Physicochemical properties				Donor sample		
	MW (g/mol)	mp (°C)	logP	pKa	Drug amount (%)	Vehicle	Solubility (mg/ml)
Theophylline	180	273[a]	-0.02[a]	1.5, 8.6[b]	5	60% PG	28±3
Hydrocortisone	362	220[a]	1.61[a]	-	2	60% PG	8.3±0.6
Adefovir	273	301[c]	-2.06[b]	1.2, 4.2, 6.8[d]	2	PB pH 4.8	70±7
Indomethacin	358	158[a]	4.27[a]	4.5[a]	2	60% PG	0.9±0.1

[a]Data retrieved from SRC PhysProp database (www.syrres.com).
[b]Calculated using ACD/Labs Software V8.14 for Solaris
[c]Taken from Ref. [25]
[d]Taken from Ref. [26]
PG = propylene glycol, PB = phosphate buffer

Skin

For the *in vitro* experiments, porcine skin was selected due to it is availability and permeability similar to the human skin [27-29]. Porcine ears were purchased from a local slaughterhouse. To ensure integrity of the skin barrier, ears were removed post-sacrifice before the carcass was exposed to the high-temperature cleaning procedure. Full-thickness dorsal skin was excised by blunt dissection, and hairs were carefully trimmed. The skin was then immersed in 0.03% sodium azide solution in saline for 5 min for preservation. The skin fragments were stored at -20°C up to two months.

Permeation experiments

The skin permeability was evaluated using modified Franz diffusion cells with an available diffusion area of 1 cm^2 and acceptor volume of approximately 17 ml. The porcine skin was slowly thawed, cut into pieces of 2x2 cm, mounted into the diffusion cells dermal side down and sealed with silicone grease. The acceptor compartment was filled with PBS at pH 7.4 with 0.03% of sodium azide as a preservative and the volume of the acceptor phase was measured and included into the calculation. The Franz diffusion cells with mounted skin samples were placed in a thermostated water bath with a constant temperature of 32 °C

equipped with a multi-place magnetic stirrer. After equilibration period of 1 h, 200 µl (i.e. an infinite dose) of the donor sample was applied to the SC side of the skin and covered with a glass slide. The acceptor phase was stirred at 32 °C throughout the experiment. Sink conditions were maintained for all the drugs. Samples of the acceptor phase (0.6 ml) were withdrawn at predetermined time intervals during 48 h (52 h in the case of hydrocortisone) and replaced with fresh buffer solution. The permeation experiment with hydrocortisone had to be prolonged to reach the pseudo steady-state. The cumulative amount of the drug permeated across the skin, corrected for the acceptor phase replacement was plotted against time, and the steady state flux was calculated from the linear region of the plot. Enhancement ratio (ER) was calculated as a ratio of the flux with and without the enhancer.

At the end of the permeation experiment, the diffusion cells were dismounted; the skin surface washed with 0.5 ml of ethanol and 0.5 ml of water and blotted dry. The exposed area of 1 cm^2 was punched out and weighted. The skin sample was then extracted with 5 ml of the appropriate mobile phase (or PBS at pH 7.4 for adefovir) for 48 h. The recovery was 98±2 % for theophylline, 101±7 % for indomethacin, 93±1 % for hydrocortisone and 97±2 % for adefovir [30]. The concentration of the drug in the extract was determined by HPLC.

Enzymatic hydrolysis of DDAK

DDAK (10 mg, 0.03 mmol) was dissolved in 10 ml of acetonitrile. 100 µl of this stock solution was added to 0.2 IU porcine esterase in 9.9 ml of PBS at pH 7.4 and the solution was incubated at 32°C. The samples of 0.1 ml were withdrawn in predetermined intervals during 120 min and 0.1 ml of acetonitrile was added to deactivate the enzyme. The sample was diluted with 1.8 ml of acetonitrile/ water (4:1) and assayed on HPLC/MS. Since this analytical method describes only the decomposition of DDAK, the presence of the expected hydrolysis product dodecanol was confirmed by TLC on silica gel using chloroform/methanol 9:1. The Rf values for dodecanol and DDAK were 0.82 and 0.25, respectively. The negative control containing DDAK without the esterase was prepared likewise.

HPLC conditions

The model drugs were determined by isocratic reversed-phase HPLC using LC-20AD pump, SIL-20AC autosampler and SPD-20A UV/VIS detector (Shimadzu, Kyoto, Japan). The data were analyzed using CSW v. 1.7 for Windows integrating software (Data Apex, Prague, Czech Republic).

Separation of theophylline was achieved on LiChroCART 250-4 column (LiChrospher 100 RP-18, 5 µm, Merck) at 35°C using methanol/0.1M NaH_2PO_4 4:6 (v/v) as a mobile phase. A flow rate of 1.2 ml/min was employed and the effluent was measured at 272 nm. The retention time of theophylline was 2.9±0.1 min.

Indomethacin samples were analyzed on LiChroCART 250-4 column (LiChrospher 100 RP-18, 5 µm, Merck) using a mobile phase containing acetonitrile/water/acetic acid 90:60:5 (v/v/v) at a flow rate of 1.5 ml/min at 40°C. UV absorption was monitored at 270 nm and the retention time was 3.9±0.1min.

Hydrocortisone was determined on LiChroCART 250-4 column (LiChrospher 100 RP-18, 5 µm, Merck) at 40°C using methanol/water/THF 60:40:1 (v/v/v). The flow rate was adjusted at 1.2 ml/min, absorption was measured at 252nm. The retention time of hydrocortisone was 4.2±0.1min.

Adefovir samples were analyzed on LiChroCART 250-4 column (Purospher STAR, RP-18e, 5 µm, Merck) with LiChroCART 4-4 guard column containing the same sorbent at

40°C. The mobile phase consisted of 10mM KH_2PO_4 and 2mM Bu_4NHSO_4 at pH 6.0 with 7% of acetonitrile at a flow rate of 1.5 ml/min. The detector wavelength was set at 260 nm [30].

HPLC-MS analysis of DDAK was performed using a chromatographic system LC 20A Prominence (Shimadzu, Kyoto, Japan) coupled with LCQ Max advantage mass spectrometer (Thermo Finnigan, San Jose, U.S.A.) with ESI source and an ion trap analyzer. The data were processed using Xcalibur software (Thermo Finnigan, San Jose, U.S.A.). DDAK was determined on Luna, phenyl-hexyl column (150 x 30 mm, 5 µm, Phenomenex, Aschaffenburg, Germany) at 40 °C using a mixture of 0.01% HCOOH and acetonitrile (30:70; v/v) as a mobile phase. A flow rate of 0.3 ml/min and an injection volume of 2 µl were used. The determination was made in selected ion monitoring mode on $[M+H]^+$ at m/z 328 for DDAK and m/z 356 for internal standard (dodecyl 8-dimethylaminooctanoate (**3f**)). The retention times of DDAK and the internal standard were 2.4±0.1 min and 2.7±0.1 min, respectively.

Reversibility of DDAK action

The reversibility of the skin barrier function after DDAK treatment was studied by measuring the transdermal electrical resistance using an LCR meter 4080 (Conrad electronic, Hirschau, Germany, measuring range 20 Ω – 10 MΩ, error at kΩ values < 0.5%, measuring frequency 120 kHz). The skin samples were mounted into the Franz diffusion cells, the acceptor compartments were filled with PBS at pH 7.4 and the cells were equilibrated at 32°C for 0.5 h as described above. 0.5 ml of PBS was introduced into a donor compartment and the baseline skin resistance ($k\Omega/cm^2$) was measured by stainless steel electrodes inserted into the donor and acceptor compartment. The buffer solution was removed from the donor compartment by a cotton swab, and 150 µl of the donor sample containing 1% (w/v) of DDAK in 60% propylene glycol (PG) was applied. The control cells received 150 µl of 60% PG without the enhancer. The donor samples were removed after two hours and the skin surface was washed with 0.5 ml of distilled water and gently blotted dry. The resistance was measured at predetermined time intervals during 8 h.

Data analysis

Kruskal-Wallis One Way Analysis of Variance on Ranks with Dunn's or Student-Newman-Keuls post test method was used for the statistical analysis. The skin electrical resistances were compared using *t*-test or Mann-Whitney Rank Sum Test (SigmaStat for Windows version 3.0.1). Data are presented as means ± SEM and the number of replicates is given in the pertinent figure.

RESULTS

Synthesis

The *N*,*N*-dimethylamino acid esters were prepared via carbodiimide coupling of a bromo acid and dodecanol or 1H,1H,2H,2H-perfluoro-1-decanol, except for dodecyl 3-bromopropanoate **2b**, which was synthesized from an acyl chloride, followed by a nucleophilic substitution of bromine with dimethylamine (Fig. 1). This synthetic pathway via the bromo esters was more convenient and provided better yields with easy purification of the products in comparison with our previous work starting from dimethylamino acid [20].

Solution of dimethylamine in THF provided similar yields but was easier to handle than liquid dimethylamine [6].

The above procedure could not be applied to the synthesis of (*R*)- and (*S*)-DDAIP because the substitution occurs at the chiral centre. Hence, reductive dimethylation of alanine dodecyl ester using sodium triacetoxyborohydride and formaldehyde was applied (Fig. 2) [24].

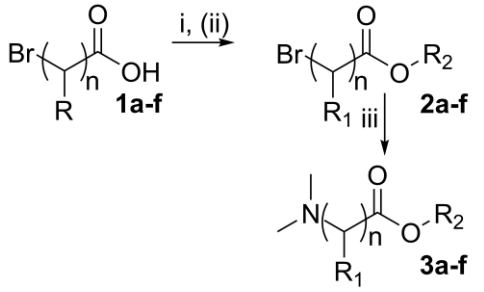

	n	R_1	R_2	synth.
a	1	$-CH_3$	$-C_{12}H_{25}$	i, iii
b	2	-H	$-C_{12}H_{25}$	ii, iii
c	3	-H	$-C_{12}H_{25}$	i, iii
d	4	-H	$-C_{12}H_{25}$	i, iii
e	5	-H	$-C_{12}H_{25}$	i, iii
f	7	-H	$-C_{12}H_{25}$	i, iii
g	1	$-CH_3$	$-C_{10}H_4F_{17}$	i, iii

Fig. 1. Synthesis of *N*,*N*-dimethylamino acid esters. Reagents and conditions: (i) dodecanol or 1H,1H,2H,2H-perfluoro-1-decanol/DCC/DMAP/ethyl acetate /0°C; (ii) 1. $SOCl_2$, reflux; 2. dodecanol/ $CHCl_3$, reflux; (iii) $(CH_3)_2NH$/THF.

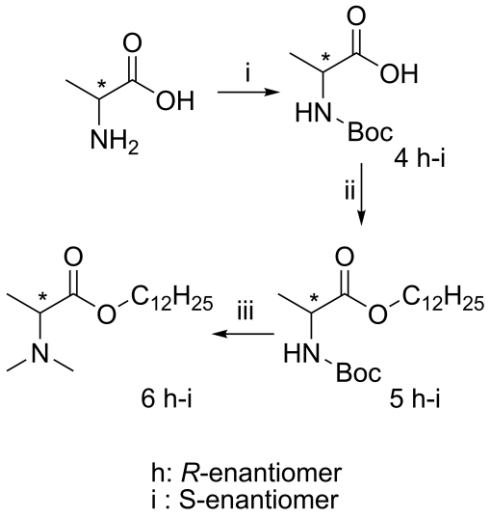

Fig. 2. Synthesis of DDAIP enantiomers. Reagents and conditions: (i) $(Boc)_2O$/1M NaOH/dioxane; (ii) $C_{12}H_{25}OH$/DCC/DMAP/ethyl acetate/0°C; (iii) 1. TFA/CH_2Cl_2 (1:1); 2. $Na[(CH_3CO)_3BH]$/35% HCHO/CH_2Cl_2.

Permeation experiments

The effect of the linking chain length on the enhancing activity of the prepared compounds was evaluated using theophylline as the model drug. The basic physicochemical characteristics of this drug are listed in Table I. The theophylline flux through the porcine skin without an enhancer was 2.4±2.5 μg/cm^2/h, and the skin concentration was 436 μg/g. All of the synthesized dimethylamino acid dodecyl esters significantly increased the theophylline permeation (Fig. 3). DDAIP enhanced the theophylline flux 5.9 times to 13.9 μg/cm^2/h with no significant difference between the (*R*) and (*S*)-enantiomers and the racemate. Its straight-chain isomer **3b**, i.e. 3-(dimethylamino)propionate, displayed significantly higher activity than DDAIP with enhancement ratio (ER) of 15.0. The highest activity was observed in aminobutanoic (**3c**), aminopentanoic (**3d**) and aminohexanoic acid (DDAK) derivatives, i.e. those with 3 to 5-carbon linking chain between the tertiary nitrogen and ester carbonyl. These enhancers allowed for reaching theophylline flux values up to 42.2±14.3 μg/cm^2/h, with the corresponding ER being 17.8, i.e. approximately 3 times higher activity than DDAIP. Further prolongation of the linking chain to 7 carbons in **3f** resulted in diminished theophylline permeation. Interestingly, replacement of a hydrocarbon chain in DDAIP by a polyfluorinated one in **3g** led to a complete loss of its permeation-enhancing activity.

When considering the effects of the enhancers on the theophylline skin concentration, neither racemic DDAIP nor its enantiomers showed any effect. On the other hand, DDAK significantly increased theophylline skin concentration to 1149±278 μg/g (Fig. 3). The solubility of the theophylline in the donor medium was 27.9±3.3 mg/ml, and was not significantly affected by any of the tested compounds.

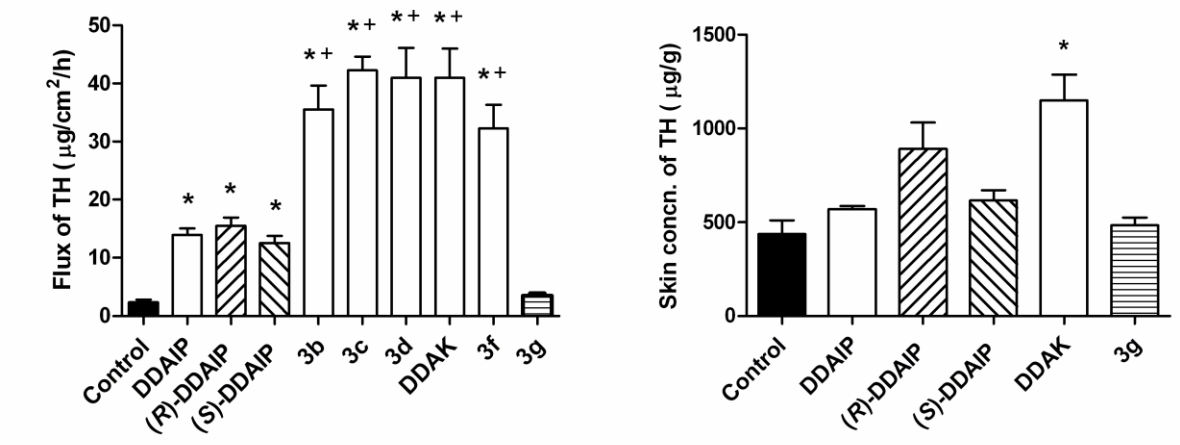

Fig. 3. Effects of the *N*,*N*-dimethylamino acid esters on theophylline (TH) flux through (left) and its concentration in the porcine skin (right). Means ± SEM, n = 8-11 (3 donors). * indicates significant difference against control ($p < 0.05$), + indicates significant difference against DDAIP ($p < 0.05$).

DDAIP – both the racemate and the enantiomers – and DDAK were further compared using hydrocortisone, indomethacin and adefovir as the model drugs covering a wide range of physicochemical properties (Table I).

The flux of hydrocortisone without an enhancer was 0.11±0.07 μg/cm^2/h, and DDAIP increased it 11.5 times to 1.27 μg/cm^2/h. The corresponding skin concentration was 168±39 μg/g. Again, no significant difference was found between the (*R*) and (*S*)-enantiomers and the racemic DDAIP. DDAK proved to be a more potent enhancer than DDAIP for hydrocortisone with the flux of 4.78 μg/cm^2/h (ER = 43.2) and the skin concentration of 484±96 μg/g (Fig. 4). The solubility of hydrocortisone in the donor vehicle was 8.3±0.6 mg/ml, and it was not significantly affected by any of the enhancers.

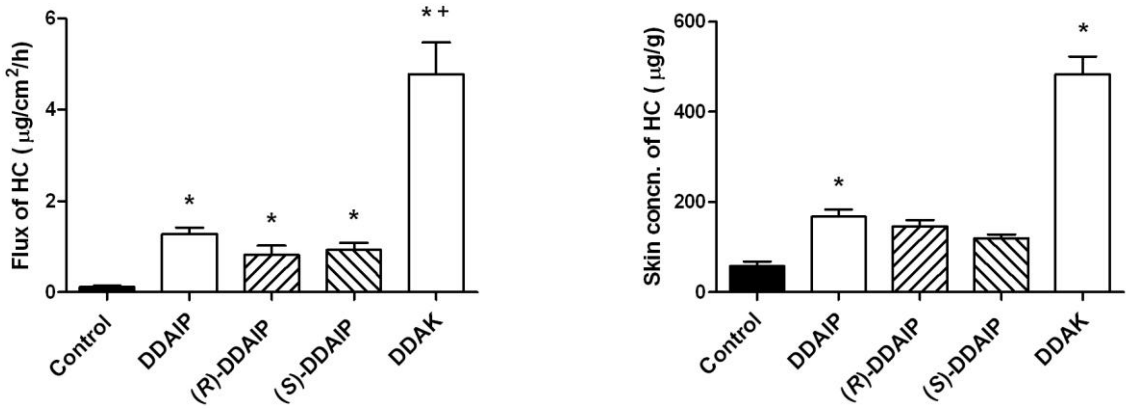

Fig. 4. Effects of the *N,N*-dimethylamino acid esters on hydrocortisone (HC) flux through (left) and its concentration in the porcine skin (right). Means ± SEM, n = 6 (2 donors). * indicates significant difference against control ($p < 0.05$), + indicates significant difference against DDAIP ($p < 0.05$).

The flux of adefovir through the porcine skin was 1.4±0.6 μg/cm^2/h, and the skin concentration was 219 μg/g. DDAIP increased the adefovir flux approximately three times, but had no effect on the amount retained in the skin. No stereoselectivity in DDAIP action was observed. The addition of DDAK into the donor sample resulted in significantly higher adefovir flux (ER = 13.6) and skin concentration (714 μg/g) in comparison with DDAIP. The permeability characteristics of the racemic DDAIP and DDAK measured under the same conditions were taken from our previous work [21, 22], and were included in Fig. 5 for comparison. The solubility of adefovir in the donor vehicle was 70±7 mg/ml, and was not significantly changed by any of the enhancers.

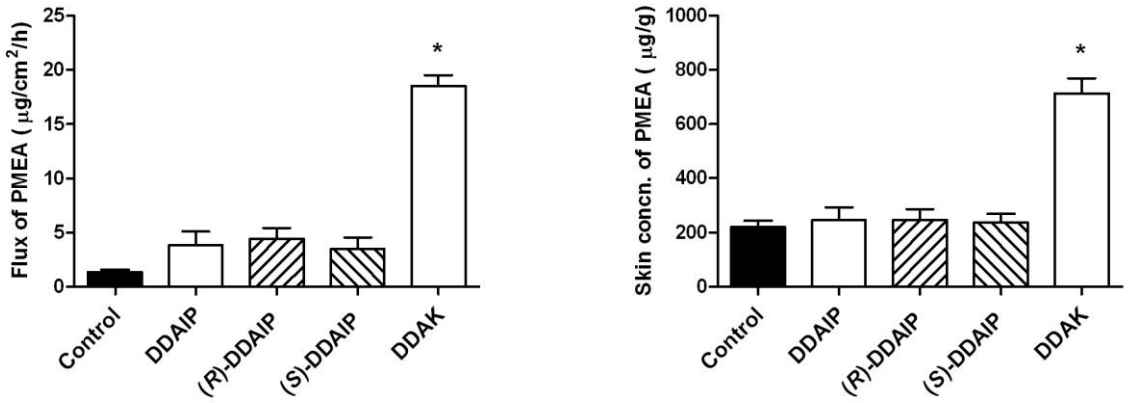

Fig. 5. Effects of the *N,N*-dimethylamino acid esters on adefovir (PMEA) flux through (left) and its concentration in the porcine skin (right). Means ± SEM, n = 4-11 (2-4 donors). * indicates significant difference against control ($p < 0.05$).

On the other hand, DDAIP (ER = 22.8) was more effective than DDAK (ER = 8.7) in enhancing the permeation of indomethacin through the porcine skin. Similar results were obtained for the indomethacin skin concentration. The donor sample with DDAIP and DDAK produced indomethacin skin concentration of 1012±173 μg/g and 482±166 μg/g, respectively (Fig. 6). The solubility of indomethacin in the donor media significantly increased from 0.9±0.1 mg/ml in the control sample to 3.4±0.2 mg/ml and 11.6±1.2 mg/ml in the samples with DDAIP and DDAK, respectively.

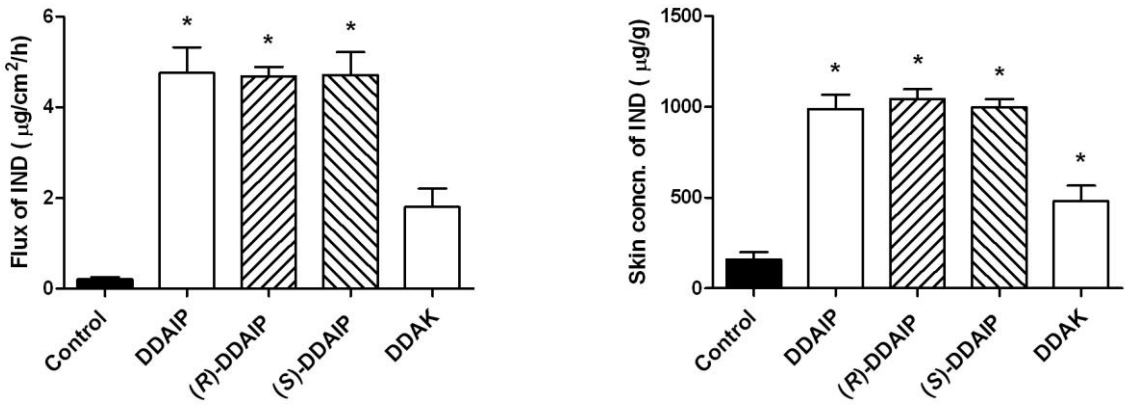

Fig. 6. Effects of the *N,N*-dimethylamino acid esters on indomethacin (IND) flux through (left) and its concentration in the porcine skin (right). Means ± SEM, n = 7 (2 donors). * indicates significant difference against control ($p < 0.05$).

Enzymatic hydrolysis of DDAK

DDAK was hydrolyzed in the presence of porcine esterase - the degradation followed a first order kinetics with the estimated half time $T_{1/2}$ of approximately 17.2 min (Fig. 7). The negative control without the enzyme showed that the compound was stable toward chemical hydrolysis.

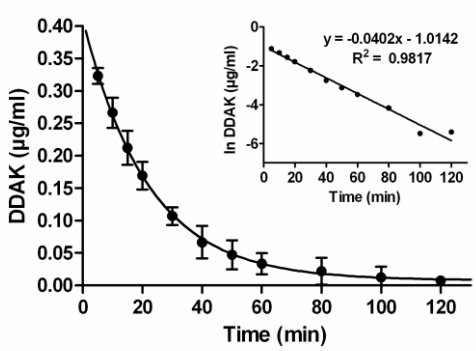

Fig. 7. *In vitro* hydrolysis of DDAK in the presence of porcine esterase (first order reaction, $T_{1/2}$ = 17.2 min). Means ± SEM, *n* = 5. Insert: plot of ln of DDAK concentration against time.

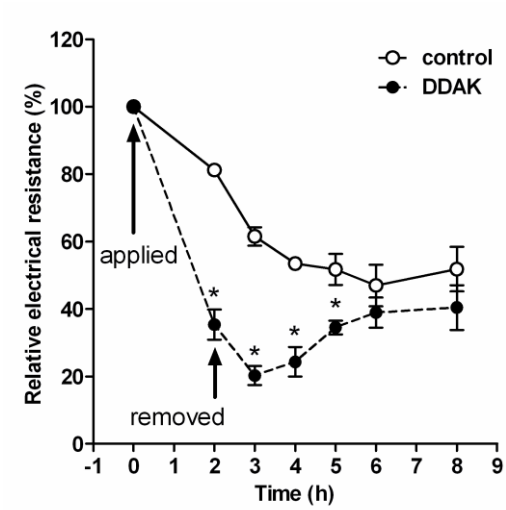

Fig. 8. *In vitro* transdermal electrical resistance of DDAK-treated and control skin as a function of time. The arrows indicate the application and removal of the donor samples. * indicates significant difference against control. Means ± SEM, *n* = 4 (2 donors).

Reversibility of DDAK action

The baseline transdermal electrical resistance was 9.1 - 14.6 kΩ/cm^2. The resistance decreased to 35 % (4.8 kΩ/cm^2) and 81 % (8.9 kΩ/cm^2, significant difference at $p < 0.05$) of the initial value after 2-h application of DDAK and control sample, respectively (Fig. 8). The resistance of the control (PG-treated sample) continued to slowly decrease until it reached approximately 5.5 kΩ/cm^2. The DDAK-treated skin resistance further dropped to 20 % (2.7 kΩ/cm^2) at 3 h, i.e. 1 h after the sample removal. Then, the resistance started to increase continually up to values of the control samples. At 6 h, i.e. 4 h after the removal of the donor samples, no significant difference between DDAK and control was observed.

DISCUSSION

Chirality of DDAIP

The purpose of this study was to investigate the structure-activity relationships in a group of dimethylamino acid transdermal permeation enhancers. The parent compound of this series, DDAIP, is a chiral compound. Since DDAIP increases the skin permeability by interacting with the skin barrier lipids [7], which represent a chiral environment, its enhancing activity may be of a stereoselective nature. The results from this study, however, did not show any significant difference between (*R*), (*S*) and racemic DDAIP in increasing either the flux or skin concentration of any of the four model drugs. This is in accordance with our previous study with 2-octyl 6-aminohexanoate as an enhancer with the chiral centre located in the hydrophobic chain [14]. Thus, the interaction of DDAIP with the skin lipids and/or the consequent barrier permeabilization is not dependent on the exact spatial orientation of its polar head.

Polyfluorination of DDAIP tail

In order to explore the impact of polyfluorination on the behavior of permeation enhancers, fluorocarbon DDAIP analogue **3g** was synthesized, and its effect on the skin transport of theophylline was evaluated. However, this compound was completely inactive. It should be noted that the chain length in **3g** was 2C-shorter than that in DDAIP - 1H,1H,2H,2H-perfluoro-1-decanol was used for the synthesis because it was commercially available. However, such shortening of the chain could not be responsible for the observed change as the decyl derivatives are usually equally or more active than their dodecyl counterparts [5, 15]. Thus, the loss of enhancing activity can be attributed to the presence of a fluorocarbon instead of a comparable hydrocarbon chain.

This effect of chain fluorination may be explained either by insufficient penetration of **3g** into the SC lipid bilayers, or its inability to disrupt the barrier lipid packing. The former explanation is probably not feasible since polyfluorinated compounds have been found to cross the skin barrier. For example, *in vitro* dermal absorption of 8-2 fluorotelomer alcohol, i.e. 1H,1H,2H,2H-perfluoro-1-decanol (the same alcohol as incorporated in **3g** molecule in this study), from a 0.5% methylcellulose vehicle and ethanol was approximately 7 and 30%, respectively, for human skin (DuPont-6997 unpublished, in [31]). Moreover, perfluorinated poison ivy allergens were elicitors of allergic contact dermatitis in pentadecylcatechol-sensitized mice [32].

The latter possible explanation, i.e. that polyfluorinated DDAIP did not disrupt the skin barrier lipid lamellae, may be connected with different behavior of a fluorocarbon chain. It was suggested that phospholipid membrane permeability after replacing a part of the hydrocarbon tail for a fluorinated one resulted from a compromise between a) increased packing disorder due to weaker lateral interaction and augmented steric repulsions and b) increased order related to increased hydrophobicity of the fluorocarbon chains. In short C_4F_9 fluorinated tails, both effects appeared to be balanced while with longer C_8F_{17} chains the hydrophobic interactions predominated, resulting in enhanced membrane ordering and rigidity [17]. This may provide a reasonable explanation of the inability of **3g** to perturb the tight SC lipid packing.

Linking chain structure

DDAK is a DDAIP analogue with longer linking chain between the tertiary nitrogen and ester bond. Its exceptional transdermal permeation-enhancing activity was identified using theophylline [20] and adefovir [21, 22], where it was even more active than DDAIP. To compare these two structurally similar enhancers in a greater detail, their effects on the permeation of four model permeants having different physicochemical properties were studied.

First, the effect of the linking chain structure between the dimethylamino group and ester carbonyl was investigated using theophylline as a model drug. DDAIP is an alanine derivative bearing the basic nitrogen on the α-carbon together with a methyl group, i.e. its linking chain could be regarded as “branched”. Its isomer **3b** having linear ethylene linking chain, i.e. a β-alanine derivative, showed significantly higher activity, suggesting a negative effect of the linking chain branching on the activity of DDAIP.

The effect of branching on the enhancing properties of various compounds was discussed in several articles. Aungst described similar enhancement produced by 5C-14C branched and unbranched fatty acids [33]. Likewise, no significant difference in permeation-enhancing ability of fatty alcohols and acids [34] and carbamates [35] with terminal methyl branching with the only exception of 12C acid was observed by Klimentova. However, similar ethyl-branched alcohols and acids showed significantly higher activity [34]. On the other hand, Chantasart described a decrease in the intrinsic enhancing potency with a higher degree of branching [36]. Hrabálek suggested that the relatively small degree of branching in the hydrophobic chain of 6-aminohexanoic acid esters did not prevent them from interacting with the lipid components of SC. However, a higher degree of branching, cyclization of the chain, and presence of an aromatic ring resulted in a loss of activity [37]. The results from this study with DDAIP and **3b** seem to support the latter studies that branching close to the polar head has negative effect on the enhancing activity.

With prolonging the linking chain between the nitrogen and ester carbonyl, the potency of the enhancers increased first, and then remained comparable in **3c**, **3d** and DDAK, i.e. in derivatives of butanoic, pentanoic and hexanoic acid, and decreased in octanoic acid-based enhancer **3f**. Neither of these enhancers changed the solubility, i.e. the thermodynamic activity of the model drug in the vehicle. The difference between DDAK and DDAIP can be explained by diverse interaction within the SC lipid bilayers. DDAK is a substance with the same hydrogen bonding activity as DDAIP, but more lipophilic and with a flexible linking chain, which could adopt an optimal conformation and probably interact more readily with SC components.

DDAK versus DDAIP

The activity of DDAK and DDAIP was further studied using hydrocortisone, adefovir and indomethacin (Table I) to find whether DDAK was able to facilitate absorption of a broader spectrum of drugs. This enhancer was more potent than DDAIP in increasing both the flux and skin concentration of hydrocortisone and adefovir confirming the results with theophylline. Neither DDAIP nor DDAK changed the solubility of these drugs in the donor vehicle, i.e. their thermodynamic activity. Thus, the reported enhancement ratios reflect a direct increase in the skin permeability.

On the other hand, the enhancing effect of DDAIP on the permeation of indomethacin was 2.6 times higher than that of DDAK. The enhancing potency of DDAIP towards indomethacin permeation was previously explained by a complex formation via hydrogen bonding between the carboxyl group of indomethacin and the tertiary amine of the enhancer [11]. This is consistent with 3.8 times increased solubility of the drug in the donor vehicle observed in this work. On the other hand, DDAK possesses similar dimethylamino group capable of interacting with indomethacin. Indeed, the solubility of indomethacin in 60% PG increased 10 times after the addition of DDAK. However, its ability to enhance indomethacin permeation through the skin was lower than that of DDAIP. In order to study the nature of the interaction, NMR and IR spectra of indomethacin, DDAIP, DDAK and their equimolar mixtures were recorded. ^{13}C-NMR spectra showed larger upfield shifts of the carbons next to nitrogen in DDAK-indomethacin complex than in the DDAIP one, consistent with the shifts of protonated DDAK. Similar changes were observed in the ^{1}H-NMR and IR spectra. Thus, DDAK was likely protonated by indomethacin. This may be explained by different basicity of the two enhancers: DDAK is a stronger base that DDAIP due to better steric availability and higher electron density of the nitrogen lone pair and is therefore capable of (partly) dissociating indomethacin, i.e. a carboxylic acid. However, the formation of an ion pair in the donor vehicle may be decreased due to its high dielectric constant and the two ionic species are likely solvated. This may explain the lower activity of DDAK towards indomethacin.

Biodegradability of DDAK

DDAK was designed as a biodegradable permeation enhancer. Similar to DDAIP, it contains ester bond and may thus be hydrolyzed by skin esterases. To determine DDAK biodegradability, we used the same porcine esterase method as was applied previously to DDAIP [6], tranexamic acid-based enhancers [16] and Transkarbam 12 [23]. However, the conditions for HPLC determination of DDAIP described by Büyütimkin et al. [6] were not applicable to DDAK analysis due to its low UV absorption, which limited the sensitivity of the assay. The enhancer concentration was thus determined using HPLC/MS. The results demonstrated that DDAK was rapidly hydrolyzed by porcine esterase with $T_{1/2}$ = 17.2 min. This is in a good agreement with DDAIP showing half life of 18.5 min [6]. The longer half life of DDAIP may be explained by steric hindrance of the ester group by the adjacent methyl. As esterases are present in the human epidermis [38, 39], the hydrolysis is likely to occur *in vivo* as well, preventing any possible harmful action of this compound on living cells. Moreover, pilot oral toxicity tests in mice and rats showed that all animals survived a DDAK dose of 2 g/kg without any signs of toxicity (BioTest Ltd, Konárovice, Czech Republic).

Reversibility of DDAK action

Electrical resistance is a simple, quick and robust method for measuring the skin barrier integrity [40]. In this study, we used this method for evaluation of the reversibility of DDAK action. The results confirmed that a) DDAK acts by direct decrease of the skin barrier resistance as suggested previously [22], b) the action of this enhancer on the skin is temporary

and c) the barrier changes induced by DDAK are reversible. The reversibility is probably connected with rapid clearance of DDAK from the SC with subsequent hydrolysis of this compound by epidermal esterases. The rapid reversibility may also explain the previously found difference in activity of this enhancer in the co-application and pretreatment protocol [22].

CONCLUSION

In this study, the transdermal permeation-enhancing potency of a series of *N,N*-dimethylamino acid esters was studied. No stereoselectivity in action of DDAIP was found. Polyfluorination of a hydrophobic chain of DDAIP resulted in a complete loss of activity. Replacement of a "branched" linking chain between nitrogen and ester of DDAIP by a linear one markedly improved the enhancing activity with optimum linking chain length found in 4-6C acid derivatives. DDAK was more potent enhancer than DDAIP for theophylline, hydrocortisone and adefovir, while DDAIP was better enhancer for indomethacin. DDAK was rapidly metabolized by porcine esterase, displayed low acute toxicity and reversible action. These results suggest that DDAK, a highly effective biodegradable transdermal permeation enhancer for a broad spectrum of drugs, is a promising candidate for future research.

ACKNOWLEDGEMENTS

This work was supported by the Centre for New Antivirals and Antineoplastics (1M0508), the Ministry of Education of the Czech Republic (MSM0021620822) and the Grant Agency of the Charles University (286/2006/B-CH/FaF).

REFERENCES

[1] Prausnitz, M. R.; Mitragotri, S.; Langer, R. Current status and future potential of transdermal drug delivery. *Nat. Rev. Drug Discov.*, **2004**, *3*, 115-24.

[2] Thomas, B. J.; Finnin, B. C. The transdermal revolution. *Drug Discov Today*, **2004**, *9*, 697-703.

[3] Thong, H. Y.; Zhai, H.; Maibach, H. I. Percutaneous penetration enhancers: an overview. *Skin Pharmacol. Physiol.*, **2007**, *20*, 272-82.

[4] Williams, A. C.; Barry, B. W. Penetration enhancers. *Adv Drug Deliv Rev*, **2004**, *56*, 603-18.

[5] Vavrova, K.; Zbytovska, J.; Hrabalek, A. Amphiphilic transdermal permeation enhancers: structure-activity relationships. *Curr. Med. Chem.*, **2005**, *12*, 2273-91.

[6] Buyuktimkin, S.; Buyuktimkin, N.; Rytting, J. H. Synthesis and enhancing effect of dodecyl 2-(N,N-dimethylamino)propionate on the transepidermal delivery of indomethacin, clonidine, and hydrocortisone. *Pharm. Res.*, **1993**, *10*, 1632-7.

[7] Suhonen, T. M.; Pirskanen, L.; Raisanen, M.; Kosonen, K.; Rytting, J. H.; Paronen, P.; Urtti, A. Transepidermal delivery of beta-blocking agents: Evaluation of enhancer effects using stratum corneum lipid liposomes. *J. Control. Release*, **1997**, *43*, 251-59.

[8] Wolka, A. M.; Rytting, J. H.; Reed, B. L.; Finnin, B. C. The interaction of the penetration enhancer DDAIP with a phospholipid model membrane. *Int. J. Pharm.*, **2004**, *271*, 5-10.

[9] Turunen, T. M.; Urtti, A.; Paronen, P.; Audus, K. L.; Rytting, J. H. Effect of some penetration enhancers on epithelial membrane lipid domains: evidence from fluorescence spectroscopy studies. *Pharm. Res.*, **1994**, *11*, 288-94.

[10] Buyuktimkin, N.; Buyuktimkin, S.; Rytting, J. H. In *Percutaneous Penetration Enhancers*, E.W. Smith; H.I. Maibach, eds.; CRC Press: New York, **1995**, pp. 91-102.

[11] Buyuktimkin, S.; Buyuktimkin, N.; Rytting, J. H. Interaction of indomethacin with a new penetration enhancer, dodecyl 2-(N,N-dimethylamino)propionate (DDAIP): Its effect on transdermal delivery. *Int. J. Pharm.*, **1996**, *127*, 245-53.

[12] Pfister, W.; Li, M.; Frank, D. Development of the novel permeation enhancers dodecyl-2-*N,N*-dimethylaminopropionate (DDAIP) and HCl salt: physiochemical properties, preclinical safety and in vitro permeation enhancement. *AAPS J.*, **2006**, *8*.

[13] Touitou, E.; Godin, B.; Kommuru, T. R.; Afouna, M. I.; Reddy, I. K. In *Chirality In Drug Design And Development*, I.K. Reddy; R. Mehvar, eds.; Marcel Dekker: New York, **2004**, pp. 67-99.

[14] Vavrova, K.; Hrabalek, A.; Dolezal, P. Enhancement effects of (R) and (S) enantiomers and the racemate of a model enhancer on permeation of theophylline through human skin. *Arch. Dermatol. Res.*, **2002**, *294*, 383-5.

[15] Kanikkannan, N.; Kandimalla, K.; Lamba, S. S.; Singh, M. Structure-activity relationship of chemical penetration enhancers in transdermal drug delivery. *Curr. Med. Chem.*, **2000**, *7*, 593-608.

[16] Vavrova, K.; Hrabalek, A.; Dolezal, P.; Holas, T.; Klimentova, J. Biodegradable derivatives of tranexamic acid as transdermal permeation enhancers. *J. Control. Release*, **2005**, *104*, 41-9.

[17] Vierling, P.; Santaella, C.; Greiner, J. Highly fluorinated amphiphiles as drug and gene carrier and delivery systems. *J. Fluorine Chem.*, **2001**, *107*, 337-54.

[18] Wang, K.; Karlsson, G.; Almgren, M.; Asakawa, T. Aggregation behavior of cationic fluorosurfactants in water and salt solutions. A cryoTEM survey. *J. Phys. Chem. B*, **1999**, *103*, 9237-46.

[19] Riess, J. G.; Krafft, M. P. Advanced fluorocarbon-based systems for oxygen and drug delivery, and diagnosis. *Artif. Cells Blood Substit. Immobil. Biotechnol.*, **1997**, *25*, 43-52.

[20] Hrabalek, A.; Dolezal, P.; Farsa, O.; Sklubalova, Z.; Kunes, J. Esters of 6-dimethylaminohexanoic acid as skin penetration enhancers. *Pharmazie*, **2000**, *55*, 759-61.

[21] Vavrova, K.; Lorencova, K.; Klimentova, J.; Novotny, J.; Holy, A. N.; Hrabalek, A. Transdermal and dermal delivery of adefovir: effects of pH and permeation enhancers. *Eur. J. Pharm. Biopharm.*, **2008**, *69*, 597-604.

[22] Vavrová, K.; Lorencová, K.; Novotný, J.; Holý, A.; Hrabálek, A. Permeation enhancer dodecyl 6-(dimethylamino)hexanoate increases transdermal and topical delivery of adefovir; influence of pH, ion-pairing and skin species. *Eur. J. Pharm. Biopharm., In Press, doi:10.1016/j.ejpb.2008.07.002*, .

[23] Hrabalek, A.; Dolezal, P.; Vavrova, K.; Zbytovska, J.; Holas, T.; Klimentova, J.; Novotny, J. Synthesis and enhancing effect of transkarbam 12 on the transdermal delivery of theophylline, clotrimazole, flobufen, and griseofulvin. *Pharm. Res.*, **2006**, *23*, 912-9.

[24] Abdel-Magid, A. F.; Carson, K. G.; Harris, B. D.; Maryanoff, C. A.; Shah, R. D. Reductive Amination of Aldehydes and Ketones with Sodium Triacetoxyborohydride. Studies on Direct and Indirect Reductive Amination Procedures. *J. Org. Chem.*, **1996**, *61*, 3849-62.

[25] Holy, A.; Gunter, J.; Dvorakova, H.; Masojidkova, M.; Andrei, G.; Snoeck, R.; Balzarini, J.; De Clercq, E. Structure-antiviral activity relationship in the series of pyrimidine and purine N-[2-(2-phosphonomethoxy)ethyl] nucleotide analogues. 1. Derivatives substituted at the carbon atoms of the base. *J. Med. Chem.*, **1999**, *42*, 2064-86.

[26] Kopecky, V., Jr.; Mojzes, P.; Burda, J. V.; Dostal, L. Raman spectroscopy study of acid-base and structural properties of 9-[2-(phosphonomethoxy)ethyl]adenine in aqueous solutions. *Biopolymers*, **2002**, *67*, 285-8.

[27] Herkenne, C.; Naik, A.; Kalia, Y. N.; Hadgraft, J.; Guy, R. H. Pig ear skin ex vivo as a model for in vivo dermatopharmacokinetic studies in man. *Pharm. Res.*, **2006**, *23*, 1850-6.

[28] Jacobi, U.; Kaiser, M.; Toll, R.; Mangelsdorf, S.; Audring, H.; Otberg, N.; Sterry, W.; Lademann, J. Porcine ear skin: an in vitro model for human skin. *Skin Res Technol*, **2007**, *13*, 19-24.

[29] Williams, A. In *Transdermal and Topical Drug Delivery: From Theory to Clinical Practice* Pharmaceutical Press, **2003**, pp. 54-58.

[30] Vavrova, K.; Lorencova, K.; Klimentova, J.; Novotny, J.; Hrabalek, A. HPLC method for determination of in vitro delivery through and into porcine skin of adefovir (PMEA). *J. Chrom. B*, **2007**, *853*, 198-203.

[31] Fasano, W. J.; Carpenter, S. C.; Gannon, S. A.; Snow, T. A.; Stadler, J. C.; Kennedy, G. L.; Buck, R. C.; Korzeniowski, S. H.; Hinderliter, P. M.; Kemper, R. A. Absorption, distribution, metabolism, and elimination of 8-2 fluorotelomer alcohol in the rat. *Toxicol. Sci.*, **2006**, *91*, 341-55.

[32] Fraginals, R.; Schaeffer, M.; Stampf, J. L.; Benezra, C. Perfluorinated analogues of poison ivy allergens. Synthesis and skin tolerogenic activity in mice. *J. Med. Chem.*, **1991**, *34*, 1024-7.

[33] Aungst, B. J. Structure/effect studies of fatty acid isomers as skin penetration enhancers and skin irritants. *Pharm. Res.*, **1989**, *6*, 244-7.

[34] Klimentova, J.; Kosak, P.; Vavrova, K.; Holas, T.; Hrabalek, A. Influence of terminal branching on the transdermal permeation-enhancing activity in fatty alcohols and acids. *Bioorg. Med. Chem.*, **2006**, *14*, 7681-7.

[35] Klimentova, J.; Kosak, P.; Vavrova, K.; Holas, T.; Novotny, J.; Hrabalek, A. Transkarbams with terminal branching as transdermal permeation enhancers. *Bioorg. Med. Chem. Lett.*, **2008**, *18*, 1712-5.

[36] Chantasart, D.; Li, S. K.; He, N.; Warner, K. S.; Prakongpan, S.; Higuchi, W. I. Mechanistic studies of branched-chain alkanols as skin permeation enhancers. *J. Pharm. Sci.*, **2004**, *93*, 762-79.

[37] Hrabalek, A.; Vavrova, K.; Dolezal, P.; Machacek, M. Esters of 6-aminohexanoic acid as skin permeation enhancers: The effect of branching in the alkanol moiety. *J. Pharm. Sci.*, **2005**, *94*, 1494-9.

[38] Prusakiewicz, J. J.; Ackermann, C.; Voorman, R. Comparison of skin esterase activities from different species. *Pharm. Res.*, **2006**, *23*, 1517-24.

[39] Montagna, W. Histology and cytochemistry of human skin. IX. The distribution of non-specific esterases. *J Biophys Biochem Cytol*, **1955**, *1*, 13-6.

[40] Davies, D. J.; Ward, R. J.; Heylings, J. R. Multi-species assessment of electrical resistance as a skin integrity marker for in vitro percutaneous absorption studies. *Toxicol. In Vitro*, **2004**, *18*, 351-8.

4. Short-Chain Ceramides Decrease Skin Barrier Properties

Skin Pharmacol Physiol, **2009**, *22*, 22-30

J. Novotný, B. Janůšová, M. Novotný, A. Hrabálek, K. Vávrová

ABSTRACT

Stratum corneum ceramides are major determinants of skin barrier function. Although their physiological and pathological role has been widely investigated, to date no structure-activity relationships have been established. In this study, a series of short-chain ceramide analogues with polar head structure identical to ceramide NS, sphingosine length of 12 carbons and acyl chain length from 2 to 12 carbons was synthesized. Their effect on skin permeability was evaluated using porcine skin and two model drugs, theophylline and indomethacin, and compared to that of a physiological ceramide NS. The results showed that ceramide chain length was crucial for their barrier properties. Ceramides with 4-8C acyl chain were able to increase skin permeability for both drugs up to 10.8 times with maximum effect at 6C acyl. No increase in permeability was found for ceramide analogues with 2C and 12C acyl and ceramide NS. The same relationships were obtained for skin concentrations of the model drugs. The relationship between ceramide acyl chain length and its ability to perturb skin barrier showed striking similarity to the behavior of short-chain ceramides in sphingomyelin/phospholipid membranes and confirmed that short-chain ceramides do not act as natural ceramides and their use as experimental tools should be cautious.

INTRODUCTION

The primary function of the skin is to protect the body from the loss of water and other physiologically important components and to prevent or limit the penetration of potential toxic compounds, allergens, irritants and microbes. The principal barrier for penetration of most compounds resides is the stratum corneum (SC), the uppermost layer of the skin, which consists of flattened dead cells, corneocytes, and intercellular lipid lamellae. The intercellular lipids are considered, as the only continuous domain through SC, to be the most important pathway for the diffusion of substances into the body. This lipidic matrix is composed of an approximately equimolar mixture of ceramides, cholesterol and free fatty acids. The unusual composition of the SC lipids with the high ceramide content and, particularly, their exceptional organization seems to be essential for maintaining the skin barrier function. This is supported by the observation that prominent skin diseases, such as atopic dermatitis and psoriasis, have diminished ceramide levels. For recent reviews on the skin ceramides, see Wertz [1], Bouwstra et al. [2, 3], Wartewig et al. [4], Kessner et al. [5] and Holleran et al. [6].

In the human SC, nine major ceramide subclasses have been identified [7]. These compounds belong to the class of sphingolipids and consist of a sphingoid base - sphingosine, phytosphingosine or 6-hydroxysphingosine, which is *N*-acylated by a long-chain saturated fatty acid, α-hydroxy acid (both with approximately 24C) or ω-hydroxy acid (30C and more). The ω-hydroxyl is further esterified with linoleic acid.

Although the physiological and pathological role of ceramides in the skin, their biosynthesis and physicochemical behavior has been widely investigated, to date no structure-activity relationships have been established. It is generally accepted that the relatively small polar head of ceramides, their ability to create an extensive hydrogen bonding network, their exceptionally long saturated chains allowing for strong hydrophobic attraction and the heterogeneity in their structure are the basic prerequisites of a competent skin barrier. Particularly, ceramide 1 (EOS) was proved to influence dominantly the formation of the long periodicity phase and lateral lipid packing [8]. Nevertheless, no systematic study has been done to investigate the importance of the individual structural features of ceramides for their diffusion resistance.

In this study, we have focused on the role of acyl chain length of skin ceramides. This structural modification has been widely discussed in studies concerning the role of ceramides in cell signaling. Short-chain analogues, particularly *N*-acetylsphingosine (C2 ceramide), have been extensively used as agonists when ceramide effects had to be elicited. However, many substantial differences between naturally occurring long-chain ceramides and their short-chain analogues were described recently (for a review, see Goñi and Alonso [9] and van Blitterswijk et al. [10] and references therein).

No such data are available for the ceramide action in the skin. Although short-chain fluorescent ceramide analogue was used to study ceramide behavior in the skin after topical application [11], it is questionable whether this result may be reproduced using natural ceramide. We have previously studied ceramide analogues based on simple L-serine esters. Compound 14S24, having the same chain length as ceramide NS, was able to repair both porcine [12] and human skin barrier disrupted by various model insults [13]. On the other hand, compound 12S12, having the same polar head but shorter chains, acted as a permeation enhancer [14]. Moreover, many potent permeation enhancers, i.e. compounds increasing skin permeability, bear one common structural feature, which is a chain of 10-12C [15]. These compounds can incorporate into the SC lipid lamellae and fluidize them, thereby promoting drug flux through the skin [16]. Similar example can be found in fatty acids. While the long-chain fatty acids are important components of the SC lipid mixture, the shorter ones act as permeation enhancers [15, 17-19]. Thus, we hypothesize, that short-chain ceramides may not have the same barrier properties as their long-chain natural counterparts.

The aim of this study was to synthesize a series of short-chain analogues of ceramide NS and to evaluate their effects on the skin permeability of two model drugs in vitro.

MATERIALS AND METHODS

Chemicals and instrumentation

All chemicals were purchased from Sigma-Aldrich (Schnelldorf, Germany). Silica gel 60 (230-400 mesh) for column chromatography, TLC plates (silica gel 60 F_{254}, aluminium back) and HPLC columns were obtained from Merck (Darmstadt, Germany).

The structure and purity of the compounds synthesized were confirmed by FTIR (Nicolet Impact 400 spectrophotometer) and ^{1}H and ^{13}C NMR spectra (Varian Mercury-Vx

BB 300 instrument, operating at 300 MHz for ^{1}H, 75 MHz for ^{13}C). The melting points were measured with a Kofler apparatus and are uncorrected.

Synthesis

(*S*)-3-hydroxy-1-methoxy-1-oxopropan-2-aminium chloride (**1**). Thionyl chloride (9 ml, 0.12 mol) was added dropwise to anhydrous methanol (120 ml) to keep the internal temperature below -15°C. The solution was stirred at -20°C for 0.5 h and then L-serine (5 g, 47.5 mmol) was added. The mixture was maintained at -20°C for additional 0.5 h and then stirred at room temperature overnight. The solvent was removed under reduced pressure and the crude was recrystallized from methanol/diethyl ether. White crystals of the product were dried over KOH. Yield = 90%. M.p. = 161-163°C, the spectra were in accordance with Ref. [20].

(*S*)-methyl 2-(*tert*-butoxycarbonylamino)-3-hydroxypropanoate (**2**). The methyl ester (**1**) (33.6 g, 0.22 mol) was dissolved in dry chloroform (400 ml) and triethylamine (TEA, 72 ml, 0.98 mol) was added. The reaction was cooled to -5°C and solution of di-*tert*-butyl dicarbonate (Boc_2O, 56.6 g, 0.26 mol) in dioxane (200 ml) was slowly added. The mixture was stirred at -5°C for 0.5 h, warmed up to room temperature (RT) and stirred overnight. Subsequently, the reaction was treated with 1M $KHSO_4$ (100 ml) and 5% $NaHCO_3$ (100 ml). The polar phases were washed with chloroform (2x 100ml) and the combined organic layers were dried over Na_2SO_4, filtered and concentrated in vacuum. The product was used without further purification.

(*S*)-3-*tert*-butyl 4-methyl 2,2-dimethyloxazolidine-3,4-dicarboxylate (**3**). The solution of protected L-serine (**2**) (10.9 g, 49.9 mmol), 2,2-dimethoxypropane (DMP, 12.2 ml, 99.8 mmol) and p-toluenesulfonic acid monohydrate ($TsOH.H_2O$, 0.13 g, 0.68 mmol) in toluene (140 ml) was refluxed for 0.5 h, then the solvent was distilled at 61°C until 10 ml of azeotrope was collected and the temperature was dropping. Additional DMP (2.9 ml, 0.10 mol) was added, the mixture refluxed for additional 0.5 h and the solvent was distilled off again (5 ml collected). The cooled reaction was partitioned between saturated $NaHCO_3$ solution (200 ml) and diethyl ether (2x450ml). The combined organic layers were washed with brine (100 ml), dried over Na_2SO_4 and concentrated in vacuum. The crude was purified on silica, using ethyl acetate/hexane (1:14 to 1:9) to give a colorless oily product. Yield = 89%. The spectra were in accordance with Refs. [21, 22].

(*S*)-*tert*-butyl 4-formyl-2,2-dimethyloxazolidine-3-carboxylate (**4**). The oxazolidine (**3**) (20 g, 77.1 mmol) was dissolved in dry toluene (170 ml) and cooled to -78°C under nitrogen. 1.0 M solution of diisobutylaluminium hydride (DIBAL-H) in toluene (130 ml, 0.13 mol) was slowly added to keep the temperature under -65°C. The reaction mixture was stirred for 2 h at – 78°C under nitrogen until the TLC analysis (hexane/ethyl acetate 4:1) shown the reaction to be complete. The reaction was quenched by slow addition of -20°C methanol (30 ml) to maintain the reaction temperature under -65°C. The resulting white emulsion was poured into stirred ice-cold 1M HCl (500 ml) and extracted with ethyl acetate (3x500ml). The combined organic layers were washed with saturated KBr solution (350 ml), dried over Na_2SO_4, filtered

and concentrated under vacuum. The product was separated on silica column (ethyl acetate/hexane 1:4) as an oily liquid. Yield = 76%. The spectra were in accordance with Refs. [21, 22].

(*R*)-tert-butyl 4-((*S*)-1-hydroxydec-2-ynyl)-2,2-dimethyloxazolidine-3-carboxylate (**5b**). 1.6M solution of butyl lithium (BuLi) in hexane (1.9 ml, 3.04 mmol) was added to -78°C solution of 1-nonyne (0.57 ml, 3.47 mmol) in dry THF (30 ml) and stirred for 1 h under nitrogen. Subsequently, hexamethylphosphoramide (HMPA, 0.9 ml, 5.16 mmol) and the aldehyde (**4**) (0.59 g, 2.58 mmol) in THF (15 ml) was added and the reaction stirred for additional 2 h at -78°C. Saturated solution of NH_4Cl (20 ml) was added to the resulting mixture; the reaction was warmed to RT, diluted with water and extracted with diethyl ether (3x100 ml). After drying and concentration of the organic phase under vacuum, the crude was purified by flash column chromatography (ethyl acetate/hexane 9:1), giving a colorless oily product in 76% yield. The spectra were in accordance with van Overmeire et al. [23].

(*R*)-tert-butyl 4-((*S*)-1-hydroxyhexadec-2-ynyl)-2,2-dimethyloxazolidine-3-carboxylate (**5a**) was synthesized likewise, the spectra were in accordance with Garner et al. [24].

(2*S*,3*R*,4*E*)-2-aminododec-4-ene-1,3-diol (**6b**, C12 sphingosine). Lithium (0.39 g, 56 mmol) was treated with methanol, diethyl ether and hexane, cut into small pieces and dissolved in -78°C ethyl amine (70 ml) under nitrogen atmosphere (about 3 h, indicated by deep blue colour of the solution). The alkyne (**5b**) (2 g, 5.66 mmol) in THF (70 ml) was added dropwise, the reaction mixture was stirred at –78°C for 2 h, and then quenched by addition of solid NH_4Cl (2.3 g). Ethyl amine was blown out by a stream of nitrogen; the resulting mixture was concentrated under vacuum and partitioned between water (100 ml) and diethyl ether (3x150). The organic phase was dried over Na_2SO_4, filtered and concentrated under vacuum. The crude was dissolved in dioxane/1M HCl (1:1) and refluxed under nitrogen atmosphere for 1 h. The formation of the sphingosine analogue, Rf = 0.71, at the expense of the starting material at the solvent front was checked by TLC using n-butanol/acetic acid/water (4:1:1). The reaction mixture was concentrated to its half and extracted with diethyl ether/hexane 1:1 (4x100 ml). The aqueous phase was then alkalized with cold 1M NaOH to pH 10 and extracted with dichloromethane (3x200ml). The combined extracts were washed with saturated solution of KBr (100 ml), dried over Na_2SO_4, treated with carbon, filtered and concentrated under vacuum. The crude in the form of waxy solid was recrystallized from diethyl ether/hexane to give NMR-homogenous product in overall yield of 43%. The spectra were in accordance with van Overmeire et al. [23].

(2*S*,3*R*,4*E*)-2-aminooctadec-4-ene-1,3-diol (**6a**, sphingosine) was prepared from the alkyne (**5a**) likewise, the spectra were in accordance with Garner et al. [24].

N-((2*S*,3*R*,4*E*)-1,3-dihydroxydodec-4-en-2-yl)acetamide (**7b**, ceramide 12/2). The sphingosine analogue (**6b**) (160 mg, 0.74 mmol) was dissolved in dry dichloromethane (10 ml) and 4-dimethylaminopyridine (DMAP, 9 mg, 0.074 mmol), acetic acid (42 µl, 0.74 mmol) and 1-ethyl-3-(3-dimethylaminopropyl)carbodiimide (WSC, 131 µl, 0.74 mmol) were added at 0°C. The reaction was stirred overnight and partitioned between water (30 ml) and dichloromethane (2x30 ml). The organic extracts were dried, concentrated and the product

was separated on silica with chloroform/methanol 50:1. Yield = 57% of a colorless waxy solid. Mp = 37-39°C. ^{1}H NMR (300 MHz, $CHCl_3$): δ 6.44 (d, J = 7.4 Hz, 1H), 5.79 (dt, J = 15.4, 6.7 Hz, 1H), 5.53 (dd, J = 15.4, 5.6 Hz, 1H), 4.33 (m, 1H), 3.89-3.99 (m, 2H), 3.71 (d, J = 10.7 Hz, 1H), 2.51 (br s, 2H), 2.02-2.11 (m; 5H), 1.27-1.37 (m, 10H), 0.88 (t, J = 6.7, 3H). ^{13}C NMR (75 MHz, $CHCl_3$): δ 171.2, 133.7, 128.7, 73.7, 61.7, 54.7, 32.2, 31.7, 29.0, 23.1, 22.5, 14.0. IR (ATR): ν_{max} 3283, 2920, 2852, 1643, 1618, 1554 cm^{-1}.

General procedure for the preparation of the succinimidyl esters of carboxylic acids: An appropriate aliphatic acid (1.82 mmol), 1-hydroxypyrrolidine-2,5-dione (0.21 g, 1.82 mmol), and DMAP (0.02 g, 0.16 mmol) were dissolved in ethyl acetate (2 ml) and cooled to 0°C. *N,N′*-dicyclohexylcarbodiimide (DCC, 0.38 g, 1.84 mmol) in ethyl acetate (1 ml) was added, the suspension was slowly warmed to RT and stirred overnight. A droplet of acetic acid was used to quench the reaction. The precipitated *N,N′*-dicyclohexylurea was filtered off and the concentrated residue was purified on a silica column with ethyl acetate/hexane.

General procedure for the preparation of the ceramides **7a** and **7c-f**: The sphingosine analogue (**6a** for the preparation of **7a,** or **6b** for the preparation of **7c-f**) (100 mg, 0.46 mmol) and an appropriate succinimidyl ester (0.46 mmol) were dissolved in dry THF (3 ml) and stirred at RT overnight. The mixture was concentrated in vacuum and the product separated on silica column using chloroform/methanol (50:1) as a mobile phase.

N-((2*S*,3*R*,4*E*)-1,3-dihydroxyoctadec-4-en-2-yl)tetracosanamide (**7a**, ceramide NS). Yield = 89%. M.p. = 94-96°C. ^{1}H NMR (300 MHz, $CHCl_3$): δ 6.24 (d, J = 6.9 Hz, 1H), 5.78 (dt, J = 15.2, 6.6 Hz, 1H), 5.53 (dd, J = 15.4, 6.5 Hz, 1H), 4.32 (m, 1H), 3.88-3.98 (m, 2H), 3.68-3.7 (m, 1H), 2.68 (br s, 2H), 2.23 (t, J = 7.5 Hz, 2H), 2.05 (q, J = 6.9 Hz, 2H), 1.56-1.66 (m, 2H), 1.25-1.37 (m, 62H), 0.87 (t, J = 6.5 Hz, 6H). ^{13}C NMR (75 MHz, $CHCl_3$): δ 173.8, 134.3, 128.8, 74.7, 62.5, 54.5, 36.8, 32.2, 31.9, 29.7, 29.5, 29.4, 29.3, 29.2, 29.1, 25.7, 22.7, 14.1. IR (ATR): ν_{max} 3312, 2919, 2849, 1646, 1549 cm^{-1}.

N-((2*S*,3*R*,4*E*)-1,3-dihydroxydodec-4-en-2-yl)butyramide (**7c**, ceramide 12/4). Yield = 64%. M.p. = 57-58°C. ^{1}H NMR (300 MHz, $CHCl_3$): δ 6.31 (d, J = 7.0 Hz, 1H), 5.78 (dt, J = 15.5, 6.4 Hz, 1H), 5.52 (dd, J = 15.2, 6.4 Hz, 1H), 4.30 (m, 1H), 3.87-3.96 (m, 2H), 3.69 (dd, J = 10.5, 4.7 Hz, 1H), 3.05 (br s, 2H), 2.21 (t, J = 7.0, 2H), 2.05 (q, J = 7.0 Hz, 2H), 1.61-1.73 (m, 2H), 1.26-1.38 (m, 12H), 0.96 (t, J = 7.2 Hz, 3H), 0.88 (t, J = 6.7 Hz, 3H). ^{13}C NMR (75 MHz, $CHCl_3$): δ 173.8, 134.2, 128.8, 74.5, 62.4, 54.5, 38.8, 32.3, 31.8, 29.1, 22.6, 19.2, 14.1, 13.7. IR (ATR): ν_{max} 3227, 2921, 2851, 1643, 1623, 1550 cm^{-1}.

N-((2*S*,3*R*,4*E*)-1,3-dihydroxydodec-4-en-2-yl)hexanamide (**7d**, ceramide 12/6). Yield = 82%. M.p. = 62-65°C. ^{1}H NMR (300 MHz, $CHCl_3$): δ 6.36 (d, J = 7.0 Hz, 1H), 5.78 (dt, J = 15.2, 6.4 Hz, 1H), 5.52 (dd, J = 15.5, 6.3 Hz, 1H), 4.30 (t, J = 4.2 Hz, 1H), 3.88-3.96 (m, 2H), 3.69 (dd, J = 8.2, 2.3 Hz, 1H), 2.89 (br s, 2H), 2.23 (t, J = 7.6 Hz, 2H), 2.05 (q, J = 6.9, 2H), 1.59-1.69 (m, 2H), 1.26-1.36 (m, 14H), 0.85-0.92 (m, 6H). ^{13}C NMR (75 MHz, $CHCl_3$): δ

174.0, 134.2, 128.7, 74.5, 62.4, 54.5, 36.8, 32.3, 31.8, 31.4, 29.1, 25.4, 22.6, 22.4, 14.1, 13.9. IR (ATR): ν_{max} 3335, 2920, 2851, 1608, 1550 cm^{-1}.

N-((2*S*,3*R*,4*E*)-1,3-dihydroxydodec-4-en-2-yl)octanamide (**7e**, ceramide 12/8). Yield = 83%. M.p. = 63-64°C. ^{1}H NMR (300 MHz, $CHCl_3$): δ 6.33 (d, J = 7.1 Hz, 1H), 5.77 (dt, J = 15.4, 6.3 Hz, 1H), 5.51 (dd, J = 15.5, 6.5 Hz, 1H), 4.29 (t, J = 5.6 Hz, 1H), 3.87-3.96 (m, 2H), 3.69 (dd, J = 10.7, 2.3 Hz, 1H), 2.81 (br s, 2H), 2.22 (t, J = 7.5 Hz, 2H), 2.05 (q, J = 6.7 Hz, 2H), 1.58-1.68 (m, 2H), 1.26-1.38 (m, 18H), 0.87 (t, J = 6.9 Hz, 6H). ^{13}C NMR (75 MHz, $CHCl_3$): δ 174.0, 134.2, 128.7, 74.4, 62.4, 54.5, 36.8, 32.3, 31.8, 31.7, 29.2, 29.1, 29.0, 25.7, 22.6, 14.1, 14.0. IR (ATR): ν_{max} 3349, 3297, 2921, 2851, 1637, 1545 cm^{-1}.

N-((2*S*,3*R*,4*E*)-1,3-dihydroxydodec-4-en-2-yl)dodecanamide (**7f**, ceramide 12/12). Yield = 86%. M.p. = 80-82°C. ^{1}H NMR (300 MHz, $CHCl_3$): δ 6.29 (d, J = 7.3 Hz, 1H), 5.78 (dt, J = 15.6, 6.7 Hz, 1H), 5.52 (dd, J = 15.4, 6.4 Hz, 1H), 4.30 (m, 1H), 3.86-3.96 (m, 2H), 3.66-3.72 (m, 1H), 2.81 (br s, 2H), 2.22 (t, J = 7.5 Hz, 2H), 2.05 (q, J = 6.9 Hz, 2H), 1.58-1.68 (m, 2H), 1.25-1.38 (m, 26H), 0.87 (t, J = 6.5 Hz, 6H). ^{13}C NMR (75 MHz, $CHCl_3$): δ 174.0, 134.2, 128.8, 74.6, 62.4, 54.5, 36.8, 32.3, 31.9, 31.8, 29.6, 29.5, 29.4, 29.3, 29.2, 29.1, 25.7, 22.6, 14.1. IR (ATR): ν_{max} 3347, 3293, 2918, 2849, 1636, 1546 cm^{-1}.

Donor samples

Donor samples were prepared as 5% w/v suspension of theophylline, and 2% w/v suspension of indomethacin, respectively, with 1% w/v of the short-chain ceramide in propylene glycol/water 6:4. All the donor samples were saturated with the pertinent model drug at these concentrations. The suspension was stirred for 5 min at 50°C and then allowed to equilibrate at 37°C for 24h before the application on the skin. The negative control samples containing the same amount of the model drug without the ceramide and the positive control containing the drug and 1% ceramide NS were prepared likewise.

For the determination of the effects of the ceramides on the solubility of the drugs in the donor solvent, the samples were prepared in triplicate as described above and allowed to equilibrate. After 24 h, the suspensions were centrifuged at 10,000g for 5 min; the supernatant was withdrawn, diluted with the pertinent mobile phase and analyzed by HPLC.

Skin

For the initial in vitro experiments, porcine skin was selected because it is easy to obtain and its permeability is close to the human skin [25-29]. Porcine ears were purchased from a local slaughterhouse. To ensure integrity of the skin barrier, ears were removed post-sacrifice before the carcass was exposed to the high-temperature cleaning procedure. Full-thickness dorsal skin was excised by blunt dissection and hairs were carefully trimmed. The skin was than immersed in 0.05% sodium azide solution in saline for 5 minutes for preservation. The skin fragments were stored at -20°C up to two months.

Permeation experiments

The effects of the short-chain ceramides on the skin permeability was evaluated using modified Franz diffusion cells [30] with an available diffusion area of 1 cm^2 and an acceptor volume of approximately 17 ml. The skin fragments were slowly thawed immediately before use and carefully inspected for any visual damage. They were cut into squares ca 2 x 2 cm, mounted into the diffusion cells dermal side down and sealed with silicone grease. The acceptor compartment of the cell was filled with phosphate-buffered saline at pH 7.4 with 0.03% sodium azide as a preservative. The precise volume of the acceptor liquid was measured for each cell and included into the calculation. The Franz diffusion cells with mounted skin samples were placed in a water bath with a constant temperature of 32°C equipped with a multi-place magnetic stirrer. After an equilibration period of 1 h, 150 µl (i.e. an infinite dose) of the donor sample was applied to the SC side of the skin and covered with a glass slide. The acceptor phase was stirred at 32°C throughout the experiment. Sink conditions were maintained. Samples of the acceptor phase (0.6 ml) were withdrawn at predetermined time intervals over 48 h and replaced with fresh buffer solution.

At the end of the permeation experiment (48 h), the diffusion cells were dismounted and the skin surface washed with 0.5 ml of ethanol and 0.5 ml of water. The exposed area of 1 cm^2 was punched out, blotted dry and weighted. The skin sample was then extracted with 5 ml of the appropriate mobile phase for 48 h and the concentration was determined by HPLC. The extraction efficacy was 98±2% for theophylline and 101±7% for indomethacin, which is in accordance with the FDA Guidance for Industry for Bioanalytical Method Validation, 2001.

HPLC assay conditions

Theophylline and indomethacin were determined by isocratic reverse-phase HPLC using LC-20AD pump, SIL-20AC autosampler and SPD-20A UV/VIS detector (Shimadzu, Kyoto, Japan). The data were analyzed using CSW v. 1.7 for Windows integrating software (Data Apex, Prague, Czech Republic).

Reverse phase separation of theophylline was achieved on LiChroCART 250-4 column (LiChrospher 100 RP-18, 5 µm, Merck) at 35°C using methanol/0.1M NaH_2PO_4 4:6 (v/v) as the mobile phase at a flow rate of 1.2 ml/min. 10 µl was injected on the column and the effluent was measured at 272 nm. The retention time of theophylline was 2.9±0.1 min.

Indomethacin samples were assayed on a LiChroCART 250-4 column (LiChrospher 100 RP-18, 5 µm, Merck) using a mobile phase containing acetonitrile/water/acetic acid 90:60:5 (v/v/v) at a flow rate of 1.5 ml/min. 20 µl was injected on the column, which was maintained at 40°C. UV absorption was monitored at a wavelength of 270 nm and the retention time of indomethacin was 3.9±0.1 min.

Data analysis

The cumulative amount of the drug penetrated across the skin, corrected for the acceptor phase replacement was plotted against time and the steady state flux was calculated from the linear region of the plot. Kruskal-Wallis One Way Analysis of Variance on Ranks with Dunn's or Student-Newman-Keuls post test method was used for the statistical analysis

(SigmaStat for Windows version 3.0.1). Data are presented as means ± SEM and the number of replicates is given in the pertinent figure.

RESULTS

Synthesis

The sphingosine analogue was prepared by addition of lithium alkynide to a protected L-serinal as a chiral building block according to Garner [21] with several synthetic modifications, which allowed us to avoid cancerogenic reagents like methyl iodide and benzene and afforded better yields. The *anti*-selectivity of the addition was improved using HMPA [23, 31]. For the *N*-acylation of sphingosine, various means of carboxyl activation were evaluated, including *N*-hydroxysuccinimide, carbodiimides, 4-nitrophenyl esters, ethylchloroformate and dimethylsulfamoyl chloride. The best yields and easiest purification was achieved with succinimidyl esters of the correspondent carboxylic acids [32], except for the ceramide 12/2, which was synthesized via carbodiimide coupling [33]. The synthetic scheme and the list of the prepared compounds are shown in figure 1.

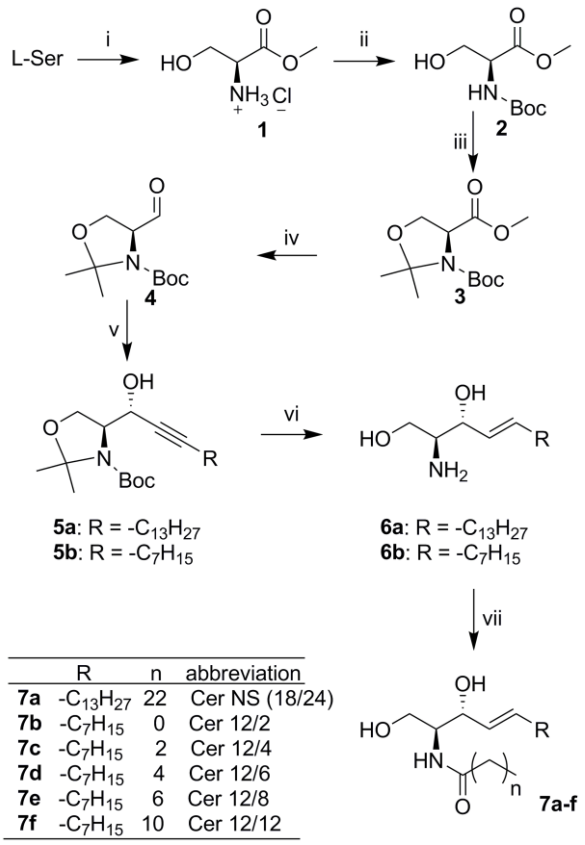

Fig. 1. Scheme of the preparation of the ceramide analogues. Reagents and conditions: (i) $SOCl_2$/MeOH; (ii) Boc_2O/dioxane/TEA/$CHCl_3$; (iii) DMP/TsOH.H_2O/toluene; (iv) DIBAL-H/toluene; (v) BuLi/1-alkyne/HMPA/THF; (vi) 1. Li/$EtNH_2$/THF; 2. HCl/dioxan (vii) succinimidyl ester/THF resp. AcOH/WSC/DMAP/THF.

Effects of the short-chain ceramide analogues on the skin permeation of theophylline

The effects of the prepared short-chain ceramide analogues on the skin permeability was evaluated using porcine skin and two model drugs with distinct physicochemical properties, theophylline and indomethacin, and compared to that of a physiological ceramide NS. The ceramides 12/4, 12/6 and 12/8, i.e. those with 4-8 carbon acyl chain length, increased the flux of theophylline 10.4, 10.8 and 8.7 times, respectively (figure 2). No increase in permeability was found for ceramide 12/2 and 12/12 and the natural ceramide NS. A similar profile was obtained for the theophylline skin concentration, again with the maximum at around 4-6C acyl. The solubility of theophylline in the donor vehicle was 25.8±1.5 mg/ml and was not significantly affected by any of the ceramide analogues.

Effects of the short-chain ceramide analogues on the skin permeation of indomethacin

Almost the same pattern of the skin permeation of the second model drug, indomethacin, versus ceramide acyl chain length was observed (figure 3). The ceramide analogue 12/6 with hexanoyl chain significantly increased both the flux (7.0 times) and skin concentration (2.6 times) of this drug. The solubility of indomethacin in the donor vehicle was 1.0±0.2 mg/ml and it was not significantly affected by any of the ceramide analogues.

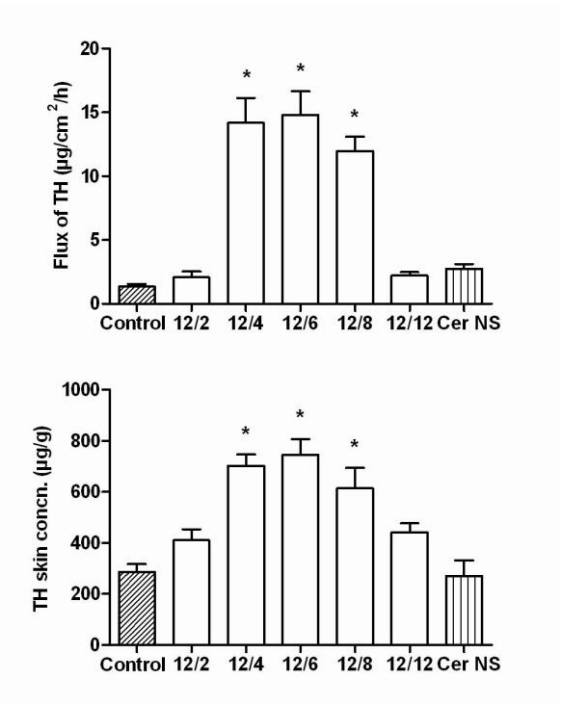

Fig. 2. Effects of the ceramide acyl chain length on theophylline (TH) flux through (upper panel) and its concentration in the porcine skin (lower panel). Data are presented as means ± SEM, n = 11-26. * indicates significant difference against control ($p < 0.05$).

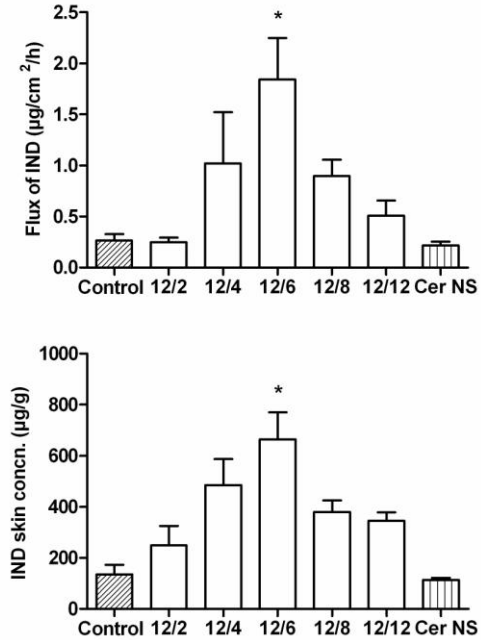

Fig. 3. Effects of the ceramide acyl chain length on indomethacin (IND) flux through (upper panel) and its concentration in the porcine skin (lower panel) Data are presented as means ± SEM, n = 5. * indicates significant difference against control ($p < 0.05$).

DISCUSSION

The objective of this work was to synthesize a series of short-chain ceramides and to evaluate their effects on the skin barrier properties. The polar head of the prepared analogues was identical to ceramide NS, i.e. a non-hydroxy acyl sphingosine, which is the most abundant ceramide in the human SC [34]. The length of sphingosine in ceramide is usually 18C. For the purpose of this initial study, the sphingosine backbone of the prepared ceramide analogues was truncated to 12C. The main reason was to pronounce the putative effects of the short-chain ceramides on the skin permeability since they may have been relatively small and difficult to distinguish due to high variability associated with skin permeation experiments. The acyl chain length of the analogues was varied from 2 to 12C. In order to differentiate these analogues having 12C sphingosine from those discussed below, they are designated ceramide 12/2, 12/4 etc. The former number indicates the sphingosine length and the latter the acyl carbon number.

The effects of the prepared short-chain ceramides on the SC barrier were studied using the permeation of two model compounds through the porcine skin. Theophylline and indomethacine were selected as the model permeants having different molecular weight (MW = 180 and 357 g/mol, respectively), lipophilicity (logP = -0.1 and 3.7, respectively), ionization constants (pKa values of theophylline are 1.7 and 8.8 and that of indomethacin is 4.5) and flux values through the porcine skin (1.4 and 0.26 $\mu g/cm^2/h$, respectively). Moreover, the permeability of theophylline proved to be a good marker of the skin barrier function [12, 35] with higher sensitivity than transepidermal water loss [13].

The results showed the importance of the ceramide chain length for the skin barrier permeability. Although it was not experimentally possible to selectively replace the natural long-chain ceramides in the native SC by the short-chain ones – they were only added to the existent skin lipid mixture, the extent of the permeability increase relative to control proved the usefulness of this experimental setup. The ceramides 12/4, 12/6 and 12/8, i.e. those with 4-8C acyl chain, were able to increase the skin permeability for both model permeants with maximum at around 6C. No increase in permeability was found for ceramide 12/12, ceramide NS and, surprisingly, the ceramide 12/2, i.e. the shortest analogue. The same relationships were obtained for the skin concentrations of the model drugs. The inactivity of 12/2 and 12/12 ceramides proved that the shortening of sphingosine to 12C alone cannot be responsible for the increased skin permeability caused by the C4-C8 analogues.

Several studies suggested that hydrogen bonding plays critical role as a cohesive force in lipid membranes [36, 37]. However, the short-chain ceramides prepared in our study perturbed the skin barrier although they had the same hydrogen bonding ability as ceramide NS. This is in accordance with recent studies demonstrating that sphingosine-based ceramides, regardless of chain length, form a network of cooperative hydrogen bonds involving the primary and allylic hydroxyl, amide and two molecules of water and not the adjacent ceramides [38] and the driving force for molecular assembly of the sphingosine ceramides is the formation of the orthorhombic chain packing [39]. Since the hydrophobic interactions are caused by the attraction of induced dipoles in the hydrophobic chains, they strongly depend on the chain length. Thus, the shorter the chain, the weaker the interaction is expected to be, causing an increased permeability of the lipid membrane. Another possible explanation is that the insertion of a shorter chain into a long-chain lamella would simply produce a free space within the membrane, which would most probably be compensated by an increased mobility of the surrounding chains. A similar mechanism has been proposed for the

action of the amphiphilic permeation enhancers [15]. A third possibility is that these short-chain ceramides could form separate phases within the long-chain lipid lamellae, similar to, for example, oleic acid [40], creating a more permeable shortcut through the membranes.

Nevertheless, the above hypotheses may only partly explain the observed relationship between the chain length and skin permeability. The permeability increased with decreasing chain length up to 6C, but decreased with further shortening of the acyl chain. The shortest ceramide analogue 12/2 did not change the skin permeability, at least under these experimental conditions.

The reasons for the difference between ceramide 12/6 and 12/2 are not known at present. However, surprisingly similar structure-activity relationships may be found in studies of the effects of short-chain ceramides on phospholipid/sphingomyelin membranes. Nybond et al. [41] studied the effects of ceramides with 2-14C acyl on the stability of the sphingomyelin-rich domains and cholesterol displacement in phospholipid/sphingomyelin/cholesterol vesicles. The stability of the ordered domains, which may have a relevance to the stability of the SC lipids, was increased upon incorporation of sphingosine, C2 ceramide and ceramides with an acyl chain of 12C and longer. However, both C4 and C6 ceramides destabilized the ordered domains.

Very similar effects of ceramide analogues on ordered membrane domain (raft) stability was reported by Megha et al. [42]. A minimum of 12C acyl chain length was required for significant raft stability and C6 and C8 ceramides were more destabilizing than the C2 analogue. In contrast to Nybond et al. [41], C2 ceramide did not stabilize the ordered domains, which may be connected with different lipid chain lengths and concentrations used for the bilayer formation. Interestingly, the effects of ceramide acyl chain length were qualitatively similar in the absence and presence of cholesterol suggesting that the ability of ceramides to stabilize/destabilize ordered lipid domains does not involve a specific ceramide-sterol interaction. Moreover, from the comparison of ceramide analogues with different polar head structure, it was suggested that the ability of lipids to pack tightly is more sensitive to small changes in the structure of their hydrophobic segments than small changes in their polar headgroups [42].

Chiantia et al. [43] demonstrated, using atomic force microscopy and fluorescence correlation spectroscopy on sphingomyelin/phospholipid bilayers, that short-chain ceramides do not form a separate phase but alter the physical properties of the liquid-ordered domains, decreasing their stability and viscosity and perturbing the lipid packing. Interestingly, the liquid ordered domain size decreased with decreasing ceramide chain length up to 6C but the trend changed in the presence in C2 ceramide. The relative diffusion coefficients for both ordered and disordered phase and partition coefficients between these two phases of fluorescent dye BodChol increased up to C6 ceramide and then decreased with further shortening of the chain.

Gidwani et al. [44] showed, using fluorescence anisotropy measurement, that C6 ceramide was 4-5 times more effective than C2 one in decreasing lipid order in plasma membranes. In contrast to these, long chain ceramides, such as C16 ceramide are of more cylindrical shape and should pack well into liquid ordered membrane.

The above differences between C2 and C6 ceramide might be explained by the different shape of the ceramide molecule after its incorporation into the membrane. Nybond et al. [41] presented energy-minimized models of the studied ceramides suggesting that C2 ceramide does not require much more space than sphingosine alone and the *N*-acetyl chain may be well

accommodated in the polar region of the bilayer without disruption of the chain packing. The 4-6C acyl chains were probably not long enough to pack efficiently with the long chain lipids and "wobbled" between the hydrophilic and hydrophobic regions, thus perturbing the lipid packing in its vicinity. When the acyl chain was 10C or longer it was very likely fully embedded in the bilayer, adjacent to the neighboring long chain bases or acyl chains. Since lipid packing is an important feature of the SC barrier properties as well, this theory may provide a reasonable explanation of our results.

Another explanation of the lower effect of ceramide 12/2 may be its lower lipophilicity compared to longer ceramides and, consequently, lower uptake into the lipophilic SC from a relatively hydrophilic vehicle. Similar difference in partitioning was suggested to be responsible for the lower cytotoxicity of C2 ceramide compared to C6 one by Shabbits et Mayer [45]. However, more studies regarding the molecular aspects of the suggested interactions and elucidation of the role of the sphingosine chain length are needed.

In conclusion, this study showed that the ceramide chain length was crucial for their skin barrier properties. The relationship between the ceramide acyl chain length and its ability to perturb skin barrier showed striking similarity to the behavior of short-chain ceramides in sphingomyelin/phospholipid membranes and confirmed that short-chain ceramides do not act as natural ceramides and their use as experimental tools should be cautious.

ACKNOWLEDGEMENTS

This work was supported by the Centre for New Antivirals and Antineoplastics (1M0508), the Ministry of Education of the Czech Republic (MSM0021620822) and the Grant Agency of the Charles University (286/2006/B-CH/FaF).

REFERENCES

[1] Wertz, P. W. Lipids and barrier function of the skin. *Acta Derm Venereol Suppl (Stockh)*, **2000**, *208*, 7-11.

[2] Bouwstra, J. A.; Honeywell-Nguyen, P. L.; Gooris, G. S.; Ponec, M. Structure of the skin barrier and its modulation by vesicular formulations. *Prog Lipid Res*, **2003**, *42*, 1-36.

[3] Bouwstra, J. A.; Ponec, M. The skin barrier in healthy and diseased state. *Biochim Biophys Acta*, **2006**, *1758*, 2080-95.

[4] Wartewig, S.; Neubert, R. H. Properties of ceramides and their impact on the stratum corneum structure: a review. Part 1: ceramides. *Skin Pharmacol Physiol*, **2007**, *20*, 220-9.

[5] Kessner, D.; Ruettinger, A.; Kiselev, M. A.; Wartewig, S.; Neubert, R. H. Properties of ceramides and their impact on the stratum corneum structure. Part 2: stratum corneum lipid model systems. *Skin Pharmacol Physiol*, **2008**, *21*, 58-74.

[6] Holleran, W. M.; Takagi, Y.; Uchida, Y. Epidermal sphingolipids: metabolism, function, and roles in skin disorders. *FEBS Lett*, **2006**, *580*, 5456-66.

[7] Ponec, M.; Weerheim, A.; Lankhorst, P.; Wertz, P. New acylceramide in native and reconstructed epidermis. *J Invest Dermatol*, **2003**, *120*, 581-8.

[8] Bouwstra, J. A.; Gooris, G. S.; Dubbelaar, F. E.; Weerheim, A. M.; Ijzerman, A. P.; Ponec, M. Role of ceramide 1 in the molecular organization of the stratum corneum lipids. *J Lipid Res*, **1998**, *39*, 186-96.

[9] Goni, F. M.; Alonso, A. Biophysics of sphingolipids I. Membrane properties of sphingosine, ceramides and other simple sphingolipids. *Biochim Biophys Acta*, **2006**, *1758*, 1902-21.

[10] van Blitterswijk, W. J.; van der Luit, A. H.; Veldman, R. J.; Verheij, M.; Borst, J. Ceramide: second messenger or modulator of membrane structure and dynamics? *Biochem J*, **2003**, *369*, 199-211.

[11] Man, M. Q.; Feingold, K. R.; Elias, P. M. Exogenous lipids influence permeability barrier recovery in acetone-treated murine skin. *Arch Dermatol*, **1993**, *129*, 728-38.

[12] Vavrova, K.; Zbytovska, J.; Palat, K.; Holas, T.; Klimentova, J.; Hrabalek, A.; Dolezal, P. Ceramide analogue 14S24 ((S)-2-tetracosanoylamino-3-hydroxypropionic acid tetradecyl ester) is effective in skin barrier repair in vitro. *Eur J Pharm Sci*, **2004**, *21*, 581-7.

[13] Vavrova, K.; Hrabalek, A.; Mac-Mary, S.; Humbert, P.; Muret, P. Ceramide analogue 14S24 selectively recovers perturbed human skin barrier. *Br J Dermatol*, **2007**, *157*, 704-12.

[14] Vavrova, K.; Hrabalek, A.; Dolezal, P.; Holas, T.; Zbytovska, J. L-Serine and glycine based ceramide analogues as transdermal permeation enhancers: polar head size and hydrogen bonding. *Bioorg Med Chem Lett*, **2003**, *13*, 2351-3.

[15] Vávrová, K.; Zbytovská, J.; Hrabálek, A. Amphiphilic transdermal permeation enhancers: structure-activity relationships. *Curr Med Chem*, **2005**, *12*, 2273-91.

[16] Smith, E. W.; Maibach, H. I. *Percutaneous penetration enhancers, 2nd ed.*, CRC Press: Boca Raton **2006**.

[17] Kanikkannan, N.; Kandimalla, K.; Lamba, S. S.; Singh, M. Structure-activity relationship of chemical penetration enhancers in transdermal drug delivery. *Curr Med Chem*, **2000**, *7*, 593-608.

[18] Klimentova, J.; Kosak, P.; Vavrova, K.; Holas, T.; Hrabalek, A. Influence of terminal branching on the transdermal permeation-enhancing activity in fatty alcohols and acids. *Bioorg Med Chem*, **2006**, *14*, 7681-7.

[19] Thong, H. Y.; Zhai, H.; Maibach, H. I. Percutaneous penetration enhancers: an overview. *Skin Pharmacol Physiol*, **2007**, *20*, 272-82.

[20] Foss, F. W., Jr.; Snyder, A. H.; Davis, M. D.; Rouse, M.; Okusa, M. D.; Lynch, K. R.; Macdonald, T. L. Synthesis and biological evaluation of gamma-aminophosphonates as potent, subtype-selective sphingosine 1-phosphate receptor agonists and antagonists. *Bioorg Med Chem*, **2007**, *15*, 663-77.

[21] Garner, P.; Park, J. M. 1,1-Dimethylethyl (S) or (R)-4-Formyl-2,2-dimethyl-3-oxazolidinecarboxylate: A Useful Serinal Derivative. *Org. Synth.*, **1991**, *70*, 18–28.

[22] Williams, L.; Zhang, Z.; Feng, S.; Carroll, P. J.; Joullié, M. M. Grignard reactions to chiral oxazolidine aldehydes. *Tetrahedron*, **1996**, *52*, 11673-94.

[23] Van Overmeire, I.; Boldin, S. A.; Dumont, F.; Van Calenbergh, S.; Slegers, G.; De Keukeleire, D.; Futerman, A. H.; Herdewijn, P. Effect of aromatic short-chain analogues of ceramide on axonal growth in hippocampal neurons. *J Med Chem*, **1999**, *42*, 2697-705.

[24] Garner, P.; Park, J. M.; Malecki, E. A Stereodivergent Synthesis of D-erythro-Sphingosine and D-threo-Sphingosine From L-Serine. *J. Org. Chem.*, **1988**, *53*, 4395-98.

[25] Jacobi, U.; Kaiser, M.; Toll, R.; Mangelsdorf, S.; Audring, H.; Otberg, N.; Sterry, W.; Lademann, J. Porcine ear skin: an in vitro model for human skin. *Skin Res Technol*, **2007**, *13*, 19-24.

[26] Simonsen, L.; Fullerton, A. Development of an in vitro skin permeation model simulating atopic dermatitis skin for the evaluation of dermatological products. *Skin Pharmacol Physiol*, **2007**, *20*, 230-6.

[27] Williams, A. In *Transdermal and Topical Drug Delivery: From Theory to Clinical Practice* Pharmaceutical Press, **2003**, pp. 54-58.

[28] Andega, S.; Kanikkannan, N.; Singh, M. Comparison of the effect of fatty alcohols on the permeation of melatonin between porcine and human skin. *J Control Release*, **2001**, *77*, 17-25.

[29] Simon, G. A.; Maibach, H. I. The pig as an experimental animal model of percutaneous permeation in man: qualitative and quantitative observations--an overview. *Skin Pharmacol Appl Skin Physiol*, **2000**, *13*, 229-34.

[30] Franz, T. J. Percutaneous absorption on the relevance of in vitro data. *J. Invest. Dermatol.*, **1975**, *64*, 190-5.

[31] Herold, P. Synthesis of D-erythro- and D-threo-sphingosine derivatives from L-serine. *Helv Chim Acta*, **1988**, *71*, 354-63.

[32] Lapidot, Y.; Rappoport, S.; Wolman, Y. Use of esters of N-hydroxysuccinimide in the synthesis of N-acylamino acids. *J Lipid Res*, **1967**, *8*, 142-5.

[33] Dhaon, M. K.; Olsen, R. K.; Ramasamy, K. Esterification of N-protected .alpha.-amino acids with alcohol/carbodiimide/4-(dimethylamino)pyridine. Racemization of aspartic and glutamic acid derivatives. *J Org Chem*, **1982**, *47*, 1962-65.

[34] Chen, H.; Mendelsohn, R.; Rerek, M. E.; Moore, D. J. Fourier transform infrared spectroscopy and differential scanning calorimetry studies of fatty acid homogeneous ceramide 2. *Biochim Biophys Acta*, **2000**, *1468*, 293-303.

[35] Yoshiike, T.; Aikawa, Y.; Sindhvananda, J.; Suto, H.; Nishimura, K.; Kawamoto, T.; Ogawa, H. Skin barrier defect in atopic dermatitis: increased permeability of the stratum corneum using dimethyl sulfoxide and theophylline. *J Dermatol Sci*, **1993**, *5*, 92-6.

[36] Karlsson, K.-A. On the character and functions of sphingolipids. *Acta Biochim Polonica*, **1998**, *45*, 429-38.

[37] Pascher, I. Molecular arrangements in sphingolipids. Conformation and hydrogen bonding of ceramide and their implication on membrane stability and permeability. *Biochim Biophys Acta*, **1976**, *455*, 433-51.

[38] Li, L.; Tang, X.; Taylor, K. G.; DuPre, D. B.; Yappert, M. C. Conformational characterization of ceramides by nuclear magnetic resonance spectroscopy. *Biophys J*, **2002**, *82*, 2067-80.

[39] Rerek, M. E.; Chen, H.; Markovic, B.; Van Wyck, D.; Patrick Garidel, P.; Mendelsohn, R.; Moore, D. J. Phytosphingosine and Sphingosine Ceramide Headgroup Hydrogen Bonding: Structural Insights through Thermotropic Hydrogen/Deuterium Exchange. *J Phys Chem B*, **2001**, *105*, 9355 -62.

[40] Ongpipattanakul, B.; Burnette, R. R.; Potts, R. O.; Francoeur, M. L. Evidence that oleic acid exists in a separate phase within stratum corneum lipids. *Pharm Res*, **1991**, *8*, 350-4.

[41] Nybond, S.; Bjorkqvist, Y. J.; Ramstedt, B.; Slotte, J. P. Acyl chain length affects ceramide action on sterol/sphingomyelin-rich domains. *Biochim Biophys Acta*, **2005**, *1718*, 61-6.

[42] Megha; Sawatzki, P.; Kolter, T.; Bittman, R.; London, E. Effect of ceramide N-acyl chain and polar headgroup structure on the properties of ordered lipid domains (lipid rafts). *Biochim Biophys Acta*, **2007**, *1768*, 2205-12.

[43] Chiantia, S.; Kahya, N.; Schwille, P. Raft domain reorganization driven by short- and long-chain ceramide: a combined AFM and FCS study. *Langmuir*, **2007**, *23*, 7659-65.

[44] Gidwani, A.; Brown, H. A.; Holowka, D.; Baird, B. Disruption of lipid order by short-chain ceramides correlates with inhibition of phospholipase D and downstream signaling by FcepsilonRI. *J Cell Sci*, **2003**, *116*, 3177-87.

[45] Shabbits, J. A.; Mayer, L. D. Intracellular delivery of ceramide lipids via liposomes enhances apoptosis in vitro. *Biochim Biophys Acta*, **2003**, *1612*, 98-106.

5. Skin Penetration of NBD-Ceramides is Chain Length-Dependent; Long-Chain Lipids Do Not Enter Nucleated Human Epidermis

(submitted)

J. Novotný, K. Pospěchová, A. Hrabálek, R. Čáp, K. Vávrová

ABSTRACT

Topical skin lipid supplementation may provide opportunities for controlling ceramide (Cer) deficiency in diseases such as atopic dermatitis or psoriasis. However, the exact mechanisms by which exogenous Cer correct the barrier abnormalities are not known. Although exogenous short-chain NBD-labeled C6-Cer was shown to rapidly traverse stratum corneum (SC) and to be uptaken and metabolized by viable epidermal layers, no such evidence is available for long-chain ceramides. Thus, we aimed at comparing skin penetration of fluorescent NBD-labeled C6, C12, and C24-Cer and pseudoCer 14S24. Fluorescent lipids were synthesized from sphingosine or L-serine ester and omega-NBD-labeled hydroxysuccinimide-activated acids. 24-NBD-lignoceric acid was prepared from dodecan-1,12-diol using lithium tetrachlorocuprate coupling. NBD-Cer at two concentrations, either alone or in equimolar mixture with cholesterol and lignoceric acid, were applied on viable human skin for 2 and 12 h, respectively. Only short-chain NBD-C6-Cer reached viable epidermis; NBD-C12-Cer and both NBD-C24 lipids penetrated solely into several upper SC layers of both intact and acetone-treated skin. These results show that the skin penetration of exogenous Cer is chain length-dependent and that exogenous long-chain NBD-labeled Cer and their analogues do not enter viable epidermis. This suggests that short-chain Cer cannot be used as general long-chain Cer mimics.

INTRODUCTION

The principal barrier for penetration of most compounds resides is the stratum corneum (SC), the uppermost layer of the skin. SC comprises of flattened anucleated cells, corneocytes, and extracellular spaces filled with lipidic matrix, which accumulates during the cell differentiation. This lipidic matrix is composed of approximately 50% of ceramides (Cer), 25% of cholesterol and 10% of long-chain fatty acids. The unusual composition of the SC lipids with high Cer content and, particularly, their exceptional organization is believed to be the limiting factor for the penetration of topically applied compounds. For recent reviews on the skin barrier formation, physiology and pathology, see [1-6].

Depletion in total Cer content with alteration in the Cer pattern is a common sign for skin disorders with diminished skin barrier function, including atopic dermatitis [7, 8] and psoriasis [9]. The formulations containing physiological lipids and, in particular, Cer supplementation can improve permeability barrier homeostasis [10-12]. In addition, several pseudoCer and Cer analogues were able to recover perturbed skin barrier [13-18].

Exogenous Cer have been suggested to act within viable epidermis. Indeed, short-chain fluorescent NBD-C6-Cer was found to traverse SC, entering the nucleated epidermal layers within two hours [12]. It was uptaken and reprocessed by keratinocytes, entering the lamellar bodies [19]. However, no such evidence is available for natural long-chain Cer. Moreover, many substantial differences between naturally occurring long-chain Cer and their short-chain analogues have been described; for a review, see [20-22] and references therein. The Cer acyl chain length was found to be crucial for their barrier properties [23]. Cer with C_{4-8} acyl chain were able to increase skin permeability for two model drugs up to 10.8 times with maximum

effect at C_6 acyl. Therefore, we hypothesized that the ability of exogenous Cer to traverse SC and enter nucleated epidermal cells may also be chain length-dependent.

The aim of this study was to synthesize a series of fluorescent Cer analogues with different acyl chain length, namely 6, 12 and 24 carbons, and to evaluate their penetration into both disrupted and intact human skin. Furthermore, we aimed at comparing the behavior of fluorescent Cer and pseudoCer 14S24 in the skin.

RESULTS

Synthesis of fluorescent lipids

For the preparation of the fluorescent long-chain NBD-C24-Cer, 24-aminotetracosanoic acid had to be synthesized first (Figure 1). Mono-bromation of dodecan-1,2-diol was achieved with HBr under microwave activation with 76% yield and in a short time in comparison with a method published previously [24]. The resulting bromo alcohol **1** was oxidized to give acid **2** [25]. Hydroxyl group of **1** was protected as tetrahydropyranyl ether **3**, followed by treatment with magnesium to give a Grignard reagent. Coupling of the chloromagnesium salt of **2** with the Grignard reagent in the presence of freshly prepared lithium tetrachlorocuprate afforded *O*-tetrahydropyranyl acid **4** in 58% yield [26]. Its hydroxyl was deprotected and the carboxylic group was esterified to yield methyl ester **5** in one step procedure using thionyl chloride in methanol. The formal one-pot conversion of hydroxyl to primary amino group was achieved by combination of Mitsunobu reaction with Staudinger reduction of the azido group [27]. The resulting hydrochloride of 24-aminotetracosanoic acid **6** was alkalized and labeled with NBD-Cl to yield **7c**. The commercially available ω-amino hexanoic and dodecanoic acids were labeled in the same manner to yield **7a-b**.

Sphingosine was synthesized by alkynylation of protected L-serinal as described previously [23, 28, 29]. Then, it was N-acylated by succinimidyl esters of the NBD acids. NBD-labeled pseudoCer 14S24 was prepared by *N*-acylation of tetradecyl L-serine [15] with **7c** using carbodiimide coupling (Figure 2).

Figure 1. Synthesis of NBD-labeled 24-aminotetracosanoic acid. Reagents and conditions: (i) 48% HBr, toluene; (ii) CrO_3, acetic acid, H_2O, acetone; (iii) dihydro-*2H*-pyran, pyridinium *p*-toluensulfonate, $CHCl_3$; (iv) CH_2Br_2, Mg, CH_3MgCl, Li_2CuCl_4, THF; (v) $SOCl_2$, MeOH; (vi) HN_3 in benzene, PhP_3, di-isopropyl azodicarboxylate, tetrahydrofurane; (vii) NBD-Cl, $NaHCO_3$, MeOH.

Figure 2. Synthesis of NBD-labeled Cer and pseudoCer 14S24. Reagents and conditions: (i) 1. *N*-hydroxysuccinimide, dicyclohexylcarbodiimide, 4-dimethylaminopyridine, $CHCl_3$; 2. sphingosine, $CHCl_3$; (ii) L-Serine tetradecyl ester, 1-ethyl-3-(3-dimethylaminopropyl)carbodiimide, 4-dimethylaminopyridine, $CHCl_3$.

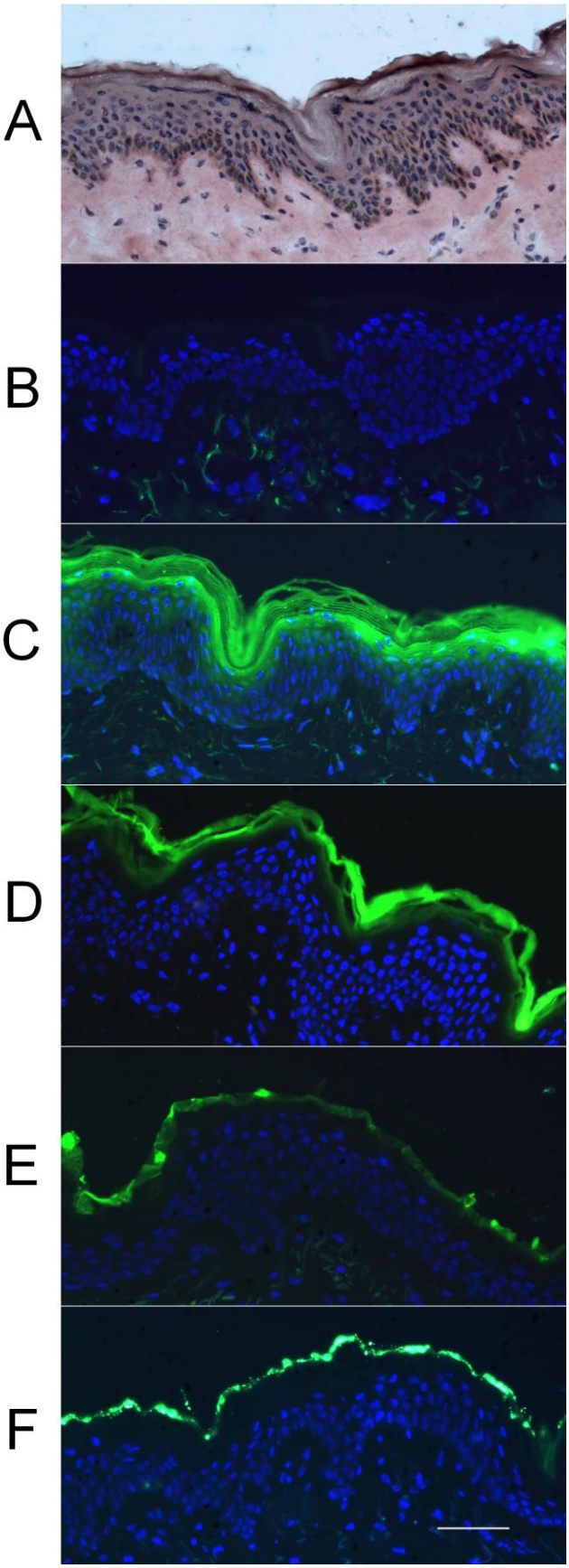

Penetration of fluorescent Cer through human skin

The first experiment was realized under similar conditions as described in [12]. The fluorescent Cer were applied as 10 µM solutions in propylene glycol/ethanol 7:3 (v/v) on intact and acetone-treated human skin for 2 h. Although *ex vivo* human skin was used, its viability was maintained throughout the experiment as assessed by 2,3,5-triphenyltetrazolium chloride (TTC) reduction. The fluorescence of Cer derivatives was clearly distinguishable from epidermal autofluorescence. NBD-C24-Cer and NBD-14S24 stayed in upper SC layers while NBD-C6-Cer and NBD-C12-Cer diffused deeper into SC. Surprisingly, neither long nor short-chain NBD-Cer penetrated into nucleated epidermal layers.

Thus, the exposure was prolonged to 12 h. Nevertheless, the results were more or less the same. In one of five replicates, NBD-C6-Cer fluorescence was visible in the nucleated epidermis while it reached only lower SC in the others. The diffusivity of NBD-C12-Cer in SC seemed to be similar; however, both 24C acyl-bearing lipids persisted in several upper SC layers. At the end of this experiment, viability of intact and acetone-treated skin was 80±4% and 63±13%, respectively, compared to freshly excised skin.

Figure 3. Penetration of exogenous fluorescent Cer with different chain length and pseudoCer 14S24 into human skin. Cer (green fluorescence) were applied on the *ex vivo* viable human skin in an equimolar mixture with cholesterol and lignoceric acid in propylene glycol/ethanol 7:3 vehicle at a total lipid concentration 1 % for 12h. Histological sections are shown using (**a**) brightfield microscopy with H&E staining, (**b**-**f**) fluorescence microscopy with nuclei of cells (blue) stained with the Hoechst 33258 dye. (**a**) and (**b**) controls, (**c**) NBD-C6-Cer, (**d**) NBD-C12-Cer, (**e**) NBD-C24-Cer, (**f**) NBD-14S24. Scale bar 50µm.

In addition, this experiment was also performed on a non-viable frozen-and-thawed skin yielding essentially the same results with slightly deeper SC penetration. In an attempt to obtain reproducible penetration of NBD-C6-Cer into viable epidermis as described previously in mice *in vivo* [12], an equimolar mixture of NBD-Cer, cholesterol and lignoceric acid at the total concentration of 1% was applied to the skin, which corresponds to 6.3-7.5 mM concentration of each lipid.
Indeed, this high-concentration donor sample resulted in reproducible penetration of the short-chain NBD-C6-Cer into the nucleated epidermal layers in both intact and acetone-treated skin. However, the longer-chain lipids were only found in SC (Figure 3).

DISCUSSION

Topical skin lipid supplementation may provide opportunities for controlling Cer deficiency and improving skin condition in diseases such as atopic dermatitis or psoriasis [1]. Indeed, it has been shown that a Cer-dominant barrier repair emollient significantly alleviated severity of atopic dermatitis [10, 11]. The mechanisms by which exogenous Cer correct the barrier abnormalities have been under debate for some time. In contrast to petrolatum, which remained restricted to SC, short-chain NBD-C6-Cer penetrated into the nucleated epidermal cells, was transported to the distal Golgi apparatus and then reprocessed [19]. However, the recent findings showed substantial differences between short and long-chain ceramides [23]. Thus, it is questionable whether topical application of long-chain Cer can also have an impact on the underlying proliferation/differentiation responses of the epidermis in addition to a direct, physical supplementation of SC lipids. These long-chain sphingolipids are considered, due to their extremely hydrophobic nature, unlikely to penetrate through intact SC [30, 31]. Thus, we aimed at studying skin penetration of NBD-labeled Cer with different chain length and of the pseudoCer 14S24.

In the first experiment, with the lipids applied at 10 μM concentration for 2 h, that is under similar conditions as described previously [12], none of the lipids penetrated into the viable epidermal layers. Thus, the exposure to NBD-Cer was prolonged to 12 h, but still no reproducible penetration of the NBD-Cer into the nucleated human epidermis was observed. This may be due the different barrier properties of mice and human skin [32, 33]. Moreover, other studies with this short-chain Cer also gave contradictory results suggesting that this effect may be vehicle and concentration-dependent. For example, no uptake of NBD-C6-Cer into hairless mice epidermis from petrolatum was found [34]. In contrast, when using a complex lipid vehicle for 2 h [34] and 1.7% solution in dimethyl sulfoxide, which is actually a potent permeation enhancer, for 4 h [35], respectively, the fluorescence was visible in the viable epidermis.

It should be noted that although *ex vivo* human skin was used in this study, viability of the tissue was maintained throughout the experiment. Only when using acetone-treated skin, its viability decreased to 63±13% at 12 h. Similar effect of short-term acetone treatment was described in tissue engineered skin [36]. Nevertheless, no significant difference was found between the penetration of NBD-lipids through intact and acetone-treated skin. In addition, one experiment was performed on a non-viable skin leading to similar distribution of the fluorescent lipids in the skin. Despite the inability of neither the short- nor the long-chain Cer to traverse SC, chain length-dependence was observed with the shorter analogues penetrating deeper into SC.

In order to obtain reliable penetration of NBD-C6-Cer into nucleated epidermal layers of the *ex vivo* human skin, i.e. to reproduce the previous *in vivo* results [12] and to be able to distinguish between the Cer homologues, the tissue was exposed to an equimolar mixture of

NBD-Cer, cholesterol and lignoceric acid at the total lipid concentration of 1% for 12 h. Under these conditions, fluorescence of the short-chain NBD-C6-Cer was observed within the viable epidermis. On the contrary, the long-chain lipids were not able to penetrate through SC, either intact or acetone-treated. Notably, both NBD-C24-Cer and NBD-14S24 stayed in several upper SC layers irrespective of the three orders of magnitude higher concentration applied.

The reason for the observed chain length-dependence in Cer penetration may be the difference in partitioning and mobility of the short- and long-chain Cer. First, the long-chain Cer are likely too hydrophobic to partition from SC into a hydrophilic viable epidermis. Indeed, free natural long-chain Cer cannot exist in solution in biological fluids or in cytosol. In addition, they belong to the category of non-swelling amphiphiles [37], implying that they cannot even give rise to micelles or other aggregates in aqueous suspension, as do, for example phospholipids and short-chain Cer [21]. For example, long-chain Cer stays relatively tightly bound to the membrane where it is generated [38, 39], while short Cer can leave the membrane and translocate to other membranes.

Based on the studies with NBD-C6-Cer, exogenous Cer are believed to be uptaken by nucleated epidermal cells, transported to the distal Golgi apparatus, metabolized and incorporated into lamellar bodies [19]. However, an elegant study comparing the effects of short- and long-chain Cer showed that although exogenous NBD-C6-Cer taken up via the plasma membrane was converted into glucosylCer in the Golgi, long-chain Cer generated in the plasma membrane did not reach the Golgi and thus were not glycosylated [40]. These data illustrate that short-chain Cer do not exactly mimic the behavior of naturally occurring long-chain Cer species.

Second, long-chain Cer were probably unable to traverse the rigid array of long-chain SC lipids since both NBD-C24-Cer and NBD-14S24 were only found in the upper SC layers. The better penetration of shorter analogues through the membranes and SC lipid lamellae may be explained by their smaller molecule and faster exchange between the lipidic bilayers. It has been found that the exchange of natural Cer between lipid membranes requires days [41], while it takes less than a minute for short chain, fluorescent Cer to exchange between lipid vesicles [42]. The easier transbilayer movement of C6 Cer than C16 Cer was observed in phospholipid membranes [43]. Short chain Cer were also found to decrease the skin barrier properties [23], which may explain their higher penetration. Such chain length dependence may be explained by stronger hydrophobic interactions between longer Cer chains. Since the hydrophobic interactions are caused by the attraction of induced dipoles in the hydrophobic chains, they strongly depend on the chain length. Thus, the shorter the chain, the weaker the interaction is expected to be, causing an increased permeability.

In conclusion, these findings imply that the mechanism of action of the long-chain Cer and Cer analogue 14S24 is likely a direct, physical supplementation of SC lipids. Moreover, these lipids are not able to penetrate into viable epidermis, which increases their overall safety in the treatment of the skin barrier diseases.

However, it should be kept in mind that these results were obtained using NBD-labeled lipids and should be confirmed using more physiological fluorescent Cer, e.g. with polyene fluorophores, or radiolabeled lipids (for an excellent comparison and discussion on these Cer tools, see [44]). Nevertheless, these results showed different behavior of short and long chain NBD-Cer in the human skin. Although short-chain Cer are useful experimental tools in many sphingolipid studies, they cannot be used as general Cer mimics, particularly when considering Cer effects in lipid membranes including SC lipid lamellae.

MATERIALS AND METHODS

Chemicals, instrumentation and synthesis of fluorescent lipids

See Supplementary Materials and Methods

Skin

Human skin from Caucasian female patients, who had undergone abdominal plastic surgery, was used. The procedure has been approved by the Ethics Committee of the University Hospital Hradec Králové, Czech Republic (No. 200609 S09P) and conducted according to the Declaration of Helsinki Principles. After excision, the subcutaneous fatty tissue was removed by a scalpel. Before the start of the experiment, the skin was maintained at 4°C for maximum of 8 h. No significant decrease in viability was observed during this period.

The penetration experiments were performed on intact and acetone-treated skin, respectively. Acetone-extracted skin was prepared by gentle rubbing of the skin surface for 1 min [45] with 1.0 ml of acetone in a cotton ball.

NBD-Cer samples

The NBD-Cer donor samples were prepared in propylene glycol/ethanol 7:3 (v/v) [12]. Two series of samples were prepared for each compound, a) 10μM solution of NBD-C6-Cer, NBD-C12-Cer, NBD-C24-Cer, and pseudoCer NBD-14S24, respectively, and b) equimolar mixture of Cer, cholesterol and lignoceric acid with total lipid amount being 1% w/v. The samples were allowed to equilibrate for 24 h at 32°C before application to the skin.

Penetration of fluorescent lipids

The tissue samples were transferred into cell culture dishes filled with Dulbecco's Modified Eagle's Medium (DMEM) supplemented with penicilline, streptomycine and amphotericine B. The level of the medium was adjusted so that the tissue specimens were incubated at the air-liquid interface [46]. After 1 h equilibration at 32°C, 50 μl of Cer donor samples were applied using rings with 1 cm^2 diameter glued to the skin surface. The skin was then incubated at 32°C for 2 h and 12 h, respectively. All the experiments were performed at least in triplicate using skin from two donors. At the end of the experiment, the donor Cer solution was wiped off with a cotton stub and the skin surface was gently washed with water. Skin specimens of approximately 10 mm^2 area were excised and immersed in Optimal Cutting Temperature embedding medium (Leica, Prague, Czech Republic), snap-frozen in liquid nitrogen and stored at −80 °C.

Skin viability

Viability of the skin was assessed by TTC reduction assay [47]. Briefly, punch biopsies of 5 mm diameter (6 replicates) were incubated in 1 ml of 1.5% TTC and 3% sodium succinate in phosphate-buffered saline at pH 7.4 (PBS) at 37°C under nitrogen. After 1 h, the skin specimens were blotted dry and the dark red formazan derivative formed by mitochondrial enzymes was extracted with 1 ml Methyl Cellosolve (2-methoxyethanol) overnight. The absorption at 490 nm was measured and corrected using skin specimens devitalized by boiling as a negative control. During the experiment, no significant decrease in viability was observed.

Fluorescence microscopy

Sections of 7 μm thickness were cut on a cryostat and placed on gelatin-coated slides. Slides were air-dried and fixed in acetone at −20 °C for 30 min. After being rinsed in PBS the slides were counterstained with Hoechst 33258 dye and examined under a fluorescence microscope.

Photo documentation and image digitizing from the microscope were performed with the Olympus AX 70, with a digital firewire camera Pixelink PL-A642 (Vitana Corp. Ottawa, Canada) with image analysis software NIS ver. 3.0 (Laboratory Imaging, Czech Republic).

CONFLICT OF INTEREST

The authors state no conflict of interest.

ACKNOWLEDGEMENT

This work was supported by the Centre for New Antivirals and Antineoplastics (1M0508) and the Ministry of Education of the Czech Republic (MSM0021620822).

SUPPLEMENTARY INFORMATION

Chemicals and instrumentation

All chemicals were purchased from Sigma-Aldrich (Schnelldorf, Germany). Silica gel 60 (230-400 mesh) for column chromatography, TLC plates (silica gel 60 F_{254}, aluminium back) and HPLC columns were obtained from Merck (Darmstadt, Germany). The reaction under microwave activation was carried out in a Milestone MicroSYNTH Ethos 1600 URM reactor. The structure and purity of the synthesized compounds were confirmed by FTIR (Nicolet Impact 400 spectrophotometer), MS (Quattro Micro triple quadrupole, Waters Micromass) and ^{1}H and ^{13}C NMR spectra (Varian Mercury-Vx BB 300 instrument, operating at 300 MHz for ^{1}H, 75 MHz for ^{13}C). The melting points were measured with a Kofler apparatus and are uncorrected.

Synthesis

12-bromododecan-1-ol (1). Dodecan-1,12-diol (15.0 g, 74.1 mmol) in toluene (220 ml) with 48% HBr (10 ml, 89.0 mmol) was refluxed in microwave reactor at 600 MW for 2x20 min. Further HBr (3.3 ml, 29.4 mmol) was then added and the reaction was refluxed for additional 20 min at 600 MW. The mixture was cooled to room temperature (RT), the toluene layer separated and extracted with saturated $NaHCO_3$ (150 ml). The organic phase was dried over Na_2SO_4 and concentrated under vacuum. Pure compound was obtained after column chromatography, using hexane/ethyl acetate (4:1). Mp = 29-30°C. Yield = 76%. ^{1}H NMR (300 MHz, $CHCl_3$): δ 3.64 (t, J = 6.6 Hz, 2H), 3.41 (t, J = 6.9 Hz, 2H), 1.80-1.90 (m, 2H), 1.52-1.61 (m, 2H), 1.27-1.44 (m, 16H); ^{13}C NMR (75 MHz, $CHCl_3$): δ 63.1, 34.1, 32.8, 29.6, 29.5, 29.4, 28.1, 25.7.

12-bromododecanoic acid (2). The alcohol (**1**) (4.0 g, 15.1 mmol) in acetone (15 ml) was slowly added to a stirred ice-cold mixture of CrO_3 (5.85 g, 58.5 mmol), acetic acid (52.4 ml) and water (6 ml). The mixture was stirred at 5°C for 2.5 h, warmed up to RT and stirred overnight. The reaction was poured into water (250 ml) and extracted with diethyl ether (3x200 ml). The crude was purified on silica column, eluting with hexane/ethyl acetate (4:1). Mp = 49-50°C. Yield = 82%. ^{1}H NMR (300 MHz, $CHCl_3$): δ 3.41 (t, J = 6.9 Hz, 2H), 2.35 (t, J = 7.5 Hz, 2H), 1.80-1.90 (m, 2H), 1.58-1.68 (m, 2H), 1.27-1.44 (m, 14H); ^{13}C NMR (75 MHz, $CHCl_3$): δ 180.1, 34.1, 34.0, 32.8, 29.4, 29.3, 29.2, 29.0, 28.7, 28.1, 24.6.

2-(12-bromododecyloxy)tetrahydro-2H-pyran (3). Dihydro-*2H*-pyran (3.21 ml, 33.6 mmol) and pyridinium *p*-toluensulfonate (180 mg, 0.72 mmol) was added to alcohol (**1**) (5.93 g, 22.4

mmol) in chloroform (55 ml) at 0°C. The reaction was slowly warmed up to RT, stirred for additional 3h and then extracted with water (200 ml). The aqueous phase was washed with chloroform (2x200ml). Combined organic layers were washed with brine, dried over Na_2SO_4 and concentrated under reduced pressure. The product was obtained after column chromatography on silica with hexane/ethyl acetate (19:1). Yield = 96%. ^{1}H NMR (300 MHz, $CHCl_3$): δ 4.57 (t, J = 3.6 Hz, 1H), 3.83-3.91 (m, 1H), 3.69-3.77 (m, 1H), 3.46-3.53 (m, 1H), 3.36-3.43 (m, 3H), 1.79-1.89 (m, 3H), 1.49-1.61 (m, 7H), 1.27-1.44 (m, 16H); ^{13}C NMR (75 MHz, $CHCl_3$): δ 98.8, 67.7, 62.3, 34.1, 32.8, 30.8, 29.7, 29.5, 29.4, 28.7, 28.2, 26.2, 25.5, 19.7.

24-(tetrahydro-2H-pyran-2-yloxy)tetracosanoic acid (4). The protected bromide (**3**) (9.36 g, 26.8 mmol) and dibromomethane (0.2 ml, 2.88 mmol) were dissolved in dry THF (15 ml). Magnesium (0.71 g, 29.2 mmol) was added and the reaction was refluxed until most of the metal dissolved (approx. 3 h). The bromoacid (**2**) (6.73 g, 22.34 mmol) was suspended in dry THF, cooled to -20°C under nitrogen and 3M solution of methylmagnesium chloride in THF (8.2 ml, 24.6 mmol) was added. After the cessation of gas evolution, freshly prepared 2M solution of Li_2CuCl_4 in THF (2.23 ml, 4.46 mmol) was added, followed by dropwise addition of Grignard compound prepared from (**3**). The mixture was stirred for 24 h at -20°C. The reaction was poured into 0.5M H_2SO_4 (400 ml) and extracted with diethyl ether (3x400 ml). The organic phase was dried over Na_2SO_4 and concentrated under reduced pressure. The crude was separated on column using hexane/ethyl acetate (25% to 80% of ethyl acetate). Mp = 69-70°C. Yield = 58%. ^{1}H NMR (300 MHz, $CHCl_3$): δ 4.58 (t, J = 3.4 Hz, 1H), 3.84-3.91 (m, 1H), 3.69-3.77 (m, 1H), 3.47-3.54 (m, 1H), 3.34-3.42 (m, 1H), 2.34 (t, J = 7.5 Hz, 2H), 1.49-1.87 (m, 12H), 1.25-1.39 (m, 36H); ^{13}C NMR (75 MHz, $CHCl_3$): δ 179.0, 98.8, 67.7, 62.3, 33.9, 30.8, 29.7, 29.5, 29.4, 29.2, 29.0, 26.2, 25.5, 24.7, 19.7; IR (ATR): ν_{max} 2912, 2846, 1701, 1691, 1471, 1034.

Methyl 24-hydroxytetracosanoate (5). Thionylchloride (0.71 ml, 9.8 mmol) was added dropwise to dry methanol (150 ml) under nitrogen not to exceed -15°C. Acid (**4**) (1.88 g, 4.0 mmol) was added and stirred at -20°C for additional 0.5 h, slowly warmed up to RT and stirred overnight. The resulting suspension was cooled to 0°C, the solid was filtered off, washed with cold methanol and dried under vacuum. The product was obtained as a colorless solid. Mp = 77-79°C. Yield = 90%. ^{1}H NMR (300 MHz, $CHCl_3$): δ 3.66 (s, 3H), 3.63 (t, J = 6.7 Hz, 2H), 2.29 (t, J = 7.5 Hz, 2H), 1.51-1.63 (m, 4H), 1.24-1.36 (m, 38H); ^{13}C NMR (75 MHz, $CHCl_3$): δ 174.3, 63.1, 51.4, 34.1, 32.8, 29.7, 29.6, 29.4, 25.7, 24.9; IR (ATR): ν_{max} 2914, 2847, 1736, 1461, 1173.

23-carboxytricosan-1-aminium chloride (6). Freshly prepared 1.2M solution of azoimide in benzene (2.51 ml, 3.0 mmol) was added to the solution of hydroxy acid (**5**) (1.0 g, 2.51mmol) in dry THF (1.25 ml), followed by triphenylphosphine (1.45 g, 5.52 mmol) in dry THF (8 ml). Subsequently, di-isopropyl azodicarboxylate (0.57 ml, 2.76 mmol) in THF (1.25 ml) was added and stirred for 3h, followed by further addition of triphenylphosphine (0.66g, 2.51 mmol). The reaction was stirred at 50°C for 3h. Then, 1M HCl (4 ml) was added and stirred overnight at RT. The mixture was concentrated under vacuum, suspended in THF/1M KOH (10 ml), refluxed for 3h, cooled to RT and neutralized with 1 M HCl. The solid was filtered off, recrystallized from acetic acid and dried over NaOH, giving a colorless solid. Mp = 151-155°C. Yield = 49%. ^{1}H NMR (300 MHz, DMSO): δ 7.75 (br s, 3H), 2.68-2.78 (m, 2H), 2.17 (t, J = 7.3 Hz, 2H), 1.41-1.53 (m, 4H), 1.16-1.29 (m, 38H). IR (KBr): ν_{max} 3428, 2917, 2850, 1729, 1472, 720.

6-(7-nitrobenzo[c][1,2,5]oxadiazol-4-ylamino)hexanoic acid (7a). 6-Aminohexanoic acid (50mg, 0.38 mmol), 4-chloro-7-nitrobenzofurazan (NBD-Cl) (76 mg, 0.38 mmol) and $NaHCO_3$ (96 mg, 1.14 mmol) were stirred in methanol (5 ml) at 0°C for 0.5 h, at RT for 1.5 h and then at 50°C for additional 1.5 h. The reaction was cooled to RT and carefully acidified with 0.1 M HCl. The solid was filtered off, purified on silica, eluting with chloroform-chloroform/methanol (50:1) and recrystallized from aqueous methanol giving an orange solid. Mp = 158-159°C. Yield = 63%. ^{1}H NMR (300 MHz, $CHCl_3$): δ ^{1}H NMR (300 MHz, $CHCl_3$): δ 9.52 (s, 1H), 8.48 (d, J = 8.8 Hz, 1H), 6.38 (d, 8.8 Hz, 1H), 3.44 (m, 2H), 2.21 (t, J = 7.2 Hz, 2H), 1.62-1.72 (m, 2H), 1.49-1.59 (m, 2H), 1.34-1.41 (m, 2H); ^{13}C NMR (75 MHz, $CHCl_3$): δ 174.6, 145.4, 144.6, 144.3, 138.1, 120.7, 99.3, 43.4, 33.7, 27.6, 26.1, 24.4; IR (ATR): ν_{max} 3348, 2927, 2856, 1729, 1697, 1585, 1492, 1290, 1256, 1168, 1117, 994.

12-(7-nitrobenzo[c][1,2,5]oxadiazol-4-ylamino)dodecanoic acid (7b). 12-Aminododecanoic acid was converted to compound **7b** using the same procedure as for **7a**. Mp = 94-96°C. Yield = 81%. ^{1}H NMR (300 MHz, $CHCl_3$): δ 8.50 (d, J = 8.7 Hz, 1H), 6.34 (m, 1H), 6.18 (d, J = 8.7 Hz, 1H), 3.49 (q, J = 6.6 Hz, 2H), 2.35 (t, J = 7.5 Hz, 2H), 1.76-1.86 (m, 2H), 1.58-1.68 (m, 2H), 1.25-1.50 (m, 14H); ^{13}C NMR (75 MHz, $CHCl_3$): δ 179.1, 144.2, 143.9, 143.8, 136.5, 123.9, 98.5, 44.0, 33.8, 29.3, 29.2, 29.1, 29.0, 28.9, 28.5, 26.9, 24.6. IR (ATR): ν_{max} 3300, 2921, 2848, 1708, 1617, 1585, 1495, 1466, 1227, 1181, 905, 724.

24-(7-nitrobenzo[c][1,2,5]oxadiazol-4-ylamino)tetracosanoic acid (7c). ω-Amino acid hydrochloride (**6**) (150 mg, 0.36 mmol), NBD-Cl (71 mg, 0.36 mmol) and $NaHCO_3$ (90 mg, 1.07 mmol) were refluxed in methanol (15 ml) for 3.5h. The reaction was cooled to RT and carefully acidified with 0.1 M HCl. The solid was filtered off, purified on silica, eluting with chloroform/methanol (50:1) and recrystallized from chloroform/hexane giving a brownish solid. Mp = 116-117°C. Yield = 56%. ^{1}H NMR (300 MHz, $CHCl_3$): δ 8.50 (d, J = 8.5 Hz, 1H), 6.26 (s, 1H), 6.17 (d, J = 8.5 Hz, 1H), 3.48 (q, J = 6.6 Hz, 2H), 2.35 (t, J = 7.5 Hz, 2H), 1.76-1.86 (m, 2H), 1.58-1.68 (m, 2H), 1.25-1.52 (m, 38H). IR (ATR): ν_{max} 3300, 2921, 2848, 1708, 1617, 1585, 1495, 1466, 1227, 1181. MS: ESI (pos) *m/z* 569.5 $(M+Na)^+$, 601.52 $(M+2Na)^+$ MS: ESI (neg) *m/z* 545.6 $(M-H)^-$

General procedure for the preparation of the NBD-labeled acid succinimidylesters (8a-c). To a 0°C solution of ω-NBD-amino acid (**7a-c**) (0.11 mmol), *N*-hydroxysuccinimide (13 mg, 0.11 mmol) and 4-dimethylaminopyridine (2 mg, 0.016 mmol) in chloroform (6 ml) was added dicyclohexylcarbodiimide (26 mg, 0.13 mmol). The reaction was stirred at 0°C for 0.5h and then at RT overnight. The suspension was concentrated under vacuum and separated on silica, eluting with chloroform/methanol (50:1).

2,5-dioxopyrrolidin-1-yl 6-(7-nitrobenzo[c][1,2,5]oxadiazol-4-ylamino)hexanoate (8a). Mp = 189-191°C. Yield = 85%. ^{1}H NMR (300 MHz, $CHCl_3$): δ 8.50 (d, J = 8.8 Hz, 1H), 6.44 (m, 1H), 6.19 (d, J = 8.8 Hz, 1H), 3.54 (q, J = 6.2 Hz, 2H), 2.87 (s, 4H), 2.67 (t, J = 6.8 Hz, 2H), 1.82-1.92 (m, 4H), 1.57-1.69 (m, 4H).

2,5-dioxopyrrolidin-1-yl 12-(7-nitrobenzo[c][1,2,5]oxadiazol-4-ylamino)dodecanoate (8b). Mp = 162-164°C. Yield = 95%. ^{1}H NMR (300 MHz, $CHCl_3$): δ 8.51 (d, J = 8.8 Hz, 1H), 6.26 (m, 1H), 6.19 (d, J = 8.8 Hz, 1H), 3.50 (q, J = 6.6 Hz, 2H), 2.85 (s, 4H), 2.61 (t, J = 7.4 Hz, 2H), 1.67-1.87 (m, 4H), 1.25-1.56 (m, 14H).

2,5-dioxopyrrolidin-1-yl 24-(7-nitrobenzo[c][1,2,5]oxadiazol-4-ylamino)tetracosanoate (8c). Mp = 146-148°C. Yield = 96%. ^{1}H NMR (300 MHz, $CHCl_3$): δ 8.51 (d, J = 8.8 Hz, 1H),

6.17 (d, J = 8.8 Hz, 1H), 3.48 (q, J = 6.2 Hz, 2H), 2.84 (s, 4H), 2.60 (t, J = 7.5 Hz, 2H), 1.69-1.85 (m, 4H), 1.25-1.56 (m, 38H).

General procedure for the preparation of NBD-labeled Cer. Succinimidyl ester (**8a-c**) (0.085 mmol) was dissolved in dry $CHCl_3$ (5 ml) and sphingosine (26 mg, 0.087 mmol) was added. The solution was stirred at RT for 48 h. Then, the reaction was concentrated under vacuum and purified on silica eluting with chloroform/methanol (0 to 2% of methanol) yielding an orange solid.

(*2S,3R,4E*)-N-(1,3-dihydroxyoctadec-4-en-2-yl)-12-(7-nitrobenzo[c][1,2,5]oxadiazol-4-ylamino)hexanamide (NBD-C6-Cer). Mp = 85-88°C. Yield = 54%. ^{1}H NMR (300 MHz, $CHCl_3$): δ): δ 8.48 (d, J = 8.7 Hz, 1H), 6.74 (m, 1H), 6.36 (d, J = 7.4 Hz, 1H), 6.17 (d, J = 8.7 Hz, 1H), 5.80 (dt, J = 14.6, 7.2 Hz, 1H), 5.55 (dd, J = 15.5, 6.3 Hz, 1H), 4.36 (br s, 1H), 3.93-4.02 (m, 2H), 3.71 (m, 1H), 3.53 (q, J = 6.3 Hz, 2H), 2.75 (br s, 2H), 2.31 (t, J = 6.9 Hz, 2H), 2.06 (q, J = 6.7 Hz, 2H), 1.72-1.89 (m, 4H), 1.49-1.59 (m, 2H), 1.21-1.39 (m, 22H), 0.87 (t, J = 6.7 Hz, 3H); ^{13}C NMR (75 MHz, $CHCl_3$): δ 173.6, 144.2, 143.9, 136.8, 134.3, 128.6, 74.4, 62.2, 54.5, 36.1, 32.3, 31.9, 29.3, 29.2, 29.1, 27.7, 26.2, 24.8, 22.7, 14.1. IR (KBr): ν_{max} 3397, 2922, 2851, 1637, 1623, 1589, 1309, 1271.

(*2S,3R,4E*)-N-(1,3-dihydroxyoctadec-4-en-2-yl)-12-(7-nitrobenzo[c][1,2,5]oxadiazol-4-ylamino)dodecanamide (NBD-C12-Cer). Mp = 92-93°C. Yield = 75%. ^{1}H NMR (300 MHz, $CHCl_3$): δ 8.48 (d, J = 8.5 Hz, 1H), 6.72 (m, 1H), 6.38 (d, J = 7.4 Hz, 1H), 6.17 (d, J = 8.7 Hz, 1H), 5.77 (dt, J = 15.5, 6.6 Hz, 1H), 5.52 (dd, J = 15.5, 6.3 Hz, 1H), 4.31 (t, J = 3.8 Hz, 1H), 3.89-3.97 (m, 2H), 3.70 (dd, J = 10.6, 2.3 Hz, 1H), 3.49 (q, J = 6.6 Hz, 2H), 2.22 (t, J = 7.6 Hz, 2H), 2.03 (q, J = 6.6 Hz, 2H), 1.75-1.85 (m, 2H), 1.56-1.66 (m, 2H), 1.24-1.47 (m, 36H), 0.86 (t, J = 6.4 Hz, 3H); ^{13}C NMR (75 MHz, $CHCl_3$): δ 174.0, 144.2, 144.1, 136.7, 134.2, 128.7, 98.5, 74.5, 62.4, 54.5, 44.0, 36.7, 32.3, 31.9, 29.6, 29.5, 29.3, 29.2, 29.1, 29.0, 28.4, 26.8, 25.6, 22.6, 14.1; IR (KBr): ν_{max} 3374, 2921, 2850, 1643, 1624, 1586, 1508, 1466, 1309, 1272.

(*2S,3R,4E*)-N-(1,3-dihydroxyoctadec-4-en-2-yl)-24-(7-nitrobenzo[c][1,2,5]oxadiazol-4-ylamino)tetracosanamide (NBD-C24-Cer). Mp = 92-94°C. Yield = 50%. ^{1}H NMR (300 MHz, $CHCl_3$): δ 8.49 (d, J = 8.5 Hz, 1H), 6.41 (s, 1H), 6.30 (d, J = 6.6 Hz, 1H), 6.17 (d, J = 8.5 Hz, 1H), 5.78 (dt, J = 15.5, 6.7 Hz, 1H), 5.52 (dd, J = 15.3, 6.3 Hz, 1H), 4.30-4.33 (m, 1H), 3.89-3.97 (m, 2H), 3.70 (dd, J = 10.6, 2.3 Hz, 1H), 3.48 (q, J = 6.6 Hz, 2H), 2.23 (t, J = 7.6 Hz, 2H), 2.05 (q, J = 6.9 Hz, 2H), 1.76-1.86 (m, 2H), 1.58-1.68 (m, 2H), 1.25-1.49 (m, 62H), 0.87 (t, J = 6.5 Hz, 3H); ^{13}C NMR (75 MHz, $CHCl_3$): δ 174.0, 143.9, 136.5, 134.2, 128.8, 98.5, 74.6, 62.5, 54.5, 44.0, 36.8, 32.3, 31.9, 29.7-29.1, 28.5, 26.9, 25.7, 22.7, 14.0; IR (KBr): ν_{max} 3420, 2919, 2850, 1654, 1624, 1585, 1571, 1467, 1302, 1271; MS: ESI (pos) *m/z* 851.0 $(M+Na)^+$; MS: ESI (neg) *m/z* 827.0 $(M-H)^-$.

Tetradecyl (*2S*)-3-hydroxy-2-(24-(7-nitrobenzo[c][1,2,5]oxadiazol-4-ylamino)tetracosanamido)propanoate (NBD-14S24). 3-hydroxy-1-oxo-1-(tetradecyloxy)propan-2-aminium chloride (27 mg, 0.080 mmol) and 4-dimethylaminopyridine (11 mg, 0.090 mmol) were stirred in dry chloroform (5 ml) at RT for 15 min. The reaction was cooled to 0°C and NBD acid (**7c**) (50 mg, 0.091 mmol) and 1-ethyl-3-(3-dimethylaminopropyl)carbodiimide (14 µl, 0.080 mmol) were added. The reaction was stirred for 48 h at RT, and then extracted with water (20 ml). The aqueous phase was washed with chloroform (2x20 ml), the combined organic layers were dried over Na_2SO_4, filtered, concentrated in vacuum, and the crude was purified on silica with chloroform/methanol

(50:1). Mp = 101-104°C. Yield = 71.5%. ^{1}H NMR (300 MHz, $CHCl_3$): δ 8.49 (d, J = 8.6 Hz, 1H), 6.43 (d, J = 6.9 Hz, 1H), 6.35 (s, 1H), 6.18 (d, J = 8.8 Hz, 1H), 4.67 (dt, J = 7.0, 3.4 Hz, 1H), 4.17 (t, J = 6.7 Hz, 2H), 3.95 (d, J = 3.0 Hz, 2H), 3.48 (q, J = 6.7 Hz, 2H), 2.66 (s, 1H), 2.27 (t, J = 7.6 Hz, 2H), 1.76-1.86 (m, 2H), 1.59-1.69 (m, 4H), 1.25-1.51 (m, 60H), 0.87 (t, J = 6.7 Hz, 3H); ^{13}C NMR (75 MHz, CHCl3): δ 173.8, 170.5, 144.2, 136.5, 123.9, 98.5, 66.1, 64.0, 54.9, 44.0, 36.5, 31.9, 29.7-29.2, 28.5, 26.9, 25.8, 25.5, 22.7, 14.1; IR (ATR): ν_{max} 3308, 2915, 2849, 1723, 1647, 1625, 1556, 1470, 1249; MS: ESI (pos) *m/z* 851.0 $(M+Na)^+$, 869.0 $(M+K)^+$; MS: ESI (neg) *m/z* 828.9 $(M-H)^-$.

REFERENCES

[1] Choi, M. J.; Maibach, H. I., Role of ceramides in barrier function of healthy and diseased skin. *Am J Clin Dermatol* **2005,** 6, 215-23.

[2] Holleran, W. M.; Takagi, Y.; Uchida, Y., Epidermal sphingolipids: metabolism, function, and roles in skin disorders. *FEBS Lett* **2006,** 580, 5456-66.

[3] Bouwstra, J. A.; Ponec, M., The skin barrier in healthy and diseased state. *Biochim. Biophys. Acta* **2006,** 1758, 2080-95.

[4] Feingold, K. R., Thematic review series: skin lipids. The role of epidermal lipids in cutaneous permeability barrier homeostasis. *J. Lipid Res.* **2007,** 48, 2531-46.

[5] Wertz, P. W., Lipids and barrier function of the skin. *Acta Derm Venereol Suppl (Stockh)* **2000,** 208, 7-11.

[6] Elias, P. M.; Feingold, K. R., *Skin Barrier* CRC Press: NY, 2006.

[7] Imokawa, G., Lipid abnormalities in atopic dermatitis. *J Am Acad Dermatol* **2001,** 45, S29-32.

[8] Imokawa, G.; Abe, A.; Jin, K.; Higaki, Y.; Kawashima, M.; Hidano, A., Decreased level of ceramides in stratum corneum of atopic dermatitis: an etiologic factor in atopic dry skin? *J Invest Dermatol* **1991,** 96, 523-6.

[9] Motta, S.; Monti, M.; Sesana, S.; Mellesi, L.; Ghidoni, R.; Caputo, R., Abnormality of water barrier function in psoriasis. Role of ceramide fractions. *Arch Dermatol* **1994,** 130, 452-6.

[10] Chamlin, S. L.; Frieden, I. J.; Fowler, A.; Williams, M.; Kao, J.; Sheu, M.; Elias, P. M., Ceramide-dominant, barrier-repair lipids improve childhood atopic dermatitis. *Arch Dermatol* **2001,** 137, 1110-2.

[11] Chamlin, S. L.; Kao, J.; Frieden, I. J.; Sheu, M. Y.; Fowler, A. J.; Fluhr, J. W.; Williams, M. L.; Elias, P. M., Ceramide-dominant barrier repair lipids alleviate childhood atopic dermatitis: changes in barrier function provide a sensitive indicator of disease activity. *J Am Acad Dermatol* **2002,** 47, 198-208.

[12] Man, M. Q.; Feingold, K. R.; Elias, P. M., Exogenous lipids influence permeability barrier recovery in acetone-treated murine skin. *Arch Dermatol* **1993,** 129, 728-38.

[13] Imokawa, G.; Yada, Y.; Higuchi, K.; Okuda, M.; Ohashi, Y.; Kawamata, A., Pseudo-acylceramide with linoleic acid produces selective recovery of diminished cutaneous barrier function in essential fatty acid-deficient rats and has an inhibitory effect on epidermal hyperplasia. *J Clin Invest* **1994,** 94, 89-96.

[14] Philippe, M.; Garson, J. C.; Gilard, P.; Hocquaux, M.; Hussler, G.; Leroy, F.; Mahieu, C.; Semeria, D.; Vanlerberghe, G., Synthesis of 2-N-oleoylamino-octadecane-1,3-diol: a new ceramide highly effective for the treatment of skin and hair. *International Journal of Cosmetic Science* **1995,** 17, 133-146.

[15] Vavrova, K.; Zbytovska, J.; Palat, K.; Holas, T.; Klimentova, J.; Hrabalek, A.; Dolezal, P., Ceramide analogue 14S24 ((S)-2-tetracosanoylamino-3-hydroxypropionic acid tetradecyl ester) is effective in skin barrier repair in vitro. *Eur J Pharm Sci* **2004,** 21, 581-7.

[16] Takagi, Y.; Nakagawa, H.; Higuchi, K.; Imokawa, G., Characterization of surfactant-induced skin damage through barrier recovery induced by pseudoacylceramides. *Dermatology* **2005,** 211, 128-34.

[17] Matsuki, H.; Kiyokane, K.; Matsuki, T.; Sato, S.; Imokawa, G., Reevaluation of the Importance of Barrier Dysfunction in the Nonlesional Dry Skin of Atopic Dermatitis Patients through the Use of Two Barrier Creams. *Exogenous Dermatology* **2004,** 3, 293-302.

[18] Vavrova, K.; Hrabalek, A.; Mac-Mary, S.; Humbert, P.; Muret, P., Ceramide analogue 14S24 selectively recovers perturbed human skin barrier. *Br J Dermatol* **2007,** 157, 704-12.

[19] Mao-Qiang, M.; Brown, B. E.; Wu-Pong, S.; Feingold, K. R.; Elias, P. M., Exogenous nonphysiologic vs physiologic lipids. Divergent mechanisms for correction of permeability barrier dysfunction. *Arch Dermatol* **1995,** 131, 809-16.

[20] Novotny, J.; Hrabalek, A.; Vavrova, K., Synthesis and structure-activity relationships of skin ceramides. *submitted* **2009**.

[21] Goni, F. M.; Alonso, A., Biophysics of sphingolipids I. Membrane properties of sphingosine, ceramides and other simple sphingolipids. *Biochim Biophys Acta* **2006,** 1758, 1902-21.

[22] van Blitterswijk, W. J.; van der Luit, A. H.; Veldman, R. J.; Verheij, M.; Borst, J., Ceramide: second messenger or modulator of membrane structure and dynamics? *Biochem J* **2003,** 369, 199-211.

[23] Novotny, J.; Janusova, B.; Novotny, M.; Hrabalek, A.; Vavrova, K., Short-chain ceramides decrease skin barrier properties. *Skin Pharmacol Physiol* **2009,** 22, 22-30.

[24] Chong, J. M.; Heuft, M. A.; Rabbat, P., Solvent effects on the monobromination of alpha,omega-diols: A convenient preparation of omega-bromoalkanols. *J Org Chem* **2000,** 65, 5837-8.

[25] Klimentova, J.; Kosak, P.; Vavrova, K.; Holas, T.; Hrabalek, A., Influence of terminal branching on the transdermal permeation-enhancing activity in fatty alcohols and acids. *Bioorg Med Chem* **2006,** 14, 7681-7.

[26] Müller, S.; Schmidt, R. R., Synthesis of two Unique Compounds, a Ceramide and a Cerebroside, Occurring in Human Stratum Corneum. *J Prakt Chem* **2000,** 342, 779-784.

[27] Fabiano, E.; Golding, B. T.; Sadeghi, M. M., A Simple Conversion of Alcohols into Amines *Synthesis* **1987**, 190-192.

[28] Garner, P.; Park, J. M.; Malecki, E., A stereodivergent synthesis of D-erythro-sphingosine and D-threo-sphingosine from L-serine. *The Journal of Organic Chemistry* **1988,** 53, 4395 - 4398.

[29] Herold, P., Synthesis of D-Erythro- and D-Threo-Sphingosine Derivatives From L-Serine. *Helv Chim Acta* **1988,** 71, 354-362.

[30] Harding, C. R.; Watkinson, A.; Rawlings, A. V.; Scott, I. R., Dry skin, moisturization and corneodesmolysis. *Int J Cosmet Sci* **2000,** 22, 21-52.

[31] Coderch, L.; Lopez, O.; de la Maza, A.; Parra, J. L., Ceramides and skin function. *Am J Clin Dermatol* **2003,** 4, 107-29.

[32] Simon, G. A.; Maibach, H. I., Relevance of hairless mouse as an experimental model of percutaneous penetration in man. *Skin Pharmacol Appl Skin Physiol* **1998,** 11, 80-6.

[33] Bond, J. R.; Barry, B. W., Hairless mouse skin is limited as a model for assessing the effects of penetration enhancers in human skin. *J Invest Dermatol* **1988,** 90, 810-3.

[34] Silvander, M.; Ringstad, L.; Ghadially, R.; Skold, T., A new water-based topical carrier with polar skin-lipids. *Lipids Health Dis* **2006,** 5, 12.

[35] Yatvin, M. B.; Stowell, M. H. B. Covalent polar lipid-conjugates with biologically active compounds for use in salves. 2002.

[36] Koria, P.; Brazeau, D.; Kirkwood, K.; Hayden, P.; Klausner, M.; Andreadis, S. T., Gene expression profile of tissue engineered skin subjected to acute barrier disruption. *J Invest Dermatol* **2003,** 121, 368-82.

[37] Small, D. M., Surface and bulk interactions of lipids and water with a classification of biologically active lipids based on these interactions. *Fed. Proc.* **1970,** 29, 1320-6.

[38] Venkataraman, K.; Futerman, A. H., Ceramide as a second messenger: sticky solutions to sticky problems. *Trends Cell Biol* **2000,** 10, 408-12.

[39] Chatelut, M.; Leruth, M.; Harzer, K.; Dagan, A.; Marchesini, S.; Gatt, S.; Salvayre, R.; Courtoy, P.; Levade, T., Natural ceramide is unable to escape the lysosome, in contrast to a fluorescent analogue. *FEBS Lett* **1998,** 426, 102-6.

[40] Tepper, A. D.; Diks, S. H.; van Blitterswijk, W. J.; Borst, J., Glucosylceramide synthase does not attenuate the ceramide pool accumulating during apoptosis induced by CD95 or anti-cancer regimens. *J Biol Chem* **2000,** 275, 34810-7.

[41] Simon, C. G., Jr.; Holloway, P. W.; Gear, A. R., Exchange of C(16)-ceramide between phospholipid vesicles. *Biochemistry* **1999,** 38, 14676-82.

[42] Pagano, R. E.; Martin, O. C., A series of fluorescent N-acylsphingosines: synthesis, physical properties, and studies in cultured cells. *Biochemistry* **1988,** 27, 4439-45.

[43] Shabbits, J. A.; Mayer, L. D., Intracellular delivery of ceramide lipids via liposomes enhances apoptosis in vitro. *Biochim Biophys Acta* **2003,** 1612, 98-106.

[44] Kuerschner, L.; Ejsing, C. S.; Ekroos, K.; Shevchenko, A.; Anderson, K. I.; Thiele, C., Polyene-lipids: a new tool to image lipids. *Nat Methods* **2005,** 2, 39-45.

[45] Nishijima, T.; Tokura, Y.; Imokawa, G.; Seo, N.; Furukawa, F.; Takigawa, M., Altered permeability and disordered cutaneous immunoregulatory function in mice with acute barrier disruption. *J Invest Dermatol* **1997,** 109, 175-82.

[46] Hensbergen, P.; Alewijnse, A.; Kempenaar, J.; van der Schors, R. C.; Balog, C. A.; Deelder, A.; Beumer, G.; Ponec, M.; Tensen, C. P., Proteomic profiling identifies an UV-induced activation of cofilin-1 and destrin in human epidermis. *J Invest Dermatol* **2005,** 124, 818-24.

[47] Bravo, D.; Rigley, T. H.; Gibran, N.; Strong, D. M.; Newman-Gage, H., Effect of storage and preservation methods on viability in transplantable human skin allografts. *Burns* **2000,** 26, 367-78.

Curriculum Vitae

Mgr. Jakub Novotný

EDUCATION

- 2004-present Ph.D. study of Bioorganic Chemistry at the Department of Inorganic and Organic Chemistry, Faculty of Pharmacy in Hradec Králové

- 2004 Master degree in Pharmacy, MSc. Thesis - Solid phase synthesis and characterization of platinum(II)- peptide bioconjugates.
- 2003-2004 Socrates/Erasmus programme, Ruprecht Karl University of Heidelberg, Institute of pharmacy and molecular biotechnology (Prof. Niels Metzler-Nolte).

EMPLOYMENT

- 2008-2009 Researcher of the MSM 0021620822 project "Research of Novel Drugs" at FaF UK in Hradec Králové
- 2009 Reimbursement specialist - State Office of Drug Control

PUBLICATIONS

J**.** Novotný, A**.** Hrabálek, K**.** Vávrová. Synthesis and Structure-Activity Relationships of Skin Ceramides. *Curr. Med. Chem*. (submitted)

J. Novotný, K. Pospěchová, A. Hrabálek, R. Čáp, K. Vávrová. Skin Penetration of NBD-Ceramides is Chain Length-Dependent; Long-Chain Lipids Do Not Enter Nucleated Human Epidermis. *J. Invest. Dermatol.* (submitted)

J. Novotný, P. Kovaříková, M. Novotný, B. Janůšová, A. Hrabálek and K. Vávrová. Dimethylamino Acid Esters as Biodegradable and Reversible Transdermal Permeation Enhancers: Effects of Linking Chain Length, Chirality and Polyfluorination. *Pharm. Res.*, **26**: 811-21 (2009).

J. Novotný, B. Janůšová, M. Novotný, A. Hrabálek, K. Vávrová. Short-Chain Ceramides Decrease Skin Barrier Properties. *Skin Pharmacology and Physiology, Skin Pharmacol Physiol*. **22**: 22-30 (2009).

M. Novotný, A. Hrabálek, B. Janůšová, J. Novotný, K. Vávrová. Dicarboxylic acid esters as transdermal permeation enhancers: effects of chain number and geometric isomers. *Bioorg. Med. Chem.* **19**: 344-7 (2009).

J. Klimentova, P. Kosak, K. Vavrova, T. Holas, J. Novotny, and A. Hrabalek. Transkarbams with terminal branching as transdermal permeation enhancers. *Bioorg. Med. Chem. Lett.* **18**: 1712-5 (2008).

K. Vavrová, K. Lorencová, J. Novotný, A. Holý, and A. Hrabálek. Permeation enhancer dodecyl 6-(dimethylamino)hexanoate increases transdermal and topical delivery of

adefovir; influence of pH, ion-pairing and skin species. *Eur. J. Pharm. Biopharm.* **70**: 901-7 (2008).

K. Vavrova, K. Lorencova, J. Klimentova, J. Novotny, A. N. Holy, and A. Hrabalek. Transdermal and dermal delivery of adefovir: effects of pH and permeation enhancers. *Eur. J. Pharm. Biopharm.* **69**: 597-604 (2008).

K. Vavrova, K. Lorencova, J. Klimentova, J. Novotny, and A. Hrabalek. HPLC method for determination of in vitro delivery through and into porcine skin of adefovir (PMEA). *J. Chrom. B* **853**: 198-203 (2007).

A. Hrabalek, P. Dolezal, K. Vavrova, J. Zbytovska, T. Holas, J. Klimentova, and J. Novotny. Synthesis and enhancing effect of transkarbam 12 on the transdermal delivery of theophylline, clotrimazole, flobufen, and griseofulvin. *Pharm. Res.* **23**: 912-9 (2006).

RESEARCH ACTIVITIES:

International Conferences:

- 10. Perspectives in percutaneous penetration (La Grande Motte 2006, France).
- 10. Gordon research conference: Barrier function of mammalian skin (Newport 2007, USA).
- 7. Cell course 2008 (Saarbrucken 2008, Germany).

Czech Conferences:

- 34. Syntéza a analýza léčiv (Brno 2005).
- 42. Pokroky v organické, bioorganické a farmaceutické chemii (Nymburk 2006).
- 35. Syntéza a analýza léčiv (Karlovice 2006).
- 36. Syntéza a analýza léčiv (Bratislava 2007, Slovakia).

Grants (principal researcher):

- Grant Agency of the Charles University (286/2006/B-CH/FaF): Synthesis of ceramides and their analogues – interaction of penetration enhancers with ceramide membrane models.